TR ECOM-0423-5
September 1969

Reports Control Symbol
OSD-1366

TURBULENT DIFFUSION IN A STABLY STRATIFIED SHEAR LAYER

Contract No. DAAB07-68-C-0423
Task IIB Research Technical Report
Deseret Test Center

Prepared by

Fazal H. Chaudhry

and

Robert N. Meroney

Fluid Dynamics and Diffusion Laboratory
Fluid Mechanics Program
College of Engineering
Colorado State University
Fort Collins, Colorado 80521

For

U. S. Army Electronics Command
Atmospheric Sciences Laboratory
Fort Huachuca, Arizona

CER69-70FHC-RNM12

ABSTRACT

Diffusion of a passive substance released from a continuous point source in a stably stratified shear layer is investigated both theoretically and experimentally. Using Monin-Obukhov's velocity profile and assuming a vertical eddy diffusivity which is a power function of the stability parameter z/L, the Eulerian turbulent diffusion equation is solved to obtain expressions for vertical and longitudinal velocities of the center of mass of a cloud in the constant stress region. These expressions give physical substance to those suggested by Gifford (1962) and Cermak (1963) as intuitive extensions of Batchelor's Lagrangian similarity theory.

The experimental investigation was made in the Army Micrometeorological Wind Tunnel at the Fluid Dynamics and Diffusion Laboratory of Colorado State University. The wind tunnel has a 6' x 6' x 80' test section. A stably stratified shear layer was produced by heating the air and cooling the wind tunnel floor. Detailed observations of the diffusion field, downwind ground and elevated point sources, have been made using Krypton-85 as a tracer. The concentration characteristics obtained from diffusion experiments show excellent agreement with those observed in the atmosphere. The data compares well with the predictions of similarity theory. It appears that the parameters evaluated in the field by Klug (1968) hold also

for the wind tunnel data. The data support the assumption of a Gaussian effect of source height, for elevated releases, on the ground level concentration. An examination of the available solutions to the three dimensional diffusion equation as compared to the data suggests that the detailed diffusion patterns obtained from the wind tunnel experiments may be preferable over such solutions which require arbitrary specification of a lateral diffusivity.

TABLE OF CONTENTS

TABLE OF CONTENTS - Continued

TABLE OF CONTENTS - Continued

LIST OF TABLES

LIST OF FIGURES

LIST OF FIGURES - Continued

LIST OF FIGURES - Continued

LIST OF SYMBOLS

Symbol	Definition	Dimension
A,B	Constants of proportionality	-
a	Constant	-
a,b	Arbitrary constants in the arguments of sine functions	L^{-1}
a_y, a_z	Constants in expressions for lateral and vertical diffusivities	-
b	Batchelor's constant	-
b'	Constant	-
c	Concentration of a diffusing substance e.g., Krypton-85	A/L^3
c_n	nth lateral moment of concentration	A/L^{n-2}
c_o	Zeroth lateral moment of concentration	A/L^2
c_{oo}	Zeroth longitudinal moment of c_o	A/L
c_{max}	Maximum concentration in the plume	A/L^3
c	Constant	-
c'	Concentration fluctuation	A/L^3
c_p	Specific heat at constant pressure	$HM^{-1}s^{-1}$
d	Half width of wind tunnel test section	L
F	weighting function applied to data in diffusivity computations	-
$f(\zeta)$	Universal function describing velocity variation	-
G	Vertical gradient of mean potential temperature	θL^{-1}

Symbols used to indicate dimension are:

M - Mass, L - length, T - time, - Temperature
A - Activity, H - Heat

Symbol	Definition	Dimension
g	Acceleration due to gravity	LT^{-2}
g	Function of σ/u_* which is used to correlate concentration data with similarity theory	-
H	Dimensionless Source elevation	-
H,h	Source elevation	L
h	Extent of data in the vertical direction	L
k	Dissipation constant Eq. 27	T^{-1}
K_1	Diffusion coefficient at reference height	L^2T^{-1}
K_H	Turbulent diffusivity of heat	L^2
K_M	Turbulent diffusivity of momentum	L^2T^{-1}
K_x, K_y, K_z	Turbulent diffusivities of mass in x,y and z directions	L^2T^{-1}
$k(\zeta)$	Dimensionless function in the expression for diffusivity	-
k	Von-Karman's constant	-
L	Stability length	L
L	Extent of data in longitudinal direction	L
m	constant	-
m	Exponent in power law variation of velocity, concentration	-
N	Number of counts recorded	-
N_B	Number of counts due to background	-
N_s	Number of counts due to the sample	-
N_a, N_b	Integer constants	-

Symbol	Definition	Dimension
n	Exponent in Sutton's expression for $R_L(\tau)$	-
n	Exponent in power law representation of k_z	-
n_o	Exponent in power law variation of ground concentration	-
O	Origin of coordinates	-
p	Constant	-
p'	Pressure fluctuation	$ML^{-1}T^{-2}$
Q	Source strength	AT^{-1}
q	Heat flux per unit area	$HL^{-2}T^{-1}$
q	Constant	-
R	Count rate	T^{-1}
R_i	Local gradient Richardson number	-
$R_L(\tau)$	Lagrangian correlation coefficient	-
$S(\zeta)$	Non-dimensional shear i.e, $kz/u_* du/dz$	-
s_1	Constant	-
T_L	Integral time scale	T
T	Local mean temperature	θ
T_∞	Temperature of ambient air	θ
t	Time	T
t_1	A variable substitution	-
t_b	Background counting time	T
t_s	Sample counting time	T
u_∞	Ambient wind velocity	LT^{-1}

Symbol	Definition	Dimension
u,v,w	Mean velocity components in x, y and z directions	LT^{-1}
u_1	Mean wind velocity at reference level z_1	LT^{-1}
u_*	Friction velocity	LT^{-1}
u',v',w'	Velocity fluctuations in x, y and z directions	LT^{-1}
w_1	Integral of z(t) w.r.t. time	LT^{-1}
x,y,z	Distances in longitudinal, lateral and vertical directions	L
z_1	Reference height	L
z_o	Friction height	L
$Z(t)$	A random function of time describing pressure fluctuations	LT^{-2}
α,β	Exponents	-
$\alpha,\alpha_o,\alpha_{oo}$	Constants	-
β	Empirical constant in log-linear law for velocity	-
γ	Empirical constant	-
Γ	Dry adiabatic lapse rate	θL^{-1}
$\Delta x,\Delta y,$ Δz	Probable error in x,y and z measurements	L
ζ	Dimensionless height z/L	-
ζ_o	Dimensionless friction height z_o/L	-
ζ_o'	Dimensionless parameter - $\gamma\ z_o/L$	-
η	Dimensionless width y/L	-
η	Lateral spread; $c(x,\eta o)/C_{max} = 0.5$	L
θ	Local temperature fluctuation	θ

Symbol	Definition	Dimension
ν	Kinematic viscosity	L^2T^{-1}
κ	Von-Karman's constant	-
ξ	Dimensionless longitudinal distance x/L	-
ρ	Mean mass density of air	ML^{-3}
σ	Constant	
σ_y, σ_z	Standard deviation of distribution of matter in a plume in the y and z directions	L
σ_θ	Stand deviation of vertical angle	-
σ_N	Standard deviation of error in count	-
σ_R	Standard deviation of error in count rate	T^{-1}
τ	Shear stress	$ML^{-1}T^{-2}$
τ_o	Wall shear stress	$ML^{-1}T^{-2}$
$\rho(\zeta)$	Universal function of	-
ψ	Gauss's ψ-function	-
ω	An index of temperature variation Eq. 29	T^{-1}
$\overline{\quad}$	Statistical average	-
'	Fluctuation in a quantity	-

Chapter I

INTRODUCTION

The term diffusion is used in many branches of science with different connotations. This report is concerned with the diffusion or transport of a passive substance by random motions of a turbulent fluid flow. The problem of air pollution is the most important single factor responsible for extensive study of the phenomenon of diffusion. The knowledge about the diffusion phenomenon also has application in other fields such as agriculture, water resources, and chemical engineering.

The human race prefers certain forms of energy (e.g. mechanical energy) and provides these preferred forms by converting them from other forms. Attempts at conversion more often result in residues and wastes which must be economically disposed. The atmosphere has absorbed this burden in gaseous and particulate form since time immemorial, but today it is being subjected to ever-increasing saturation. Both private and industrial consumption of fuels is on the rise. What's more, the atmosphere is absorbing waste nearly around the clock, although its capacity to dilute and disperse the pollutants is at its lowest ebb during the night. It is this aspect of diffusion with which this report deals particularly.

The most common mode of release of pollutants into the atmosphere is by continuous emission through sources, at ground level and those elevated above the surface. Because

the size of such sources are usually smaller than the eventual spreading size in the turbulent atmosphere, they are regarded as point or line sources. The transport of a passive substance downstream from a source can be accounted for either by applying a conservation principle to the rate of change of this substance in an arbitrary control volume, or by considering the statistical properties of random motion of individual particles in the turbulent flow field. The first approach, which focuses attention at a fixed point in space, is called the Eulerian description of diffusion. The second, in which the motion of a particle is followed, is called Lagrangian description. Although the latter approach is more fundamental, its progress is at a standstill because there is not enough practical knowledge about the statistical properties of flow fields. Eulerian description has been used much more extensively despite the fact that it stems from some general assumptions about the transfer mechanism.

The problem of atmospheric diffusion is complicated by the varying flow conditions which are introduced by large changes in surface temperatures. The problem is only partially solved in adiabatic atmosphere and introduction of a severer variation of temperature in the vertical gives play to bouancy forces. The effect of thermal stratification on the velocity of wind has been a subject of discussion for a long time. It is the reasoning of Monin and Obukov (1954) in the surface layer of atmosphere which is responsible for the recent progress in the present understanding of the temperature

and wind velocity distribution. The behavior of plumes under different conditions of stability can be readily understood qualitatively but the problem is to relate diffusion to parameters, such as wind characteristics, thermal stratification etc. The effect of thermal stratification is to suppress or enhance the capacity of atmosphere to diffuse according to whether the temperature increases with height (as after sunset) or falls rapidly. When the atmosphere has the first property it is said to be in inversion condition. The pollutants are too sluggish to dispense during inversions and pose a safety problem. The progress in dealing with diffusion under such conditions has been slowed by the lack of sufficient observations; the micrometeorologists had to rely on observations in the open.

A number of field investigations have been made to understand diffusion in a stably stratified turbulent boundary layer in the last decade; however, these measurements are difficult to interpret because of the numerous uncontrolled variables involved. Moreover, reliable field data are neither sufficient nor accurate enough to gather both an understanding of the phenomenon and provide verification to some of the existing hypotheses regarding diffusivities. Hence, laboratory studies of the phenomenon under carefully controlled conditions are required. The Army Meteorological Wind Tunnel offers an excellent opportunity to undertake experiments on diffusion in stable stratification. Koehler (1967) obtained diffusion data for a continuous point source

at ground level with helium as a tracer. Helium, however, is not a suitable tracer to probe buoyancy effects due to density stratification because it is buoyant in air itself. A new tracer is thus necessary for studying the diffusion in a stably stratified boundary layer.

The present study is part of a long range program of wind tunnel simulation of turbulent shear flows related to atmospheric science. The modeling criteria in the meteorological wind tunnel have been discussed by Cermak et al., (1966). Plate and Lin (1966) and Chuang and Cermak (1966) showed that the velocity profiles in thermally stratified shear layer of the wind tunnel are similar to those observed in the atmosphere during diabatic conditions. The turbulence structure of the stably stratified shear layer produced in the wind tunnel has been reported by Arya (1968). This study attempts to extend these wind tunnel investigations to include diffusion phenomena. Detailed observations of diffusion field, downwind ground and elevated point sources, have been made using Krypton-85 as a tracer. The data have been analysed to obtain different diffusion characteristics. These characteristics seem to agree with those observed in the atmosphere. The data has been compared to theoretical predictions. Also, a theoretical effort has been made to incorporate the Monin-Obukhov' velocity profile into the Eulerian description of diffusion and produce results which support the extension of Lagrangian similarity theory of Batchelor (1964).

Chapter II

BACKGROUND

This chapter traces the background of the present study in general as well as in particular viz, diffusion in a stably stratified boundary layer flow. The general theoretical background covers the two distinct approaches, the Eulerian description of diffusion and the Lagrangian or statistical approach. The experimental studies have been reviewed with reference to field or wind tunnel investigations.

2.1 Eulerian Description of Diffusion

In a field of small scale turbulence, the diffusion may be considered by analogy with the molecular diffusion Thus the Chaotic turbulent motions may be characterized by the magnitude of turbulent fluctuation of velocity u' and the scale of turbulence l, then a coefficient of turbulent diffusion $K \sim u'l$ can be introduced as a coefficient of proportionality between an average turbulent flux of a given substance $\overline{c'u'}$ and the gradient of its average concentration $\nabla\bar{c}$ or

$$\overline{u'c'} = - K \nabla\bar{c} \quad .$$

This assumption of proportionality between diffusive flux and the concentration gradient was formulated by Schmidt (1925) who termed K as an "exchange coefficient." It is variously referred to as coefficient of eddy diffusion, eddy diffusivity etc., and the description of concentration field

using this coefficient is sometime known as gradient type diffusion.

In order to describe diffusion of a substance in three dimensions, the concept of eddy diffusion is generalized by introducing three eddy diffusion coefficients, K_x, K_y and K_z which are assumed to be functions of position. An application of the conservation principle and use of the concept of eddy diffusivity gives the following equation of turbulent diffusion:

$$\frac{dc}{dt} = \frac{\partial}{\partial x}\left(K_x \frac{\partial c}{\partial x}\right) + \frac{\partial}{\partial y}\left(K_y \frac{\partial c}{\partial y}\right) + \frac{\partial}{\partial z}\left(K_z \frac{\partial c}{\partial z}\right). \qquad (1)$$

The nature of the coefficients K_x, K_y and K_z (e.g. whether these are scalar functions of position or componants of a vector function, etc.) has been discussed by Calder (1965). He shows that even under customary conditions, equation 1 can not be a generally valid form of diffusion equation. If K_x, K_y and K_z are diagonal elements of a symmetric diffusivity tensor, it is necessary for the tensor to have oxyz as principal axes in order that equation 1 is valid at all points of the medium. Thus equation 1 is applicable only in a preferred set of axes. In a meteorological situation, it appears plausible to postulate existence of such a set of axes with reference to a vertical plane such that the mean velocity vector can be approximately regarded everywhere parallel to it (vit, ox and oz in the plane and oy perpendicular to it).

Relative to these axes, the diffusion equation has the form

$$\frac{\partial c}{\partial t} + u\frac{\partial c}{\partial x} + w\frac{\partial c}{\partial z} = \frac{\partial}{\partial x}\left(K_x\frac{\partial c}{\partial x}\right) + \frac{\partial}{\partial y}\left(K_y\frac{\partial c}{\partial y}\right) + \frac{\partial}{\partial z}\left(K_z\frac{\partial c}{\partial z}\right) . \quad (2)$$

Since most of the attempts in seeking solutions to the
1 have been made with $u = w = 0$, ... no direct verification of this postulate is available.

If the mean vertical velocity w is assumed zero and the longitudinal dispersion term neglected, being much smaller than the convective term $u\frac{\partial c}{\partial x}$, the equation of diffusion becomes

$$\frac{\partial c}{\partial t} + u\frac{\partial c}{\partial x} = \frac{\partial}{\partial y}\left(K_y\frac{\partial c}{\partial y}\right) + \frac{\partial}{\partial z}\left(K_z\frac{\partial c}{\partial z}\right) . \quad (3)$$

The coefficients K_y and K_z of equation 3 are, generally speaking, variables and not known at the outset. Analytic solutions of equation 3 for standard conditions can be obtained only by making particular assumptions about these coefficients. The extent to which these assumptions represent the physical phenomena will depend on how sound these assumptions are.

Roberts (1921) assumed K_x, K_y, K_z and u as constant and obtained solutions of the diffusion equation for various types of sources. The vertical and cross wind concentration distributions determined by this theory follow the Gaussian law. The predictions of concentration however, do not agree with observations. The theoretical rate of decrease of concentration is too slow. These

discrepancies in the solutions make the hypothesis of constant eddy diffusivity an unacceptable one. Although these solutions must be merited as being the first attempt at solving problems of diffusion through conservation principle, their failure to conform to observation produced the unfortunate impression that the whole concept of eddy diffusivity was inadequate. This delayed for some time, the progress towards use of equation 2 in evaluating diffusion problems.

Bosanquet and Pearson (1936) introduced an improvement and solved the diffusion equation by assuming a linear variation of K_y and K_z with height above the surface in a uniform wind. In meteorological work, it is often convenient to use a power law profile in the form

$$u = u_1 \left(\frac{z}{z_1}\right)^m \tag{4}$$

where u_1 is the mean velocity at the reference height z_1. The exponant $m = \frac{1}{7}$ gives a good representation of the velocity variation in the neighborhood of a smooth boundary for conditions of neutral stability. Now if the shear stress is assumed independent of height in the lower layers of atmosphere i,e.,

$$K_M(z) \frac{du}{dz} = \text{constant} \tag{5}$$

the corresponding expression for the diffusivity of momentum K_M is

$$K_M(z) = k_1 \left(\frac{z}{z_1}\right)^{1-m} \tag{6}$$

where k_1 is the diffusivity at height z_1. Equations 4 and 6 are known as Schmidt's conjugate power-laws. On the assumption that Reynold's analogy applies, K_z, the diffusion coefficient in z direction, is thus determined. Using the conjugate power laws O.F.T. Roberts (see Calder (1949)) found an exact solution of the two dimensional diffusion equation

$$u \frac{\partial c}{\partial x} = \frac{\partial}{\partial z} \left(k_z \frac{\partial c}{\partial z}\right) \tag{7}$$

for concentration distribution from an infinite cross-wind line source.

Sutton (1934) obtained a relation for K_z as

$$K_z = \frac{(0.251)^{1-n}}{1-n} \nu^n \left[\left(\frac{\partial u}{\partial z}\right)^3 \left(\frac{\partial^2 u}{\partial z^2}\right)^{-2}\right]^{(1-n)} \tag{8}$$

by application of Taylor's continuous movement theory (discussed in next section), Prandtle's mixing length theory, and Reynold's analogy to his hypothesized functional form for the correlation coefficient, R_ξ, viz.,

$$R = \left(\frac{\nu}{\nu + \overline{w'^2}_\xi}\right)^n . \tag{9}$$

Substituting the power law for velocity $\bar{u}$ in equation 4 into equation 8, he recovered the conjugate power law

$$K_z = a_z u_1^{1-n} z^{1-m} \tag{10}$$

where a_z is now a known constant in terms of n and some other physical constants of the atmosphere. This seems to be the first attempt to incorporate the shear effect due to the known velocity distribution into the diffusion problem. With the velocity and coefficient of diffusion given by equations 6 and 10, Sutton solved the two dimensional diffusion equation 7 for evaporation from a semi infinite strip $0 \leq x \leq x_o$. The theoretical results showed excellent agreement with experiments. Sutton (1934) remarks on this agreement, "Thus it appears despite lack of confirmatory experiments, there is good reason for stating that the process of evaporation, as regards the wind velocity, size and shape of the area, are connected with wind shear as set forth in this theory."

Frost (1946) also used the conjugate power law for K_z to obtain a solution for diffusion from infinite cross wind line source flush with the ground and showed that the theoretical predictions were confirmed by meteorological observations.

Sutton (1947) showed that although his solution (1934) for an infinite line source predicted the law of decrease of ground concentration fairly accurately, the computed height of smoke (the distance from the ground at which the concentration falls to one tenth of that at the ground) was in marked disagreement with the observed height. He could not resolve it and thought that either the scale of atmospheric turbulence was so different from that arising

in the wind tunnels that the value of Von Karman's constant k = 0.4 was no longer applicable or the surface of earth cannot be regarded as smooth.

Calder (1949) treated the question of surface roughness in a simple fashion by adopting ordinary aerodynamic formula (with k = 0.4) for wind velocity and proved that the diffusion results can be predicted satisfactorily. Calder's work established that the diffusion equation, with some realistic assumptions, was adequate to describe the two dimensional problem. The assumptions were (a) horizontal shear stress is independent of height (b) mean mass and momentum transfers are described by the same diffusion coefficient i.e., Reynolds' analogy.

Davies (1947, 1950A) for the first time, introduced a variable lateral diffusivity to extend the above treatment to three dimensional problem of eddy diffusion described by the equation

$$u \frac{\partial c}{\partial x} = \frac{\partial}{\partial y} \left(K_y \frac{\partial c}{\partial y}\right) + \frac{\partial}{\partial z} \left(K_z \frac{\partial c}{\partial z}\right) . \qquad (11)$$

He assumed a simple power law for K_y as

$$K_y = a_y u_1^{1-n} z^m \qquad (12)$$

which when inserted into equation 11, along with the conjugate power law, led to a tractable partial differential equation. There was a significant improvement (compared with the two dimensional theory) in the agreement between theory

and experiments for rates of evaporation and the diffusion of vapor. Davies (1950B), in an effort to find a more exact power law, expressed K_y as

$$K_y = a_y u_1^{1-n} z^{\alpha} \tag{13}$$

where α is to be determined (a_y depends upon ν). By assuming a similarity solution for c viz;

$$c = \text{const}\ x^{no}\ \psi\left(\frac{y}{x^{1/q}}, \frac{z^{\beta}}{x^{1/q}}\right) \tag{14}$$

and substituting in equation 11, he found β and q subject to the condition that the equation is independent of x. Also using continuity condition, α was determined in terms of m, the index of power law for velocity and n_o, the index of decrease of ground concentration. At this stage, if a satisfactory experimental law, giving the variation of peak concentration along x-axis from a point source, were known, K_y is completely known according to the form in equation 13. When, however, the appropriate values of α, q, and n_o are substituted into equation 11 it leads to an equation in two variables $\left(\frac{y}{x^{1/q}}, \frac{z^{\beta}}{x^{1/q}}\right)$ which is not separable. It is only in the particular case when $\alpha = m$ that the equation is separable. The solution did not provide a good comparison with experiment at large distances. Davies (1952) now assumed a dependence of K_y on y also given by

$$K_y = a_y u^{1-n} z^{m} y^{(1-2m)} \tag{15}$$

in the wind tunnels that the value of Von Karman's constant k = 0.4 was no longer applicable or the surface of earth cannot be regarded as smooth.

Calder (1949) treated the question of surface roughness in a simple fashion by adopting ordinary aerodynamic formula (with k = 0.4) for wind velocity and proved that the diffusion results can be predicted satisfactorily. Calder's work established that the diffusion equation, with some realistic assumptions, was adequate to describe the two dimensional problem. The assumptions were (a) horizontal shear stress is independent of height (b) mean mass and momentum transfers are described by the same diffusion coefficient i.e., Reynolds' analogy.

Davies (1947, 1950A) for the first time, introduced a variable lateral diffusivity to extend the above treatment to three dimensional problem of eddy diffusion described by the equation

$$u \frac{\partial c}{\partial x} = \frac{\partial}{\partial y} \left(K_y \frac{\partial c}{\partial y}\right) + \frac{\partial}{\partial z} \left(K_z \frac{\partial c}{\partial z}\right) . \qquad (11)$$

He assumed a simple power law for K_y as

$$K_y = a_y u_1^{1-n} z^m \qquad (12)$$

which when inserted into equation 11, along with the conjugate power law, led to a tractable partial differential equation. There was a significant improvement (compared with the two dimensional theory) in the agreement between theory

and experiments for rates of evaporation and the diffusion of vapor. Davies (1950B), in an effort to find a more exact power law, expressed K_y as

$$K_y = a_y u_1^{1-n} z^{\alpha} \tag{13}$$

where α is to be determined (a_y depends upon ν). By assuming a similarity solution for c viz;

$$c = \text{const} \; x^{no} \; \psi\left(\frac{y}{x^{1/q}} , \frac{z^{\beta}}{x^{1/q}}\right) \tag{14}$$

and substituting in equation 11, he found β and q subject to the condition that the equation is independent of x. Also using continuity condition, α was determined in terms of m, the index of power law for velocity and n_o, the index of decrease of ground concentration. At this stage, if a satisfactory experimental law, giving the variation of peak concentration along x-axis from a point source, were known, K_y is completely known according to the form in equation 13. When, however, the appropriate values of α, q, and n_o are substituted into equation 11 it leads to an equation in two variables $\left(\frac{y}{x^{1/q}} , \frac{z^{\beta}}{x^{1/q}}\right)$ which is not separable. It is only in the particular case when $\alpha = m$ that the equation is separable. The solution did not provide a good comparison with experiment at large distances. Davies (1952) now assumed a dependence of K_y on y also given by

$$K_y = a_y u^{1-n} z^{m} y^{(1-2m)} \tag{15}$$

and obtained an analytic solution to equation 11. He assumed coefficients a_y and a_z related as

$$\frac{a_y}{a_z} = \left[\frac{\overline{u'^2}}{\overline{w'^2}}\right]^{(1-n)} , \qquad (16)$$

a_z being known from Calder's work (1949), a_y could be calculated. In the conditions of neutral stability, the solution gave good agreement with experimental results for cloud height and width. A slight discrepancy was found between the theoretical and observed values of n_o but the magnitude of peak concentration compared well.

After Taylor (1954,a,b) applied the Eulerian diffusion equation to the dispersion of soluble matter in a fluid flowing in a straight pipe, Aris (1956) presented an extremely useful approach to render the diffusion equation more tractable. Instead of seeking a direct solution of the differential equation 1, which is nearly impossible for general values of the wind shear and eddy diffusivities, he investigated the integrated forms of this equation, which are equations for the moments of c viz.,

$$c_n(x,z) = \int_{-\infty}^{\infty} y^n c(x,y,z)\, dy. \qquad (17)$$

The advantages of forming the differential equations for these functions are that they are now two-dimensional and the boundary conditions on the moments are known. The first function, c_o gives the total amount of concentration on

any transverse line, x = constant, z = constant, the second function c_1, the displacement of centroid of c_o the third, c_2 gives the spread of the substance in y-direction and so on. If the plume is symmetric, about x-z plane, c_o and c_2 suffice to describe c for all practical purposes.

Smith (1957) employed Aris's moment method with a fair measure of success in tackling the problem of an elevated continuous point source diffusion. As suggested by Sutton (1953), K_y was taken equal to K_z, as given by equation 6, to obtain a more realistic rate of decay of axial concentration. He obtained exact solutions for zeroth and second moments of the concentration distributions along lines lying along the cross wind direction at ground level for a general power law velocity distribution (i.e., the value of m). For a special case, when m takes values 0, 1/3, 1/2 and 1, the differential equation is simplified and thus allows these moments to be determined along lines at general height. Smith plotted the results for different m and noted that the interpolation curves for the height and distance (downstream from the elevated point source) of maximum concentration show the greatest variation of these factors for small m. For $m = 1/2$, the differential equation yields an exact solution for concentration, and the cross wind distribution always has a Gaussian form. If it is assumed that, for all m, the cross wind distribution is Gaussian, a formulation of concentration can be given in terms of the known zeroth and second moments. Rate of

decrease of concentration, for neutral flow $m = 1/7$, given by assumption of the power law for K_z and K_y is like $x^{-1.67}$. This index compares well with its observed value of 1.76. This fact was recognized by Davies (1950 B, index) but he preferred to assume different power laws for K_z and K_y (giving value of the index as 1.4 in one case and 1.58 in an other) because if these were supposedly equal, it would require a uniform wind speed with height.

Later, Saffman (1962) investigated the effect of wind shear on horizontal spread from an instantaneous point source at the ground by the moments method, according to whether the height, to which the material may rise, is bounded or not. Tyldesley and Wallington (1965) repeated the same conditions for short distances, numerically using both analog and digital methods. Fischer (1964), Yotsukura and Fiering (1964) and Sayer (1967) have used the method of moments to solve diffusion equation for two dimensional flow in open channels, both analytically and numerically.

2.2 Lagrangian Approach to Diffusion

The Eulerian description of diffusion, although it helps to find concentration distributions, is not based directly on the characteristics of a turbulent flow field. It would be more realistic to approach the problem from the Lagrangian point of view. Taylor (1921) proceeded to determine the essential properties of the motion of a

turbulent fluid which makes a passive substance diffuse through it. He considered the motion of a fluid element in an isotropic, homogeneous, and stationary turbulence and arrived at the well known result.

$$\sigma_x^2(t) = 2\overline{u'^2} \int_0^t \int_0^{t_1} R_L(\tau)\, d\tau\, dt_1 \qquad (18)$$

where $\sigma_x^2(t)$ is the variance of the motion in x direction and $\overline{u'^2}$ is the mean square value of the instantaneous velocity fluctuation in that direction. Also, $R_L(\tau)$ is the Lagrangian correlation coefficient given by,

$$R_L(\tau) = \frac{\overline{u'(t)\ u'(t+\tau)}}{\overline{u'^2}} \quad . \qquad (19)$$

In the words of Taylor, Equation 18 "is rather remarkable because it reduces the problem of diffusion, in a simplified type of turbulent motion to the consideration of a single quantity, namely, the correlation coefficient between the velocity of a particle at one instant and that at a time, τ , later." Equation 18 can be approximated for both small and large times.

For a small time interval, $R_L(\tau)$ does not appreciably differ from unity such that

$$\sigma_x^2 = \overline{u'^2}\ t^2 \quad . \qquad (20)$$

In other words, the standard deviation of a particle from its initial position is proportional to t (for small t) as would be expected, the fluctuating velocity being nearly the same.

For diffusion times larger than the Lagrangian time scale of turbulence defined as

$$T_L = \int_0^\infty R_L(\tau)\, d\tau \qquad (21)$$

$$\sigma_x^2(t) = 2(\overline{u'^2}\, T_L)\, t \qquad t >> T_L \qquad (22)$$

Thus, the turbulent diffusion after large intervals proceeds like molecular diffusion.

Assuming a three dimensional Gaussian distribution of concentration in a diffusion cloud, having dispersions $\sigma_x^2(t)$, $\sigma_y^2(t)$ and $\sigma_z^2(t)$ given by equation 18, Frenkiel (1963) provided equations for concentration from different kinds of sources. He showed that these solutions were equivalent to those obtained from diffusion equations with constant diffusion coefficients if

$$\sigma_x^2(t) = 2\,\overline{u'^2}\, t \quad \text{and so on.} \qquad (23)$$

Equation 18 provides an excellent method for estimating dispersion but the exact form of the function $R_L(\tau)$ is not known for the practical flow situations. Sutton (1934), on dimensional grounds, proposed a functional form for $R_L(\tau)$ as

$$R_L(\tau) = \left(\frac{\nu}{\nu + \overline{w'^2}\,\tau}\right)^n \qquad (24)$$

with n as an adjustable constant that, according to Sutton,

"specifies the rapidity of mixing and is a simple measure of the degree of turbulence." This function satisfies the conditions

$$R_L(0) = 1$$

$$R_L(\tau) = 0 \quad \text{as} \quad \tau \to \infty \tag{25}$$

which is to be expected on physical grounds. Substituting equation 24 into Taylor's theorem equation 18, he determined the variances of $\sigma^2(t)$. The solution of the diffusion problem is thus reduced to that of finding the functions representing the distribution of concentration, which satisfy the equation of continuity and the boundary conditions. Sutton (1934) assumed a Gaussian distribution and thus presented a number of formulas for different kinds of sources. These were further extended by Sutton (1947) who showed that improved agreement with observation could be obtained by their use. Further progress in Lagrangian approach is described in the next section.

2.3 Diffusion in a Thermally Stratified Boundary Layer

The preceding review shows that the problem of diffusion in a turbulent boundary layer is only partially solved for neutral conditions of flow. Introduction of a thermal stratification in the flow complicates the problem further, which now must include the diffusion as affected by buoyancy forces. Qualitatively these forces will either enhance or suppress the vertical mixing, depending if the

thermal stratification is unstable or stable, satisfactory analysis of the problem has not yet been completed. The progress in this direction is very recent and is based primarily on empiricism.

Sutton's (1934) theory was perhaps the first to admit the treatment of diffusion in a thermally stratified atmosphere. He regarded n, the index in his expression for $R_L(\tau)$ equation 24, as an adjustible constant which is an "indicator of the degree of turbulence present in the medium". It appeared to Sutton (1934) that, to a first approximation, n was independent of the mean velocity and height and was primarily affected only by those factors which tend to damp out or enhance the turbulence. For meteorological purposes n was regarded as a function of temperature gradient and of roughness of surface. Sutton (1953) found that it was not easy to relate n to the temperature gradient and moderate wind over level surfaces.

Barad and Haugen (1959) and Haugen et al. (1961) used project Prairie Grass data to test Sutton's hypothesis (1934). They found that the data for a continuous point source observed the hypothesis only if two different values for n were assumed, one to characterize lateral diffusion (n_y) and other to characterize vertical diffusion (n_z). The data showed that whereas n_y and n_z did vary systematically with stability, the range of variation of n for a given stability was rather large. Thus it is difficult to assign a value of n for a given stability.

Csanady (1964) constructed a correlation function for the r.m.s. vertical velocity w using the equations of motion. By boundary-layer type approximations in the atmosphere, he reduced the Navier-Stokes and energy equations to

$$\frac{dw}{dt} = g\left(\frac{\theta}{T}\right) + z(t) \tag{26}$$

$$\frac{d\theta}{dt} = - gw - k\theta \tag{27}$$

where θ is the local temperature fluctuation, g the vertical gradient of mean potential temperature, and k is a dissipation constant of dimension $(\text{time})^{-1}$, and $z(t)$ $\left(= \frac{1}{p} \frac{\partial p'}{\partial z}\right)$ is a random variable with statistical properties which are assumed known from measurements in neutral flow. By integrating the first equation 26, he eliminated w from the two equations and obtained a second order differential equation for θ. The solution for θ gave w from which he constructed the Lagrangian correlation function for w subject to the condition that the statistical properties of $z(t)$ and hence of its integral

$$w_1 = \int_{t_o}^{t} z(t)\, dt$$

are known. Assuming w_1 to have a correlation function as

$$\overline{w_1(t)\, w_1(t+\tau)} = w_1^2\, e^{-p\tau}\ , \tag{28}$$

the Lagrangian correlation function $R_L(\tau)$ for w is

$$R_L(\tau) = e^{-p\tau/2} \left(\cosh \frac{mp\tau}{2} - \frac{1}{m} \sin h \frac{mp\tau}{2}\right) \qquad (29)$$

where $m = \sqrt{1 - 4 \frac{\omega^2}{p^2}}$, and $\omega^2 = \frac{gG}{T}$.

The above result is for the case $G > 0$ i.e., stable stratification. Substitution of equation 29 for $R_L(\tau)$ into equation 18 gives

$$\sigma_z^2(t) = \frac{8\ \overline{w'^2}}{p^2(1-m^2)} \left[1-e^{-pt/2} \left(\cosh \frac{mpt}{2} - \frac{1}{m} \sin h \frac{mpt}{2}\right)\right] \qquad (30)$$

The outstanding feature of the equation is that it shows $\sigma_z^2(t)$ tends to an asyptotic value for large t, i.e.,

$$\sigma_z^2(t) = \frac{8\ \overline{w'^2}}{p^2(1-m^2)} = \frac{2T}{gG}\ \overline{w'^2} \text{ as } t \to \infty \quad . \qquad (31)$$

A comparison of equation 31 with experimental data of Hilst and Simpson (1960) and Gifford (1960) shows that the theory predicts the main features of turbulent diffusion process in a stratified atmosphere remarkably well. This result, however, is only applicable in nearly uniform flows away from the boundary.

No other attempts seem to have been made to derive $R_L(\tau)$ for atmospheric conditions so that no further development of Taylor's theorem has appeared in the literature.

Other developments consider the mean velocity and temperature distributions in the surface layer of the atmosphere as more basic in the treatment of diffusion in a stratified flow condition. Thus, progress towards describing velocity distribution is reviewed next.

Nearly all attempts at describing velocity variation in the atmosphere have been empirical or semi empirical. Rossby and Montgomery (1935) examined mixing length arguments and found that the velocity profile should satisfy the equation

$$\frac{du}{dz} = \frac{u_*}{kz} (1 + \beta \, Ri)^{1/2} \qquad (32)$$

where β is a constant, and Ri is Richardson number defined as

$$Ri = \frac{g/T \, \frac{\partial}{\partial z} (T+\Gamma z)}{(\frac{\partial u}{\partial z})^2} \qquad (33)$$

where Γ is dry adiabatic lapse-rate. Equation 32 reduces to logrithmic law for neutral conditions ($Ri = 0$) but Deacon (1949) found that β increased systematically with stability. Holzman (1943) suggested on intuitive and empirical grounds, a different form for mixing length and gave the following equation:

$$\frac{du}{dz} = \frac{u_*}{kz} (1-\sigma \, Ri)^{-1/2} \, . \qquad (34)$$

In near neutral condition i.e., for small Ri, both equation 32 and 34 are identical and lead to the famous log + linear law of Monin and Obukhov, to be described later.

A number of authors (e.g. Sutton (1936, 1937) and Bjorgum (1953)) advocate the possibility of using the logrithmic law under any conditions of stability. Others like Frost (1947) and Best (1935) propose an approximation of the wind profile by a power function as

$$\frac{u}{u_1} = \left(\frac{z}{z_1}\right)^m \quad . \tag{4}$$

The index m is regarded as a function of stability.

Deacon (1949) generalized the logrithmic velocity distribution and proposed the form

$$\frac{du}{dz} = a\, z^{-\beta} \tag{35}$$

where a is a constant and β depends upon stability, being greater than one for unstable conditions and less than one for stable ones. The integral form of equation 35, with "a" chosen as

$$a = \frac{u_*}{k\, z_o^{1-\beta}}$$

to provide transition to adibatic form as $\beta \to 1$, is

$$\frac{u}{u_*} = \frac{1}{k(1-\beta)} \left[\left(\frac{z}{z_o}\right)^{\beta-1} - 1\right] \tag{36}$$

Deacon's observations show that the magnitude of β determined from mean profiles is systematically related to the conditions of stability given by the Richardson number, Ri. In the constant shear stress region, assuming that momentum and

mass are transported in exactly the same manner in all conditions of stability, equation 35 gives

$$K_z = ku_* z_o \left(\frac{z}{z_o}\right)^{\beta} \tag{37}$$

as in Calder's treatment (1949), Deacon used a power law variation for velocity viz.,

$$\frac{u}{u_*} = q\left(\frac{z}{z_o}\right)^{\alpha} \tag{38}$$

(q and α found by comparison with equation 36) to solve the two dimensional diffusion equation 7. Deacon compared his solution with observations and found good agreement. Sutton (1953) noted that this agreement is good only for near-neutral conditions and that there is large discrepancy for large instability. Deacon's profile in equation 36 and the expression for K_z have been shown by Pasquill (1949) and Rider (1954) to hold to an adequate degree in unstable conditions but fail in the stable ones, the diffusivity being seriously under estimated. Rounds (1955) derived solutions to the diffusion equation 7 by direct use of Deacon's profile for an infinite line source at arbitrary height.

Deacon's profile and the results thereof are not recognized as a universal treatment of non-adiabatic diffusion. Monin and Obukhov (1954) considered the influence of stratification on the turbulent state in the surface layer of the atmosphere on dimensional grounds. They

developed a similarity theory with the turbulent state being determined by three parameters viz, shear stress τ, vertical heat flux q and the parameter $\frac{g}{T}$, which do not vary with height. The only scale of velocity is $u_* (= \sqrt{\tau/\rho})$ and the only scale of length is

$$L = \frac{u_*^3}{k \frac{g}{T} (- \frac{q}{\rho c_p})} \tag{39}$$

with L positive for stable stratification and negative for an unstable one. All dimensionless variables can be functions of dimensionless height $\zeta (= \frac{z}{L})$ only. The constant value of $\frac{kz}{u_*} (\frac{du}{dz})$ is now a function of ζ or

$$\frac{du}{dz} = \frac{u_*}{kz} \phi(\zeta) \quad . \tag{40}$$

Monin and Obukhov considered a Taylor series expansion of $\phi(\zeta)$ and retained only the first term, ζ. Thus for small ζ

$$\frac{du}{dz} = \frac{u_*}{kz} (1+\beta\zeta) \quad . \tag{41}$$

The constant β can be determined from observations under near neutral conditions. Integration of equation 41 gives Monin-Obukhov log + linear law as

$$u = \frac{u_*}{k} [\ln \frac{z}{z_o} + \beta \frac{z}{L}] \quad . \tag{42}$$

If, at this point, an equality between diffusivity of momentum and heat is assumed, it may be shown that z/L is equivalent to Ri (for small Ri) and hence, from equation 42 it follows that

$$K_z = ku_* \, z \, (1-\beta \, Ri) \, . \tag{43}$$

Ellison (1957) obtained the following more general equation by interpolation between extremes of stratification viz, between conditions of neutral stability and free convection:

$$K_z = ku_* \, z \, (1-\gamma \, Ri)^{\frac{1}{4}} \, . \tag{44}$$

This equation is said to give correct results in limiting cases and for small and large negative values of Ri.

According to Monin-Obukhov's similarity theory, the general form for K_z is

$$K_z = ku_* \, L \, \kappa(\zeta) \, . \tag{45}$$

Monin and Yaglon (1965) suggest, following Deacon, that in the case of stable stratification, for near neutral conditions, it is possible to approximately replace $\kappa(\zeta)$ by a power function of the type $K_1 \, \zeta^n$ with the index somewhat less than 1. For strong stability (i.e., when it is a matter of broad interval of values of ζ) it may be sufficient to consider only the limiting values of $\kappa(\zeta)$. As

$$\begin{aligned} \kappa(\zeta) &= \alpha_o \, \zeta \quad \text{for } \zeta \to 0 \\ \kappa(\zeta) &= \alpha_{oo}/Ri \quad \text{for } \zeta \to \infty \end{aligned} \tag{46}$$

where α_o and α_{oo} are constants.

Monin and Obukhov (1959c) used this fact to solve the equation

$$\frac{\partial c}{\partial t} = \frac{\partial}{\partial z}\left(K_z \frac{\partial c}{\partial z}\right) \tag{47}$$

for an instantaneous line source. With asymptotic properties, as stated in equation 46, he estimated $\kappa(\zeta)$ by

$$\kappa(\zeta) = \begin{cases} \zeta & \text{for } \zeta \leq 1 \\ 1 & \text{for } \zeta \geq 1 \end{cases} \tag{48}$$

The solution of equation 47 would also permit evaluation of diffusion from a steady line source for a uniform wind.

Monin and Yaglon (1965) suggest that the solution of equation 47, $c(z,t)$, may be used, as a rough approximation, to find diffusion from point sources assuming average values, for u, K_x and K_y. The concentration for an instantaneous point source could then be approximated by

$$c(x,y,z,t) \simeq \frac{1}{4\pi (K_x K_y)^{\frac{1}{2}} t} \exp\left[-\frac{(x-ut)^2}{4K_x t} - \frac{y^2}{4K_y t}\right] c(z,t). \tag{49}$$

As coefficients K_x and K_y are not known off-hand, application of this approximation becomes difficult.

Laikhtman (1961) suggested a similar method for incorporating horizontal diffusion. He assumed a Gaussian distribution of the pollutant in the lateral direction and coupled it with the solution $c(x,z)$ of the diffusion equation 7 to give

the following solution for a continuous point source

$$c(x,y,z) = \frac{1}{\sqrt{2\pi\ \sigma_y^2}} \exp\left[-\frac{y^2}{2\ \sigma_y^2}\right] c(x,z) \qquad (50)$$

where σ_y^2 is given by Taylor's theorem equation 18. He suggests that, in addition to use of the approximations in equations 22 and 23, the following interpolation formula may be used:

$$\sigma_y^2 \sim \frac{t^2}{1+\beta t} \qquad (51)$$

Iordanov (1966) solved diffusion equation 47 for elevated unsteady line source in unstable stratification approximating $\kappa(\zeta)$ as

$$\kappa(\zeta) \begin{cases} \zeta & \text{if } \zeta \leq 1 \\ \zeta^{4/3} & \text{if } \zeta \geq 1 \end{cases} . \qquad (52)$$

He also suggested a solution for the point source problem similar to that given by Laikhtman (1961).

Yamamoto and Shimanuki (1960) for the first time obtained a numerical solution for the two dimensional diffusion equation 7 (infinite line source) for the general velocity distribution of the similarity theory of Monin and Obukhov viz.,

$$\frac{du}{dz} = \frac{k}{u_* z}\ \phi(\zeta) \qquad (53)$$

where $\phi(\zeta)$ satisfies a fourth order equation

$$\phi^4 - \gamma\zeta\phi^3 - 1 = 0 \quad . \tag{54}$$

The above equation is equivalent to Ellison's interpolation formula equation 44. The vertical diffusivity K_z was computed from equation 53 by assuming constant vertical shear stress and Reynold's analogy, as

$$K_z = \frac{ku_* z}{\phi(\zeta)} \quad . \tag{55}$$

They obtained concentration as a function of two variables $(x/z_o, z/z_o)$ for a series of values of parameter $\zeta_o = \gamma z_o/L$ (which arises from dependence of $u(z)$ on z_o). This study shows that the index characterizing the decrease of ground concentration with distance is in general, a function of x/z_o and ζ_o. For the neutral stability the index is found to be nearly constant and equal to 0.9, which agrees completely with observation. For the stable case it decreases with distance but approaches a near constant value of 0.65 for large distances from the source.

Yamamoto and Shimanuki (1964) extended the above treatment to three dimensional problem of diffusion from a point source at the ground for arbitrary stratification. They solved diffusion equation 11 with $u(z)$ and K_z as given by equations 53, 54 and 55 and assumed K_y to have the form

$$K_y = ku_* z\ \alpha(\zeta_o) \tag{56}$$

where $\alpha(\zeta_o)$ is an unknown function. Substitution of equations 55 and 56 into equation 11 led to the following simplified equation which was solved numerically,

$$\frac{f}{k^2}\frac{\partial c}{\partial (x/z_o)} = \frac{\partial}{\partial (y/\alpha^{\frac{1}{2}} z_o)}\left(\xi \frac{\partial c}{\partial (y/^{\frac{1}{2}} z_o)}\right) + \frac{\partial}{\partial \xi}\left(\frac{\xi}{\phi}\frac{\partial c}{\partial \xi}\right) \qquad (57)$$

where $f = \int_1^{\xi} \frac{\phi}{\xi}\, d\xi$, $\xi = \frac{z}{z_o}$.

The function $\alpha(\zeta_o)$ was determined by comparison of lateral spread of smoke at fixed distance (as given by above solution) with those observed. It increased monotonically with respect to stability parameter ζ_o , the value being about 13 in neutral conditions ($\zeta_o = 0$), about 3 for $\zeta_o = .01$, and about 100 for $\zeta_o = -.014$. Yamamoto and Shimanuki (1964) compared the computed cross-wind concentration distribution with the observed data. Though there was general agreement the scatter of the data forbids a reliable conclusion. The rate at which peak concentration decreases with distance, as expressed by a power index, agrees with the observed value for neutral stability.

2.4 Similarity Theories and Diffusion

The last decade has seen a new approach emerge to deal with atmospheric diffusion. It is the Lagrangian similarity theory initiated by Batchelor (1959). Its counterpart in general fluid mechanics viz, Eulerian similarity of turbulent flows, was developed by Monin and Obukhov (1954)

and was used with considerable success toward determining of velocity and temperature profiles in the diabatic surface layer of atmosphere. Monin (1959) used it to predict the shape of the boundary of smoke plumes within the surface layer. Batchelor stated his ideas originally in 1959 in an unpublished report, but later (1964) presented them more fully. The Lagrangian similarity approach relies on one hypothesis and one assumption. For the neutrally stratified flow, the similarity hypothesis is that the rate of decrease of average displacement $\bar{z}$ of a marked particle above the ground is uniquely determined by the friction velocity $u_* \ (=\sqrt{\tau/\rho})$ within the layer of constant shear stress. Hence on dimensional grounds

$$\frac{d\bar{z}}{dt} = bu_* \tag{58}$$

where b is a universal dimensionless constant. The similarity assumption is that the rate of increase of mean displacement $\bar{x}$ down wind from the source is equal to mean wind speed at the level $c\bar{z}$ i.e.,

$$\frac{d\bar{x}}{dt} = u\ (c\bar{z}) \tag{59}$$

where c is another dimensionless constant. Combining the expressions for $d\bar{z}/dt$ and $d\bar{x}/dt$ through further dimensional analysis with logrithmic velocity distribution and integrating, an equation of the path of a point which moves with mean velocity of a marked particle is obtained as

$$\bar{x} = \frac{1}{bk} \left(\bar{z} \ln \frac{c\bar{z}}{z_o} - \bar{z} + A \right) \qquad (60)$$

where k is Von-Karman constant and A is another constant dependent on the initial position of the particle. The similarity hypothesis may be used to predict spacial distribution of mean concentration of some quantity released at the source. According to Batchelor (1964), the coordinate fluctuations about their mean $(x-\bar{x}, y, z-\bar{z})$ depend only on u_* and t and it follows on dimensional grounds that the probability density of these fluctuations has the same shape at all times. Also, the length scale is u_*t or $\bar{z}$. This enables an expression for concentration from a continuous point source to be written as

$$c(x,y,z) = Q \int_0^\infty \frac{1}{\bar{z}^3} f \left(\frac{x-\bar{x}}{\bar{z}}, \frac{y}{\bar{z}}, \frac{z-\bar{z}}{\bar{z}} \right) dt. \qquad (61)$$

As the functional form of this probability density is not known, only asymptotic results for $x \to \infty$ can be derived. The variation of ground concentration due to a point source (for $x \to \infty$) is roughly the same as observed, i.e., power index of x is -2.

The successful verification of the similarity theory of Monin and Obukhov (discussed in section 2.3) led to the possibility of extension of Lagrangian similarity to diabatic flows. Using the velocity profile in equation 42, Monin and Obukhov (1959) developed the following equations for the upper boundary of smoke flowing out of a point source:

$$\frac{dx}{dt} = \frac{u_*}{k} [f(\zeta) - f(\zeta_o)]$$

$$\frac{dz}{dt} = Lu_* \phi(\zeta) \quad . \tag{62}$$

The function ϕ was derived by Monin (1959), from energy balance, as being related to function f by

$$\phi(\zeta) = [1 - \frac{1}{f'(\zeta)}]^{\frac{1}{4}} \quad . \tag{63}$$

Combining equations 62 and 63 Monin obtained the boundaries of smoke plumes for different stabilities.

Gifford (1962) approximated $\phi(\zeta)$ for stable stratification as

$$\phi(\zeta) = \frac{1}{2} \left\{ [\frac{1+(\beta-1)\zeta}{1+\beta\zeta}]^{\frac{1}{4}} + 1 \right\} \tag{64}$$

and presented a number of curves for $\bar{x}$. It should be noted that the equations used by Gifford (1962), though similar to Monin's, were in terms of $\bar{x}$ and $\bar{z}$ viz,

$$\frac{d\bar{z}}{dt} = bu_* \phi(\bar{\zeta})$$

$$\frac{d\bar{x}}{dt} = \frac{u_*}{k} [f(\bar{\zeta}) - f(\zeta_o)] \quad . \tag{65}$$

He used these curves and equation 61 to obtain axial concentrations due to a continuous point source at ground for different ζ_o. The calculated index values agree with observed values remarkably well for many stability conditions. Gifford (1962)

comments, on the basis of this agreement the hypothesis of Lagrangian similarity in diabatic flows seems to be strongly supported.

Cermak (1963), using an exponential velocity distribution in place of equation 42, obtained explicit equations for the power indices of x describing the variation of axial concentrations, due to elevated, continuous point and line sources. He found that his predictions agreed with an assorted data for a range of length scales extending over three orders of magnitude. He also extended the Lagrangian similarity hypothesis to stratified flows and included height of a source as another variable. A slightly modified approach was suggested by Panofsky and Prasad (1965) which makes use of root mean square vertical componant of eddy velocity $\sqrt{w'^2}$ instead of u_*. They assume the equations of motion of center of mass of the cloud for general stratification

$$\frac{d\bar{z}}{dt} = \sqrt{w'^2} \qquad (66)$$

$$\frac{d\bar{x}}{dt} = u$$

and then

$$\frac{d\bar{z}}{dx} = \frac{\sqrt{w'^2}}{U} = \sigma_\theta$$

where σ_θ is standard deviation of the vertical angle and is a universal function of z_o/L and z/z_o. They

computed this universal relation from data and used it to integrate equation 67 numerically to give distribution of $\bar{z}$ with x for unstable conditions of flow. They also calculated relative decrease of concentration with distance from the source and found that the powers of x indicating rapidity of this decrease were quite reasonable. Panofsky and Prasad were, however, skeptical of the asymptotic form of equation 61, namely,

$$c_{max} \alpha \frac{Q}{u(\bar{z})^2} \tag{68}$$

because it implied a constant coefficient of proportionality. By comparing this proportionality with the approximate variation of c_{max}, given by the assumption of Gaussian distribution of concentration namely,

$$c_{max} \tilde{=} \frac{Q}{\pi \sigma_y \sigma_z \bar{u}} , \tag{69}$$

they argued that the Lagrangian similarity requires both lateral and vertical dispersions to be proportional to each other. But in near-neutral conditions the ratio of the two dispersions was found to be 2 and in unstable conditions the same ratio was 3, which, according to them, proves that equation 68 is not correct.

Pasquill (1966) critically examined the extension of Batchelor's Lagrangian similarity by Gifford (1962) and Panofsky and Prasad (1965) to diabatic flows and the experimental verification thereof. He observed that the

interest had been confined to relative changes of concentration with distance from the source and that the actual magnitude of the vertical spread at a fixed distance in relation to parameters u_* and L, had been virtually ignored with obvious implications on the variation of concentration with roughness and stability. In order to test whether the similarity theory provides a satisfactory representation of vertical spread, he compared the values of $\bar{z}$, computed from curves given by Monin (1959), Gifford (1962), and Panofsky and Prasad (1965) with the observations of Haugen et. al. (1961), for specified values of constants and roughness. The effect of stability variation on vertical spread as predicted by similarity theory was found to be considerably less severe than that shown by the experimental data. This discrepancy was ascribed to shortcomings in the extension of similarity theory to stratified conditions. Pasquill questioned the representativeness of the empirical functions used to describe the effects of stability e.g., $\phi(z/L)$, σ_θ, etc.

Pasquill (1966) contended that a more important error might lie in the formal representation, in which $d\bar{z}/dt$ at a given height is regarded as uniquely determined by diffusive conditions at that height alone. The existing extensions of theory identify the influence of stability on $d\bar{z}/dt$, with that on intensity of turbulent transfer at level z, that is, as represented by $\phi(z/L)$ or σ_θ. This would be acceptable only, according to Pasquill, if the influence

of stratification is a linear function of height. It is analogous to asserting that the mean K_z determining the vertical spread is proportional to $K_z(\bar{z})$ which is only true if K_z is a linear function of height. It is, however, evident that the influence of stratification on vertical transfer is not simply a linear function of height. For the effective K_z it is not adequate merely to take, say

$$K_z = ku_* z (1+\alpha) \tag{69}$$

where α is a constant. It is necessary to recognize that dK/dz, respectively, increases or decreases with height in unstable or stable conditions.

Pasquill (1966) argues that it is, thus, difficult to see how to represent the vertical spread by z alone that is without some how taking into account the shape of the vertical distribution. He suggested as an alternative that vertical spread may be represented by the height of cloud z_{max}, and the equation

$$\frac{dz_{max}}{dt} = bu_* \tag{70}$$

should replace equation 65. A much more encouraging reconciliation of observations and similarity was achieved through this arbitrary specification.

Koehler (1967) used

$$\phi (z/L) = \frac{1}{1+\beta(z/L)} \tag{71}$$

which is similar to equation 63 for small z/L.

Chatwin (1968) showed that the different results of similarity theory of Batchelor (1964) (for neutral flow) can be derived from the diffusion equation by assuming existence of an eddy diffusivity. Chatwin obtained, analytically, the different constants involved in the similarity formulations and found that their values were supported by experimental results.

2.5 Diffusion Experiments

Most of the diffusion experiment have been made in the field although these programs were expensive and the conditions were subject to change. This was partly due to the difficulty experienced in reproducing field conditions in the laboratory and partly due to the misgivings about the existing laboratory data. These have been highlighted by Sutton (1953) as follows: "It is a matter of great difficulty to produce in wind tunnels fully developed profiles in substantial layers of fluid having density gradients comparable with those observed in the lower atmosphere, so that there is little in the way of evidence from controlled experiments to guide the worker in this field. The micrometeorologist must rely for his data almost entirely on observations made in the open, where control is impossible and conditions are rarely, if ever, exactly the same on different occasions." With the construction of the Army Micrometeorological wind tunnel

at the Fluid Dynamics and Diffusion Laboratory of Colorado State University, this difficulty is very much a matter of the past.

Field Studies

Because field programs are very expensive and time consuming, only limited objectives are planned for them. The usual objectives are ground concentrations and the plume dimensions from continuous sources. All the recent experiments have been summarized in "Meteorology and Atomic Energy," 1968, published by the U. S. Atomic Energy Commission, (TID-24190).

Wind Tunnel Experiments

Most of experimental studies in wind tunnels have been carried out at the Fluid Dynamics and Diffusion Laboratory of Colorado State University. As these investigations are made in controlled conditions and are economical, complete mappings of concentration have often been attempted. Plate and Lin (1966), Chuang and Cermak (1966), Malhotra and Cermak (1963) and Arya (1968) have demonstrated the reliability of wind tunnel shear layer for modeling atmospheric flows. It has been shown that the wind tunnel generated thermally stratified shear layer obeys the same universal functions as the atmosphere. A summary of diffusion experiments made in the wind tunnel is presented in Table 1.

Chapter III

EXPERIMENTAL EQUIPMENT AND TECHNIQUES

The experimental work was carried out in the Micro-meteorological Wind Tunnel at the Fluid Dynamics and Diffusion Laboratory, Colorado State University. The main purpose was to determine the concentration field produced by ground and elevated point source releases of a gas in the wind tunnel turbulent shear layer with a temperature gradient. The equipment and technique used in these experiments are presented in the following sections. A description of the commercial instruments and their specifications are presented in appendix A.

3.1 Wind Tunnel

The layout of the wind tunnel, used in this study, is shown in figure 1. This tunnel is generally operated on a closed circuit principle. The air leaving the power-section slowly expands into a diverging duct which has heat exchanger coils located at its end. These coils enable air temperature to be set at a desired level, and also provide humidity control with the help of a set of steam nozzles. After turning 180^{o}, air enters the converging section through turbulence damping screens, which eliminate all large scale velocity fluctuations. The flow is, thus, uniform across the entire test section at the entrance and has low ambient turbulence level of the order of 0.03%.

The test section is 80 ft long and has a cross section of approximately 6 ft by 6 ft. The first 6 ft length of the test section has been roughened with ½" gravel attached to its perimeter in order to thicken the boundary layer and, thus, reduces the wall effects. Also a trip fence at the entrance is utilized to further stabilize the flow patterns. The ceiling of the tunnel is adjustible for control of pressure gradient in the direction of flow, which, in this study, was adjusted to zero. At a distance of 40 ft from the entrance, the test section floor changes from smooth plywood to smooth aluminum which covers another 40 ft length. The aluminum floor can be heated or cooled and its temperature can be kept constant along its length with varying temperatures between $20^{o}F$ and $350^{o}F$. The air temperature can be selected and can be maintained between $40^{o}F$ and $80^{o}F$. For the present study, the temperature of the plate was held at about $40^{o}F$ and that of air in the free stream at $120^{o}F$. The air speed can be controlled both by varying the RPM of the drive motor and the pitch of the propeller.

3.2 Velocity and Temperature Measurement

A pitot-static tube in conjunction with a capacitance type pressure meter was used to measure the mean dynamic pressure and hence the mean velocity. The pitot-static tube was of standard design having four 0.016 inch diameter static holes located ½" from the rounded nose. The stagnation hole was 0.046 inch in diameter and tube diameter was 0.116 inch. The two ports of the pitot-tube were connected to

the pressure meter by means of vinyl tubing. This pressure meter was calibrated against a standard Meriam Model 34FB2TM Micromanometer. No appreciable difference was noticed for the range used.

The mean temperature of the air was measured with a Chromel-Alumel thermocouple with its reference junction in an ice bath. The thermocouple had an adequate response. The thermocouple e.m.f. was determined by a sensitive millivoltmeter for adjusting ambient air temperatures.

3.3 Concentration Measurement

Krypton-85 was used as a tracer for obtaining concentration distribution. It is a radioactive noble gas. It is produced by nuclear fission of uranium and averages about 5% of total Krypton. Krypton-85 has a half life of 10.6 years so that there is no appreciable decay during a diffusion experiment. The gas decays by emission of beta particles with a maximum energy of 0.67 Mev in 99.6% of the disintegrations. In the remaining 0.4%, the emission of a beta particle with maximum energy of 0.15 Mev is followed by 0.51 Mev Gamma ray. The half value thickness for Kr-85 beta radiation is about 25 mg/cm^2 of aluminum. The maximum permissible concentration (M.P.C.) of Krypton-85 occupational exposure is 6×10^{-6} microcuries per cc for 40-hour week. Optimum procedure, for keeping exposures below M.P.C., has been worked out in Appendix B.

Krypton-85 has many advantages over the other tracers used in wind tunnel diffusion studies. It is diluted with

air about a million times before use and as such, has properties very similar to those of air. Its detection procedure is fairly simple and direct. Above all, Krypton-85 technique is much more economical than those provided by other tracers.

The Krypton-85 technique is suitable for studying diffusion from continuous sources and hence a detailed description of the different steps involved in its use is given below.

3.3.1 Procurement, transfer and dilution of Krypton-85

Krypton-85 is available in the form of a gas and can be obtained in glass or metal containers depending on the quantity involved. For this study it was rocured in a returnable metal container from Oak Ridge National Laboratory. Its concentration was about 67 millicuries per cc at standard temperature and pressure. Keeping in view the safety and economy, the gas in this form was considered unsuitable for release in the wind tunnel. The extent of dilution required before use has been given in Appendix B.

The transfer and dilution was accomplished with the help of an arrangement shown in figure 2. The gas was transferred to four empty nitrogen cylinders which were tested for pressure integrity before use. These were connected by means of a web type manifold which also helped to manage the cylinders during release. This manifold was placed at one end of a straight manifold carrying connections to a vacuum pump, compressed air cylinder, a vacuum and pressure gauge, and the metallic gas container. This

container was connected to the straight manifold by a copper tubing 3/16" I.D. using standard hoke fitting B24. A number of valves were provided to facilitate the transfer and dilution procedure described below:

1. With valves 3, 4, 5, 6, 7, 8 and 9 open, the vacuum pump was switched on till the vacuum gauge showed minus 15 inches of mercury. Valve 3 was then closed.

2. After testing the gas container for leaks, valves 1 and 2 were opened to transfer the bulk of Krypton-85. Valve 4 was then closed.

3. The pressure in the container was raised to about 30 psi and the contents were transferred to the four cylinders by opening valve 4. This process of raising the pressure and discharging was repeated about thirty times to ensure complete transfer and minimize the hazard of exposure to excessive concentrations.

4. Valves 1 and 2 were then closed and the gas cylinders were then pressurized with compressed air by opening valve 10 to 800 psi.

5. The straight manifold was then disconnected and a pressure regulator was connected in its place to the web manifold used to join the four cylinders. The gas was now ready for use at regulated pressure.

3.3.2 Calibration of diluted gas

The activity of diluted Krypton-85 was determined by the relative counting technique. Activity of a suitable

standard source is compared to that of the unknown source which, in this study, was in the form of a gas. Thallium-204 was chosen as a reference standard. It is a pure beta emitter and maximum energy of its beta particles is very close to that of 99% betas of Krypton-85. Thallium-204 standard had an activity of 8 microcuries and was 1 1/8 inch in diameter.

The arrangement employed for calibration of Krypton-85 is shown in figure 3. An end window G.M. Tube was mounted on a tube stand inside an iron shield. A door on the side of the shield gives access to the sample mount having a number of shelves. A special planchet, shown in figure 4, was used to hold the Krypton-85 sample. It was a cylindrical container made of lucite plastic and was mounted on a 2 3/4 inch by 2 3/4 inch aluminum plate .04 inch thick. It had the same inside diameter as that of the Thallium-204 standard. The planchet was covered with a thin Mylar (polyethelene terephthalate) film (0.63 milligrams per cm^2) glued to the walls in order to make it air tight. It was provided with inlet and outlet taps. A pressure meter was inserted between the inlet and the outlet. The following procedure was used to calibrate a gas sample.

1. The thallium-204 standard was placed under the G.M. tube on an aluminum plate of same thickness as the one below the planchet to provide similar backing material for both. It was also covered with Mylar film. The count was recorded on a scalar described in Appendix A.

2. The standard was now replaced by the planchet assembly such that the distance of the center of the planchet from the G.M. tube window was identical with that of the standard in 1 above. Krypton-85 was now passed through the planchet at a rate of about 1 cc per minute measured by a flow meter. The pressure inside the planchet was maintained at .004 mm of mercury. There was no appreciable deformation of the mylar film. The gas was passed for about half an hour to ensure complete exchange. Five different counts were taken and were averaged.

3. The two sources of radiation were nearly identical so that

$$\frac{\text{Activity of standard} = 8\mu\text{curies}}{\text{net count rate for standard}} = \frac{\text{Activity of sample}}{\text{net count rate for sample}} .$$

Now the activity of the sample is the product of concentration of the sample and the inside volume of the planchet (8.15 cc). The concentration was thus computed from

$$\text{concentration of Kr-85 sample} = \frac{8\ \mu\ \text{curies}}{8.15\ \text{cc}} \times \frac{\text{net count rate on sample}}{\text{net count rate on standard}} .$$

3.3.3 G.M. detectors

1. construction

Eight halogen quenched thin stainless steel wall G.M. tubes were used to study the concentration distribution in the wind tunnel. Metal wall G.M. tubes were specially preferred over the glass wall ones in order to do away with the problem of charge build up on the tube walls. Each metal tube is provided with a glass jacket around it which has inlet and outlet ports for the sample. The jacket was designed such that a defective G.M. tube could be easily replaced. This makes the Krypton-85 technique more versatile and economical. The jacket, figure 5, consists of three parts (a) The glass cylinder, (b) Lucite plastic holder, and (c) the plastic ring. The glass cylinder is glued to the lucite holder which slips down the G.M. tube phenolic base. An o-ring between the plastic holder and the phenoloc base ensures the assembly is air tight. The assembly is held against the corners of the base by the plastic ring which is screwed to it. The G.M. tube assembly is housed in a lead shield 1 inch wall thickness. A four pin socket sits on top of a small aluminum cylinder fixed to a 2 inch thick lead disc, figure 6. This disc forms the bottom piece of the lead shield. The G.M. tube leads and the two plastic tubings for Krypton-85 sample are let out of the shield through an elbow hole (½ inch in diameter) in the disc. The G.M. tube is thus completely shielded from cosmic radiation. Characteristic curves were plotted for all the G.M. tubes and their operating voltages determined.

2. calibration

A diluted gas sample, whose concentration was known (section 3.3.2), was passed through all the G.M. tubes connected in a series for five minutes to ensure complete exchange. The count was recorded for each G.M. tube. The counting yield was then calculated by

$$c.y. = \frac{\text{concentration}}{\text{net count rate}} \ (\mu\mu ci/cc/cpm) \quad .$$

This factor was nearly the same for all G.M. tubes.

3.3.4 Release system

The tracer release system is shown schematically in figure 7. The diluted Krypton-85 gas in four cylinders was first heated or cooled, as the case might be, before release. For the purpose of heating, the gas was taken from the gas regulator in a Mayon tubing to a 12" coil of copper tubing with a 3/16 inch inside diameter. This coiled tubing was placed at the end of the test section to avoid flow disturbance. The vertical position of the coils in the wind tunnel and length of the copper tubing were adjusted to match gas temperature of release with the temperature in the wind tunnel at the position of the source. The heated gas was let out of the wind tunnel near the position of the point source for metering through a calibrated flow meter. It was then connected to the source under the wind tunnel floor. The source was designed such that it would have a suitable outlet diameter

and its stem induced minimum disturbance in the flow field during the elevated releases. The horizontal portion of the source was streamlined to the same end. The source could be raised or lowered easily with the help of two wooden bits which were indented to hold the vertical stem of the source.

3.3.5 Sampling system

Samples were drawn from the wind tunnel through a rake of eight sampling tubes 1/16 inch in diameter mounted on a carriage as shown in figure 10. The carriage could be moved vertically and laterally by a remote control outside the wind tunnel. The distance between the individual sampling tubes could be varied easily by moving the clamping blocks along a horizontal bar.

The sampling equipment outside the wind tunnel is shown schematically in figure 8 and pictorially in figure 9. The eight samples drawn from the wind tunnel in Mayon tubing 1/8 inch inside diameter were first metered through separate flow meters. The sampling flow rate was fixed at 250 cc per minute keeping in view the velocity in the wind tunnel. (Appendix B). The samples were then passed through G.M. tube jackets. A vacuum pump was used to suck the samples and throw them back into the wind tunnel. Each sampling line had an electric valve (normally closed type) inserted into it in order to avoid intermixing of the samples in different lines. These valves could be opened or closed at the same time by a common switch.

Output from each G. M. tube could be connected to the same scaler and high voltage. Although the count for each G.M. tube had to be recorded one by one, this sampling scheme helped conserve Krypton-85 because eight samples were taken for one release of the gas.

3.3.6 Disposal of Krypton-85

Because the wind tunnel operates on a recirculating principle, if the gas was released repeatedly, it would accumulate in it. This creates a higher background, lowering the accuracy of measurement and could be hazardous in terms of exposure. Thus a means of emptying the wind tunnel after a few runs was necessary during data collection. The high pressure zone of the wind tunnel just upstream of heat exchangers was opened to atmosphere by a 24 inch square duet at a point about 30 ft. from the ground. The flow through this duct could be regulated by a shutter at its base. After every few releases, the shutter was opened and the wind tunnel was run at about 40 ft per second. Opening a wind tunnel window in the test section facilitated the emptying process. This would bring the background in the wind tunnel back to normal in about 15 minutes. The concentration of Krypton-85 disposed into the atmosphere was kept below the maximum permissible concentration in air.

3.4 Experimental Procedure

A typical diffusion experiment was conducted according to the following procedure:

1. The wind tunnel was started and the flow conditions were established for the experiment.

2. Point source position in the vertical was adjusted. The copper tubing coils were positioned such that the temperature of Krypton-85 at release matched the temperature of the air at that elevation.

3. The distance between the individual sampling tubes on the rake was adjusted according to their axial position downwind from the source. Also the position of sampling tubes in the vertical was set at a desired level.

4. The common valve was opened and the electric valves were switched on to open. The pump was then started and was left running for one minute to flush the jackets. The sampling flow rate was set at 250 cc per minute through all the G.M. tubes by means of a control needle valve at the inlet to the flow meters.

5. The necessary release rate through the source was then established at Krypton-85 flowmeter.

6. Samples were drawn for about three minutes and then the electric valves were closed and the common valve was also closed. This enclosed Krypton-85 gas air mixture sample in the jackets. The gas was then stopped.

7. The samples enclosed around the G.M. tube were then counted, one by one, by the scaler for a minute or more. Counting time, to increase accuracy, was increased for very dilute samples.

8. The above procedure was then repeated for a new position of the sampling probes.

9. Background concentration of Krypton-85 in the wind tunnel was obtained after every few runs. This was taken as a datum for concentration measurements. The net count rate, when multiplied by the counting yield of the respective G.M. tubes, gave the concentration of Krypton-85 in the sample.

Chapter IV

THEORETICAL ANALYSIS

The concept of Lagrangian similarity, originally proposed by Batchelor (1959, 1964) to study diffusion, in neutral condition has been applied to thermally stratified flows by many authors, (Gifford (1962), Cermak (1963), Klug (1968)). As brought out by Pasquill (1966), these developments suffer from rather arbitrary specification of the vertical velocity of a cloud's centre of mass. A sound extension of the Lagrangian similarity theory to thermally stratified flow situations can be accomplished by the use of the differential equation describing distribution of concentration along with the knowledge available regarding the effect of such stratification on the flow field and transfer processes. The method is similar to that used by Chatwin (1968) for neutral flow.

4.1 Wind Profile in Stably Stratified Boundary Layer

When vertical temperature gradients are due to heat transfer from the boundary and the turbulence is homogeneous in the horizontal, then according to Monin-Obukhov's Similarity theory the stationary turbulent regime is completely determined by the parameters $u_* = (\tau/\rho)^{1/2}$, $q/\rho c_p$ and g/T_o (τ is the turbulent shear stress and q the turbulent heat flux). The first two parameters do not vary in the surface layer. Thus the only length-scale possible is the value

$$L = \frac{u_*^3}{k \frac{g}{T_o}(- q/\rho C_p)}$$

All dimensionless variables can be functions only of the stability parameter $\zeta = z/L$. The average velocity can be represented by

$$u(z) = \frac{u_*}{k} [f(\zeta) - f(\zeta_0)] \tag{71}$$

where z_o is the roughness and $f(\zeta)$ is the universal function. Monin and Obukhov (1953, 1954) have suggested the following form for $f(\zeta)$

$$f(\zeta) = \ln\zeta + \beta\zeta \qquad |\zeta|<1 \tag{72}$$

It has been verified in various observational studies (Plate and Lin (1966)) in the atmosphere and in the wind tunnel that the velocity profile is adequately represented by this so called Monin-Obukhov's log-plus-linear law for the stable and forced convection cases. The velocity is then given by

$$u(z) = \frac{u_*}{k} [\ln \frac{\zeta}{\zeta_o} + \beta(\zeta - \zeta_o)] \tag{73}$$

4.2 Diffusion in Stably Stratified Boundary Layer

The distribution of concentration c in a cloud of contaminant released in a plane homogeneous turbulent shear layer can be described by the diffusion equation

$$\frac{\partial c}{\partial t} + u(z)\ \frac{\partial c}{\partial x} = \frac{\partial}{\partial z}\ (-\overline{w'c'}) + \frac{\partial}{\partial y}\ (-\overline{v'c'}) + \frac{\partial}{\partial x}\ (-\overline{u'c'}) \qquad (74)$$

where u', v' and w' are fluctuations of velocity about the mean in x, y and z directions and c' is the fluctuation of concentration. As $\overline{u'c'} << \bar{u}(z)c$, it is reasonable to make a boundary layer type approximation and neglect the last term on the right of equation 74. The simplified equation is

$$\frac{\partial c}{\partial t} + u(z)\ \frac{\partial c}{\partial x} = \frac{\partial}{\partial z}\ (-\overline{w'c'}) + \frac{\partial}{\partial y}\ (-v'c') \qquad (75)$$

If a vertical mass eddy diffusivity K_z is assumed, then

$$-\overline{w'c'} = K_z\ \frac{\partial c}{\partial z}$$

and equation 5 becomes

$$\frac{\partial c}{\partial t} + u(z)\ \frac{\partial c}{\partial x} = \frac{\partial}{\partial z}\ (K_z\ \frac{\partial c}{\partial z}) + \frac{\partial}{\partial y}\ (-\overline{v'c'}) \qquad (76)$$

A formulation for K_z is now required. In neutral flow mass eddy diffusivity is usually considered identical with diffusivity of momentum. The latter under the condition of constant shear stress can be written as

$$K_M = ku_*z$$

In thermally stratified flows, eddy diffusivity for heat K_H appears to be the same as that for mass K_z as suggested

by Swinbank's measurements (see Panofsky (1968)). The ratio K_H/K_M has been observed to be fairly constant (see Arya (1968), Record and Cramer (1968)) so that a coefficient of mass diffusion can be evolved. The eddy diffusivity for momentum K_M in constant flux region is generalized for stratified flows as

$$K_M = \frac{ku_* z}{s} \tag{77}$$

where s is non-dimensional wind shear defined as

$$s = \frac{kz}{u_*} \frac{du}{dz} \quad . \tag{78}$$

In neutral atmosphere, s is unity. A number of forms have been suggested for s taken as a function of z/L. The most general is the interpolation formula first found by Ellison (1957) and is given by

$$s^4 - \frac{\gamma z}{L} s^3 = 1 \tag{79}$$

where γ is a constant. Figure 39 shows plot of s vs $\gamma z/L$ with field data from different sources. Also plotted is Arya's (1968) wind tunnel data for stably stratified flows. Under near neutral condition, equation 79 leads to the Monin-Obukhov law equation 73 provided that

$$\gamma = 4\beta$$

The form most suited to the present analysis is a power function type as suggested by Monin and Yaglom (1965) following

Deacon (1949) which makes it possible to also approximate the diffusivity as a power function i.e.,

$$s = s_1 \left(\frac{z}{L}\right)^p \tag{80}$$

and

$$K_M = \frac{ku_* z}{s_1 \left(\frac{z}{L}\right)^p}$$

or

$$K_M = \frac{ku_* L}{s_1} \left(\frac{z}{L}\right)^n \qquad n=1-p \tag{81}$$

As argued above, K_z can be taken proportional to K_H so that

$$K_z = \frac{K_H}{K_M} \frac{ku_* L}{s_1} \left(\frac{z}{L}\right)^n$$

or

$$K_z = b' u_* L \left(\frac{z}{L}\right)^n \tag{82}$$

where $b' = \frac{k}{s_1} \left(\frac{K_H}{K_M}\right)$.

Rewriting equation 76 with K_z and $u(z)$ as in equations 82 and 73 and non-dimensionalizing the lengths x, y, and z using L as ξ , η and ζ produces

$$\frac{\partial c}{\partial t} + \frac{u_*}{Lk} \left[\ln \frac{\zeta}{\zeta_o} + \beta(\zeta-\zeta_o)\right] \frac{\partial c}{\partial \xi} = \frac{\partial}{\partial \zeta} \left(b' u_* L^{-1} \zeta^n \frac{\partial c}{\partial \zeta}\right) +$$

$$\frac{\partial}{\partial \eta} \left(-L \overline{v'c'}\right) \tag{83}$$

4.3 The Vertical and Horizontal Velcity of a Cloud of Contaminant in Stably Stratified Boundary Layer

Aris moment method will be used to reduce the number of variables through integration. To consider the position of the center of mass of the cloud in the vertical, $\bar{z}$, in relation to its average axial position, it is more convenient to study the flow in horizontal layers. If c_o is defined as

$$c_o = \int_{-\infty}^{\infty} c(\xi, \zeta, \eta, t)\, d\eta \tag{84}$$

the diffusion equation 83 upon integration with respect to η, becomes

$$\frac{\partial c_o}{\partial t} + \frac{u_*}{Lk}\left[\ln \frac{\zeta}{\zeta_o} + \beta(\zeta-\zeta_o)\right] \frac{\partial c_o}{\partial \xi} = \frac{\partial}{\partial \zeta}\left(b' u_* L^{-1}\, \zeta^n \frac{\partial c_o}{\partial \zeta}\right) \tag{85}$$

It is advantageous to define the properties of the cloud, i.e., $\bar{\xi}$, $\bar{\zeta}$, σ_ζ etc., in terms of c or c_o subject to the condition that

$$\int_{-\infty}^{\infty}\int_{o}^{\infty}\int_{-\infty}^{\infty} c\, d\xi\, d\zeta\, d\eta = \int_{o}^{\infty}\int_{-\infty}^{\infty} c_o\, d\xi\, d\zeta = 1 \tag{86}$$

Thus,

$$\begin{aligned}
\bar{\zeta} &= \int_{o}^{\infty}\int_{-\infty}^{\infty} \zeta\, c_o\, d\xi\, d\zeta \\
\bar{\xi} &= \int_{o}^{\infty}\int_{-\infty}^{\infty} \xi\, c_o\, d\xi\, d\zeta \\
\sigma_\zeta^2 &= \int_{o}^{\infty}\int_{-\infty}^{\infty} (\zeta-\bar{\zeta})^2\, c_o\, d\xi\, d\zeta \quad .
\end{aligned} \tag{87}$$

Consider a plane ground source which releases a puff of contaminant at $t = 0$. The concentration distribution would be determined by equation 85 subject to the following boundary and initial conditions on c_o :

$$
\begin{aligned}
&(1)\quad c_o = 0 \quad \text{at} \quad \xi = \pm\infty \\
&(2)\quad c_o = 0 \quad \text{at} \quad \zeta = +\infty \\
&(3)\quad b' u_* L^{-1} \zeta^n \frac{\partial c_o}{\partial \zeta} = 0 \quad \text{at} \quad \zeta = 0 \\
&(4)\quad c_o = \delta(\xi)\ \delta(\zeta) \ \text{at} \quad t = 0 \quad .
\end{aligned}
\tag{88}
$$

the zeroth longitudinal moment of equation 85 is produced by integrating with respect to ξ and specifying condition 1, equations 88

$$
\frac{\partial c_{oo}}{\partial t} = \frac{\partial}{\partial \zeta} \left[b' u_* L^{-1} \zeta^n \frac{\partial c_{oo}}{\partial \zeta} \right] \tag{89}
$$

where $$c_{oo} = \int_{-\infty}^{\infty} c_o \, d\xi \quad .$$

The solution of equation 89 subject to conditions 3 and 4 and 5 in equation 88 is given by Monin and Yaglom (1965) as,

$$
C_{oo}(\zeta, t) = \frac{1}{(2-n)^{\left(\frac{n}{2-n}\right)} \Gamma\left(\frac{1}{2-n}\right) (b' u_* L^{-1} t)^{\left(\frac{1}{2-n}\right)}} \; x
$$

$$
\exp \left[- \frac{\zeta^{(2-n)}}{(2-n)^2 b' u_* L^{-1} t} \right]
$$

or

$$c_{oo}(\zeta,t) = \frac{\alpha}{\Gamma(\frac{1}{\alpha})(\alpha^2\sigma)^{\frac{1}{\alpha}}} \exp[-\frac{\zeta^\alpha}{\alpha^2\sigma}] \qquad (90)$$

where

$$\alpha = 2-n$$

$$\sigma = b'u_* L^{-1} t \quad .$$

The first longitudinal moment is obtained by multiplying equation 85 by ξ and integrating with respect to ξ and ζ

$$\frac{\partial}{\partial t}\int_0^\infty d\zeta \int_{-\infty}^{\infty} \xi\, c_o\, d\,\xi + \frac{u_*}{Lk}\int_0^\infty [\ln\frac{\zeta}{\zeta_o} + \beta(\zeta-\zeta_o)]\,(\int_{-\infty}^{\infty}\xi\frac{\partial c_o}{\partial \xi}\, d\xi)d\zeta$$

$$= \int_0^\infty \frac{\partial}{\partial\zeta}(b'u_* L^{-1}\,\zeta^n \frac{\partial}{\partial\zeta}\int_{-\infty}^{\infty}\xi\, c_o\, d\xi)\, d\zeta \qquad (91)$$

where by definition $\int_0^\infty d\zeta \int_{-\infty}^{\infty} \xi\, c_o\, d\xi = \overline{\xi}$ (92)

As $\overline{\xi}$ is a function of time alone, the partial derivative may be replaced by a total derivative. Integrating by parts and using condition 1 of equation 88, the second inner integral on the left is,

$$\int_{-\infty}^{\infty} \xi\, \frac{\partial c_o}{\partial \xi}\, d\xi = \xi\, c_o \Big|_{-\infty}^{\infty} - \int_{-\infty}^{\infty} c_o\, d\xi$$

$$= - c_{oo}(\zeta,t) \qquad (93)$$

with equations 92 and 93 and the fact that $\overline{\xi}$ does not vary with ζ equation 91 reads as

$$\frac{d\bar{\xi}}{dt} = \frac{u_*}{Lk} \int_0^\infty [\ln \frac{\zeta}{\zeta_o} + \beta(\zeta-\zeta_o)]\ c_{oo}(\zeta,t)\ d\zeta \qquad (94)$$

Substituting c_{oo} from equation 90, in the above one obtains,

$$\frac{d\xi}{dt} = \frac{u_*}{Lk} \frac{\alpha}{\Gamma(\frac{1}{\alpha})(\alpha^2\sigma)^{(\frac{1}{\alpha})}} \int_0^\infty [(\ln\zeta + \beta\zeta - (\ln\zeta_o + \beta\zeta_o)]x$$

$$\exp\ (-\frac{\zeta^\alpha}{\alpha^2\sigma})\ d\zeta$$

$$= \frac{u_*}{Lk} \frac{\alpha}{\Gamma(\frac{1}{\alpha})(\alpha^2\sigma)^{(\frac{1}{\alpha})}} [\int_0^\infty \ln\zeta\ e^{\frac{\zeta^\alpha}{\alpha^2\sigma}}\ d\zeta + \beta \int_0^\infty \zeta\ e^{-\frac{\zeta^\alpha}{\alpha^2\sigma}}\ d\zeta -$$

$$(\ln\zeta_o + \beta\zeta_o) \int_0^\infty e^{-\frac{\zeta^\alpha}{\alpha^2\sigma}}\ d\zeta]$$

and with the transformations:

$$\frac{\zeta^\alpha}{\alpha^2\sigma} = t_1$$

$$\zeta = (\alpha^2\sigma)^{\frac{1}{\alpha}}\ t_1^{\frac{1}{\alpha}}$$

$$d\zeta = \frac{(\alpha^2\sigma)^{\frac{1}{\alpha}}}{\alpha}\ t_1^{(\frac{1}{\alpha}-1)}\ dt_1$$

the above equation becomes

$$\frac{d\xi}{dt} = \frac{u_*}{Lk} [\frac{1}{\alpha\ \Gamma(\frac{1}{\alpha})} \int_0^\infty \ln\ t_1\ e^{-t_1}\ t_1^{(\frac{1}{\alpha}-1)}\ dt_1 + \ln(\alpha^2\sigma)^{\frac{1}{\alpha}} +$$

$$+ \beta(\alpha^2\sigma)^{\frac{1}{\alpha}} \frac{\Gamma(\frac{2}{\alpha})}{\Gamma(\frac{1}{\alpha})} - (\ln \zeta_o + \beta \zeta_o)] \qquad (95)$$

The integral on the right hand side is a derivative of the Gamma function, as known as the digamma function. It may be evaluated as

$$\int_o^\infty \ln t_1 \; e^{-t_1} \; t_1^{(\frac{1}{\alpha}-1)} dt_1 = \Gamma(\tfrac{1}{\alpha}) \; \psi(\tfrac{1}{\alpha}) \qquad (96)$$

where $\psi(\frac{1}{\alpha})$ is Gauss' ψ-function:

$$\psi(\tfrac{1}{\alpha}) = - \gamma - \alpha + \sum_{n=1}^{\infty} \frac{1}{n(n\alpha+1)} \quad . \qquad (97)$$

Finally, equation 95 may now be written as

$$\frac{d\bar{\xi}}{dt} = \frac{u_*}{Lk} [\ln((\alpha^2\sigma)^{\frac{1}{\alpha}} \; e^{\frac{1}{\alpha}} \; \psi(\tfrac{1}{\alpha})) + \beta(\alpha^2\sigma)^{\frac{1}{\alpha}} \frac{\Gamma(\frac{2}{\alpha})}{\Gamma(\frac{1}{\alpha})} -- (\ln \zeta_o + \beta\zeta_o)] \qquad (98)$$

In order to evaluate, the first vertical moment $\frac{d\bar{\zeta}}{dt}$, equation 85 is multiplied by ζ and integrated as

$$\frac{\partial}{\partial t} \int_o^\infty \int_{-\infty}^\infty \zeta \; c_o \; d\xi \; d\zeta + \frac{u_*}{Lk} \int_o^\infty \zeta \; [\ln \frac{\zeta}{\zeta_o} + \beta(\zeta-\zeta_o)] \; (\int_{-\infty}^\infty \frac{\partial c_o}{\partial \xi} \; d\xi) d\zeta$$

$$= \int_o^\infty \zeta \; \frac{\partial}{\partial \zeta} [b' u_* L^{-1} \; \zeta^{-n} \; \frac{\partial}{\partial \zeta} \; (\int_{-\infty}^\infty c_o \; d\xi)] d\zeta \quad . \qquad (99)$$

Now,

$$\int_{-\infty}^{\infty} \frac{\partial c_o}{\partial \xi}\, d\xi = c_o \Big|_{-\infty}^{\infty} = 0$$

with this evaluation, integrating the right hand side by parts, the equation for $\bar{\zeta}$ is

$$\frac{d\bar{\zeta}}{dt} = \zeta [b' u_* L^{-1} \zeta^n \frac{\partial c_{oo}}{\partial \zeta}] \Big|_{-\infty}^{\infty} - \int_o^{\infty} b' u_* L^{-1} \zeta^n \frac{\partial c_{oo}}{\partial \zeta}\, d\zeta$$

the first term on right is zero by virtue of condition 3 in equations 88. By substituting c_{oo} from equation 90, the above equation reduces to

$$\frac{d\bar{\zeta}}{dt} = - b' u_* L^{-1} \int_o^{\infty} \zeta^{(2-\alpha)} \frac{\alpha}{\Gamma(\frac{1}{\alpha})(\alpha^2\sigma)^{(\frac{1}{\alpha})}} \exp[-\frac{\zeta^\alpha}{\alpha^2\sigma}](-\frac{\alpha\zeta^{(\alpha-1)}}{\alpha^2\sigma})\, d\zeta$$

$$= + \frac{b' u_* L^{-1} \alpha^2}{\Gamma(\frac{1}{\alpha})(\alpha^2\sigma)^{(\frac{1}{\alpha}+1)}} \int_o^{\infty} \zeta\, e^{-\frac{\zeta^\alpha}{\alpha^2\sigma}}\, d\zeta$$

or

$$\frac{d\bar{\zeta}}{dt} = b' u_* L^{-1} \alpha (\alpha^2\sigma)^{\frac{1}{\alpha}-1} \frac{\Gamma(\frac{2}{\alpha})}{\Gamma(\frac{1}{\alpha})} \qquad (100)$$

Expressing σ in terms of t (see equation 90)

$$\frac{d\bar{\zeta}}{dt} = \alpha^{(\frac{2}{\alpha}-1)} (b' u_* L^{-1})^{\frac{1}{\alpha}} \frac{\Gamma(\frac{2}{\alpha})}{\Gamma(\frac{1}{\alpha})} t^{\frac{1}{\alpha}-1} \qquad (101)$$

Integrating equation 101 with respect to t and expressing $\bar{\zeta}$ in terms of σ a final solution is found:

$$\bar{\zeta} = \frac{\Gamma(\frac{2}{\alpha})}{\Gamma(\frac{1}{\alpha})} \quad (\sigma^2\alpha)^{\frac{1}{\alpha}} \tag{102}$$

or

$$(\alpha^2\sigma)^{\frac{1}{\alpha}} = \frac{\Gamma(\frac{1}{\alpha})}{\Gamma(\frac{2}{\alpha})} \quad \bar{\zeta} \quad .$$

Incorporating this value for $(\alpha^2\sigma)^{\frac{1}{\alpha}}$, the equations 98 and 100 now give,

$$\frac{d\bar{\xi}}{dt} = \frac{u_*}{\bar{L}k} \left[\ln \left(\frac{\Gamma(\frac{1}{\alpha})}{\Gamma(\frac{2}{\alpha})} \quad e^{\frac{1}{\alpha}\,\psi(\frac{1}{\alpha})} \quad \bar{\zeta}\right) + \beta\,\bar{\zeta} - (\ln\,\zeta_o + \beta\,\zeta_o)\right] \tag{103}$$

$$\frac{d\bar{\zeta}}{dt} = \frac{b'u_*}{L} \quad \alpha \quad \left[\frac{\Gamma(\frac{2}{\alpha})}{\Gamma(\frac{1}{\alpha})}\right]^{\frac{1}{\alpha}} \quad \bar{\zeta}^{(1-\alpha)} \tag{104}$$

These equations can be written in a more familiar form, with some rearrangement, as

$$\frac{d\bar{x}}{dt} = \frac{u_*}{k} \left[\ln \frac{c\bar{\zeta}}{\zeta_o} + \beta(\bar{\zeta}-\zeta_o)\right] \tag{105}$$

$$\frac{d\bar{z}}{dt} = bu_* \; \phi(\bar{\zeta}) \tag{106}$$

where

$$c = \frac{\Gamma(\frac{1}{\alpha})}{\Gamma(\frac{2}{\alpha})} \exp\left[\frac{1}{\alpha}\ \psi\ (\frac{1}{\alpha})\right]$$

$$b \simeq k\ \alpha\ \left[\frac{\Gamma(\frac{2}{\alpha})}{\Gamma(\frac{1}{\alpha})}\right]^{\frac{1}{\alpha}} \quad (\frac{K_H}{K_M}) \tag{107}$$

$$s(\zeta) = \frac{kz}{u_*}\ \frac{du}{dz} = s_1(\zeta)^{\alpha-1}$$

Equations 105 and 106 are in exactly the same form as those presented by Gifford (1962) with the exception of the constant c. In the application of these results different forms of $\phi(\zeta)$ have been used by different authors. Monin (1959) derived this function by turbulent energy balance as

$$\phi(\zeta) = (1-\alpha' Ri)^{1/4}$$

which is equivalent to $s(\zeta)$ given by equation 79. Assuming that α is equivalent to $1/R_{i_{crit}}$ and using the relationship

$$\frac{R_i}{R_{i_{crit}}} = \frac{1}{f'(\zeta)}$$

he found

$$\phi(\zeta) = \left[1 - \frac{1}{f'(\zeta)}\right]^{1/4} \tag{108}$$

Gifford (1962) used the above form and substituted a log-linear law for $f(\zeta)$. Koehler (1967) used a log-linear law to evaluate $\phi(\zeta)$ as the reciprocal of $s(\zeta)$ i.e.,

$$\phi(\zeta) = \frac{1}{s(\zeta)} = \frac{1}{1+\beta\zeta} \tag{109}$$

Figure 40 shows $\phi(\zeta)$ as a function of ζ given by different formulas. As will be seen in chapter V, the form suggested by Monin (1959) fits the wind tunnel data very well. Equation 105 and 106 degenerate into the set of original postulates by Batchelor for neutral flow as,

$$\frac{d\bar{x}}{dt} = \frac{u_*}{k}\left[\ln \frac{c\bar{z}}{z_o}\right] \tag{110}$$

$$\frac{d\bar{z}}{dt} = bu_*$$

The values of the constants are,

$$c = e^{-\gamma} = 0.561$$
$$b = k = 0.41 \tag{111}$$

which were also obtained by Chatwin (1968).

A comparison of equations 105 and 106 with Gifford's (1962) extension of Lagrangian Similarity indicates the potential for the basic Eulerion diffusion equation 74 to describe the phenomenon. The latter not only produces the same form for the statistics as those derived from Lagrangian considerations but also enables the constants to be judged

and evaluated. The results of this analysis explain and answer the many serious objections raised by Pasquill (1966) against the Lagrangian similarity. His main objection is that it is inadequate to regard $d\bar{z}/dt$ as uniquely determined by diffusive conditions at the given height. It is now clear that the assertion, that $d\bar{z}/dt$ depends only upon the intensity of turbulent transfer at that height alone, is not analogous to saying that K_z is a linear function of height. The form of K_z used in this analysis is not linear and yet $d\bar{z}/dt$ depends upon $\bar{z}$ with, of course, some weighting factor. Pasquill's condition on dK_z/dz viz; it should decrease with height in stable flow regime is also satisfied in this analysis.

4.3.1 Determination of constants b and c

The constants b and c as given by equations 107 can be determined knowing α the exponent in the power function type of expression for $s(\zeta)$, and K_H/K_M. From the wind tunnel data, Arya (1968) found

$$\alpha = 1.3$$

and

$$\frac{K_H}{K_M} \simeq 0.7$$

the function ψ is tabulated in the hand book of Mathematical functions by Abramowitz and Stegan. The value of $\psi(1.3)$ is obtained using the recurrence relation

$$\psi\left(\frac{1}{\alpha}\right) = \psi\left(1+\frac{1}{\alpha}\right) - \alpha \quad .$$

With this evaluation b and c are

$$c = \frac{\Gamma(\frac{1}{1.3})}{\Gamma(\frac{2}{1.3})} \exp\left[\frac{1}{1.3}\,\psi(\frac{1}{1.3})\right] = 0.608$$

$$b = (0.4)(1.3)\left[\frac{\Gamma(\frac{2}{1.3})}{\Gamma(\frac{1}{1.3})}\right]^{\frac{1}{1.3}}(0.7) = 0.28 \qquad (112)$$

These values of b and c may be compared to those in equations 111. The value of b is smaller in stable flow than that in neutral flow. The two values differ to the same extent that K_H/K_M differs from unity. It is so because the factor $\alpha\left[\frac{\Gamma(\frac{2}{\alpha})}{\Gamma(\frac{1}{\alpha})}\right]^{\frac{1}{\alpha}}$ is fortuitously approximately equal to 1. Thus there is no justification in taking b equal to k, the Von-Karman's constant, in the non adiabatic case.

4.4 Locus of the Centre of Mass of the Plume

The relation between $\bar{\xi}$ and $\bar{\zeta}$ is now obtained by dividing equation 105 by equation 106 as

$$\frac{d\bar{\xi}}{d\bar{\zeta}} = \frac{1}{bk}\left[\ln\frac{c\bar{\zeta}}{\zeta_o} + \beta(\bar{\zeta}-\zeta_o)\right]\frac{1}{\phi(\bar{\zeta})} \qquad (113)$$

Equation 113 can be integrated numerically using different specifications for $\phi(\bar{\zeta})$. Figure 111 compares the solutions obtained with different $\phi(\bar{\zeta})$ for the values of ζ_o. Also plotted is Gifford's (1962) solution with c = 1. The

difference caused by this constant is appreciable for small $\bar{\zeta}$. The functions giving small $\phi(\bar{\zeta})$ values produce slowly rising plumes.

4.5 Maximum Ground Level Concentration in Stable Flow

Batchelor's Lagrangian similarity arguments relating the concentration to the plume dimensions at the ground level due to continuous release from a point source at the ground, has been extended by Gifford (1962) and Cermak (1963) to include stability variation. Their developments show

$$\frac{u_* c_{max}}{kQ} \alpha \frac{1}{\bar{\zeta}^2 u(\bar{\zeta})} \tag{114}$$

This is true when the constant c is taken equal to one. However, if c is other than one, equation 114 will be modified. Batchelor (1964) introduced c intuitively to account for the fact that the average velocity of the cloud may not be exactly equal to fluid velocity at $\bar{\zeta}$ and regarded it to be "little less than unity." As already shown in this development for nonadiabatic flow and in that of Chatwin (1968) for neutral flows that c is not equal to one, a revision of the argument leading to equation 114 is necessary and is attempted below.

According to the similarity hypothesis of Batchelor (1964), the fluctuations $(x-\bar{x}, y, z-\bar{z})$ in the position of a marked fluid particle about the mean have statistical properties which depend only upon u_* and t and hence

their probability density F has the same shape at all times. Only the length scale of this function F increases in proportion to $\bar{z}$. As both F and $\bar{z}$ are functions of time, the probability of finding the contaminant in the neighborhood of (x,y,z) or its concentration at this point due to a continuous ground source of strength Q is

$$c(x,y,z) = \int_0^\infty \frac{Q}{\bar{z}^3} F\left(\frac{x-\bar{x}}{\bar{z}}, \frac{y}{\bar{z}}, \frac{z-\bar{z}}{\bar{z}}\right) dt \qquad (115)$$

If the variable of integration, t, is eliminated using equations 105 and 106, the concentration is given by

$$c(x,y,z) = \int_{-\infty}^{\infty} \frac{Q}{\bar{z}^2} \frac{F\left(\frac{x-\bar{x}}{\bar{z}}, \frac{l}{\bar{z}}, \frac{z-\bar{z}}{\bar{z}}\right)}{\frac{bu_*}{s(\bar{\zeta})}\left[\frac{x-\bar{x}}{\bar{z}} + \frac{d\bar{x}}{d\bar{z}}\right]} d\left(\frac{x-\bar{x}}{\bar{z}}\right) \qquad (116)$$

The exact form of the function F is not known but an approximation as to its shape is possible for estimating axial ground concentration. As most of the contaminant is concentrated around $x = \bar{x}$, the function $F\left(\frac{x-\bar{x}}{\bar{z}},0,1\right)$ can be approximated by a Dirac Delta function $\delta\left(A \cdot \frac{x-\bar{x}}{\bar{z}}\right)$ where A is a constant to be determined by experiment. As x approaches $\bar{x}$, $\bar{z}$ can be considered approximately constant and hence its functions $s(\bar{\zeta})$ and $d\bar{x}/d\bar{z}$ are also constant. With these arguments, equation 116 reduces to

$$c(\bar{x},0,0) = c_{max} = \frac{Q}{\bar{z}^2 \frac{bu_*}{s(\zeta)}\frac{d\bar{x}}{d\bar{z}}} \int_{-\infty}^{\infty} \delta\left(A \cdot \frac{x-\bar{x}}{\bar{z}}\right) d\left(\frac{x-\bar{x}}{\bar{z}}\right)$$

or

$$c_{max} = \frac{Q}{A\, z^2 \frac{u_*}{k}\left[\ln \frac{c\bar{\zeta}}{\zeta_o} + \beta(\bar{\zeta}-\zeta_o)\right]} \tag{117}$$

The coefficient $1/A$ has been evaluated by Klug (1968) taking $c = 1$. It is found to be independent of $\bar{\zeta}$ and is instead a function of σ_v/u_*. This coefficient will not be appreciably different if c is given by equation 113 because its effect becomes negligible with increasing $\bar{x}$. The function

$$\frac{A\, c_{max}\, u_*\, L^2}{Qk} = \frac{1}{\bar{\zeta}^2\left[\ln \frac{c\bar{\zeta}}{\bar{\zeta}} + \beta(\bar{\zeta}-\zeta_o)\right]}$$

has been plotted as a function of $(bk\bar{\xi})$ in figure 42, for different $\phi(\zeta)$. With the same reasoning maximum ground level concentration from a line source at the ground would be given by

$$B\,\frac{c_{max\ line}\, u_*\, L}{Qk} = \frac{1}{\bar{\zeta}\left[\ln \frac{c\bar{\zeta}}{\zeta} + \beta(\bar{\zeta}-\zeta_o)\right]} \tag{118}$$

where B is a constant for the line source problem.

The maximum ground level concentration due to an elevated source cannot, however, be derived by the above method as simply. Although equation 113 can be solved for this case with a suitable boundary condition, the maximum concentrations (using this solution for $\bar{z}$) calculated from equation 117 are unrealistic near the elevated source. The ground level concentration near the elevated source does not rise but rather maintains itself before it starts to decrease to asymptotically approach the point source solution. The reason is that the approximation regarding the shape of the density function is not valid for an elevated source. In fact, no simple minded approximation seems possible.

Panofsky and Prasad (1965) have shown that the relation for c_{max} as derived is very much like the one obtained on the assumption of a Gaussian distribution. This suggests that the result in equation 117 might be extended to the case of an elevated point source if the effect of source height on ground concentration is assumed Gaussian

$$c_{max}(\text{elevated}) = c_{max}(\text{ground}) \quad \exp[-\frac{h^2}{2\sigma_z^2}] \qquad (119)$$

For $\alpha = 1.3$ (section 4.3.1)

$$\sigma_z^2 = 1.68\ \bar{z}^2$$

$$c_{max}(\xi,h) = \left(\frac{Qk}{Au_*L^2}\right) \frac{1}{\bar{\zeta}^2 \left[\ln \frac{c\bar{\zeta}}{\zeta_o} + \beta(\bar{\zeta}-\zeta_o)\right]} \exp\left[-H^2/3.36\zeta^2\right] \tag{120}$$

where $H = h/L$.

The concentration given by this equation will be used to compare the experimental data with theory.

Chapter V

EXPERIMENTAL RESULTS & DISCUSSION

The results of diffusion experiments performed in the stably stratified shear layer of the Army Meteorological Wind Tunnel and the procedures used in the analysis of data are presented in this chapter. The combination of test variables is discussed and the data are presented. Mean velocity and temperature profiles characterizing the turbulent flow field are presented and discussed. The diffusion data is compared with theory and the similarities to the atmosphere are noted. The mass transfer coefficient is compared with the momentum transfer coefficient measured by Arya (1968) at 78' section of the wind tunnel. A probable error analysis is included.

5.1 The Combination of Test Variables

The objectives of this study were: (a) to obtain concentration distributions downwind ground and elevated point sources in the stably stratified turbulent shear layer of the micrometeorological wind tunnel. (b) to analyze these distributions to obtain diffusivity information. (c) to compare the plume characteristics with the predictions of different theories and with the characteristics of diffusion in the atmosphere. With this end in view, a complete mapping of the plume concentrations, from various ground & elevated sources were obtained for several downwind cross-sections. Ground source releases were studied for three density stratifications, one neutral and two stable. Measurements on

elevated point sources, placed at 2 inches, 4 inches and 8 inches above the tunnel floor, were made for the same stable stratification as shown in summary Table II. The temperature of the floor and free stream were held constant at $40^{o}F$ and $120^{o}F$ respectively for all the stable conditions of flow. Free stream velocities of approximately 20 and 10 fps were used for ground source experiments and 10 fps for elevated point sources. The latter was preferred to ensure moderately stable conditions of flow and at the same time to reduce the spurious gravity flow circulations experienced at lower velocities in the wind tunnel. The test section and the thermal shear layer are illustrated in Figure 11. The sources were situated at 25 feet downwind from the leading edge of the cooled aluminum plate and 65 feet from the leading edge of the momentum boundary layer. The measurements of concentration, velocity and temperature were made in the last 15 feet of the wind tunnels 80 feet test section.

5.2 Characteristics of the Turbulent Flow Field

The Army micrometeorological wind tunnel has an advantage over any other facility in that its long test section provides a normally developed momentum boundary layer of a substantial thickness (see Cermak et al. (1966)). The boundary layer thickness grows rather slowly in the test length between stations 65 feet and 80 feet. Figure 12 shows the velocity profiles above the

floor at 70 feet and 78 feet stations. The variation in velocity is not appreciable such that a plane homogeneity of flow may be assumed. This practically fulfills one of the requirements for modeling of the atmospheric boundary layer.

Although the thermal boundary layer was not initiated at the same point as the momentum boundary layer, its rate of development is rather fast as shown by Plate and Lin (1966). The thermal boundary layer thickness reaches 35 percent of the local momentum boundary layer in the first 10 feet after a step change in floor temperature, and 50 per cent after the next 10 feet. The change in the thermal boundary layer thickness subsequently is smaller. It grows about 2 inches from the source position to the end of the test section. Figure 13 shows temperature profiles above the surface measured at 70 and 78 ft. stations. The temperature at station 78 is consistently greater and the difference a little more than that in velocity profiles. Both the velocity and temperature are growing in this region but the mean quantities do not change appreciably. Thus the assumption of homogeneity may be useful only in studying the mean concentration, etc. This assumption may however be misleading when considering velocity or temperature fluctuations or the turbulent fluxes in the test length of the wind tunnel. These fluctuations and fluxes may vary considerably within this region.

Arya (1968) has measured turbulent fluctuations of velocity, $\sqrt{u'^2}$ $\sqrt{v'^2}$ and $\sqrt{w'^2}$, turbulent momentum flux $\overline{u'w'}$ and the turbulent heat flux $\overline{w't'}$ at only the 78 feet station of the micrometeorological wind tunnel for three different velocities. His measurements relevant to this study are shown in figures 14 and 15. Arya noted that the simplifying assumptions, which are usually made in the surface layer of atmosphere viz, plane homogeneity and constant fluxes, are only partially true in these stably stratified shear layer studies. While plane homogeneity is approximately realized as noted above, the thickness of the layer in which the vertical fluxes are approximately constant is less than 2 inches. Experimental data on velocity profiles in the wind tunnel boundary layer, however, follows Monin-Obukhov's log-linear law $\beta = 10$ (based on assumption of constant fluxes) beyond the constant flux layer despite the large change in momentum flux. The stability parameter z/L has been found to correlate the data very well. The different flow parameters of the boundary layer are recorded in Table III.

Veenhuizen (1969) has investigated experimentally the secondary flow in the micrometeorological wind tunnel under neutrally stratified conditions at a station 40 feet downwind from the leading edge of the boundary layer. He finds that secondary flows are present in this wind tunnel but maximum secondary velocity measured is less than 2 percent of the free stream in all cases studied. Figure

16 presents the vertical distribution of the vertical secondary flow at 3 different lateral positions. Similar measurements under stable conditions of flow are, however, not available in the wind tunnel section used for the present study. It is difficult to evaluate the effect of thermal stratification on the secondary flow; however, it might be expected to decay somewhat. A numerical experiment performed for a diffusion plume over a flat boundary with and without secondary flows of the appropriate magnitude did not predict any large concentration excursions.

The above details of the flow field serve to caution that one should not treat the wind tunnel diffusion results as those of a true model of the atmospheric boundary layer in all respects. A comparison of diffusion characteristics with those of the atmosphere serves to check the effect of the dissimilarity noted above.

5.3 Results of Diffusion Experiments

Concentration distributions were measured at $x = 1, 2, 3, 5, 7, 9, 11, 13$ and $15'$ for sources as described in section 4.1 The ground source data is presented in tabular form for neutral and stable runs in Table III. All the ground source releases had the same source strength. A check on the accuracy of the data was performed by integrating the concentration profiles to calculate

$$Q = \int_0^\infty \int_{-\infty}^{\infty} u(z)\ c(x,y,z)\ dydz$$

for all the x positions. Figure 17 shows the Q values obtained in this manner and the value indicated in Table I based on the Kr-85 concentration at the source and the flow rates. The total amount of Krypton-85 passing at different axial positions as calculated numerically are within $\pm$ 9% of the value released at the source. As expected, the derivation gets bigger as one moves away from the source. Uncertainty analysis of concentration measurements by themselves will be presented in section 4.6.

5.3.1 Point source at ground level

In order to bring out the effect of stability the isoconcentration contours downwind of a point ground source under both stable and neutral conditions of flow (u_∞ = 10 fps) are plotted on the same graph for different axial positions as shown in Figures 18-26. At first glance one would observe that the outer contours for the 2 cases tend to match each other at most of the x positions and that the deviation increases as one moves inward the plume section. In other words the concentration profiles in stable conditions are peakier than those in neutral flow for the same free stream velocity. Also, the lateral spread is greater and the vertical spread is smaller than the respective spreads in neutral flow.

The variation of maximum concentration with axial distance downwind for ground sources under various stability conditions is shown in figure 27. It is customary to express this variation in terms of a power index in the

empirical formula

$$c_{max} \propto x^{-m} .$$

The value of this index m for the point source at ground level in the case of the neutral stability condition is 1.78, which compares well with the values of 1.76 to 1.8 usually associated with the atmospheric diffusion (Sutton 1957 and Cramer 1957). Effects of stability is reflected in the index value of 1.7 for the ground source under relatively mild stability conditions. The values of the index compare favorably with those previously suggested by Shih (1966) for equivalent longitudinal positions.

The vertical and lateral spreads of the plumes under various stability conditions are shown in figures 28, 29, and 30. Configurations of one-tenth and one-half concentrations at the centerline of the cloud are indicated on each of these figures. The upper part shows the vertical spread and the lower part of each figure shows the lateral spread. A comparison of vertical and lateral spreads for the same freestream velocity under neutral and stable conditions reveals that while the vertical spread is reduced by about 30 percent due to thermal stratification, the lateral spread registers only about 10 percent variation. The plumes generally open up much quicker laterally than vertically near the sources. The ratio of lateral to vertical spread near the source is more than 2 for all cases but levels off to a steady value away from the source.

This ratio is approximately 1.45 and 1.65 for the same free stream velocity under neutral and stable flow conditions respectively. In the case of slightly stable flow (u_∞ = 20 fps) the lateral spread is less and vertical spread is more than the moderately stable case (u_∞ = 10 fps). This makes the effects of stability variation reverse in the vertical and lateral directions. It is difficult to comprehend this phenomenon especially if an appeal is made to turbulence measurements under the stability conditions by Arya (1968). According to these measurements the lateral velocity fluctuations in the slightly stable case are more than three times as much as those under the moderately stable case and also the lateral intensity is greater than the vertical in both cases. One would thus expect the lateral spread to be more in the slightly stable case than that in moderately stable flow. Similar occurrence was also observed by Yamamoto and Shimanuki (1964) in their numerical solution for a point source under varying stability conditions. According to this solution the ratio of lateral to vertical spread decreases as one moves from extremely stable toward neutral conditions.

The vertical and lateral spreads of the plumes are also plotted on a logarithmic paper in terms of the one-half maximum concentration viz, σ and η in figures 31 and 32. The vertical growth of the plume under stable conditions follows the law

$$\sigma \propto x^{0.86} \tag{122}$$

Under neutral conditions this growth is faster and is approximately

$$\sigma \propto x \tag{123}$$

The lateral growth is faster in the case of moderate stability than the neutral ones for the same freestream velocity. The slightly stable case does not however fall between the aforementioned cases.

5.3.2 Elevated point source

The diffusion data from the elevated point source placed at 2, 4 and 8 inches above the boundary under the same stability conditions have been analysed to construct figures 33, 34 and 35 which show the plume spreads both vertically and laterally. Configurations of 10, 50 and 100 percent of the maximum core concentrations through the centerline of the plume are plotted on each of the figures. The core maximum remains aloft, and at the same elevation for emission from the 8 inch high source. The maximum falls slightly with downward distance in the case of the 4 inch high source. The vertical spread (upper limb) from the source at H = 2" is exactly like that from the ground source under similar conditions of stability. The vertical spread (upper limb) from the sources at H = 4" and H = 8" is, however, about 15 percent and 40 percent

higher respectively than that experienced by a ground source. Lateral spreads of the plumes from elevated sources show a peculiar property. As the elevation of the source increases from zero (ground level), the lateral spread decreases by about 15% at H = 2", recovers at H = 4" and increases from then on.

The most important information on diffusion downwind on elevated source is provided by the ground level concentration variation with distance. This concentration is plotted in figure 36 for source elevations of 0.2, 4 and 8 inches. It rises to a peak value at some distance downwind and then falls and tends to assume the ground source type of concentration variation asymptotically with distance. These branches of ground level concentration for different elevations have approximately similar shape and points to the possibility of a multiplying factor, an exponential function of H, which can be applied to ground source concentration to give that for an elevated source. Figure 37 shows the variation of maximum core concentration with axial distance for the source at three different elevations. Also plotted is the maximum concentration from the ground source under similar conditions of stability. The maximum core concentration varies slowly with distance for smaller source elevation but the rate of decrease increases with increasing source height and tends to the slope of the line for ground source. The same data is plotted in figure 38 to emphasis the effect of source elevation on the maximum

core concentration. This effect is shown to decay at large distances from the source. This plot also suggests that for $H/L > 0.5$, the maximum core concentration will become independent of the source height.

5.4 Comparison of Diffusion Data With Theory

The diffusion data presented in section 4.3 can be compared with the various theoretical results presented in chapter II and IV. For this purpose, three different solutions of the problem have been chosen. Both ground and elevated point source data will be used in the comparison.

5.4.1 Comparison with the Lagrangian similarity theory

The experimental data is in general agreement with the results of logrithmic similarity theory based on the function $\phi(\zeta)$ given by Monin (1959) using the constants as determined in chapter IV. The rate at which the plumes rise and the rate of attenuation of ground concentrations match with the predictions of the theory. Figure 43 shows average non-dimensional plume rise $\bar{z}/L$ plotted against the non-dimensional axial distance for the ground source under two different stable conditions of the flow. The data shows good agreement with the theoretical curves. The law of theoretical growth given by theory is

$$\bar{z} \alpha x^{0.82} \qquad (124)$$

which checks very well with that determined from the data equation 122. The attenuation of boundary concentrations, under two stable conditions of flow, from both ground and elevated sources is compared with predictions of similarity theory in figures 44 and 45. The data shows excellent agreement. The assumption of a Gaussian variation of boundary concentration for the case of elevated sources seems also reasonable. The agreement of data with results from this assumption improves for large h/L. The constant of proportionality A in the relations for concentrations was evaluated according to Klug's (1968) method. It correlates the data for the stable runs remarkably well. Under neutral conditions, while the law of decrease of concentration with distance for a ground source as given by similarity theory checks with experimental data (Figure 46), the constant of proportionality is not the same as given by Klugs method. The data fits the theoretical curve for A = 3.2 while that obtained by the above method is double as much. Such a conclusion was also reached by Kao and Cermak (1966) about the wind tunnel data under neutral conditions.

By integrating the point source data in the lateral direction, equivalent line source data was produced. This data is recorded in Table V. The ground concentration for the ground line source are also compared with predictions of similarity theory for the three stratifications in figure 47, 48 and 49. The agreement is good. The constant of

proportionality B is now near about 1. More line source data at other stratifications is required to evaluate B in the manner Klug treated point source data.

5.4.2 Comparison with Smith's solution

Effects of source elevation on the ground concentration is studied in comparison with Smith's (1957) solution of the point source problem assuming power law variation of velocity and diffusion coefficients. Figure 50 shows the data for plumes issued at 3 different heights in stable stratification of flow along with the theoretical curve given by Smith. Although the general form of variation is the same, the theory predicts a slower rise and a slower attenuation of ground concentration. This data also allows a comparison of the ground concentration computed from the reciprocal theorem given by Smith (1957). According to this theorem, if concentration distribution for a ground source is known, the axial ground concentration downwind of an elevated point source may be determined from it. Figure 51 and 52 show the axial ground concentrations downwind of sources at 2" and 4" elevations respectively, obtained from the ground source data by application of the reciprocal theorem of Smith compared with the values measured directly. The reciprocal theorem is based on the fact that the solutions of the diffusion equation for power law variation of velocity etc., are Green's functions. The comparison shows that this is only approximately true in the flow investigated.

5.4.3 Comparison with Yamamoto-Shimanuki solution

The solution of point source problem is fraught with difficulties due to the unknown lateral diffusivity. Efforts have been made either to avoid it as in similarity theory or to assume some form of variation for it and obtain solutions to the diffusion equation. The most up to date solution for all stabilities is that obtained numerically by Yamamoto and Shimanuki (1964). The details of this solution are given in chapter II. They have presented the solution $c(x/z_o\ ,\ y/\alpha^{1/2},\ z/z_o)$ for the different stability parameters $\zeta_o' = -\gamma z_o/L$ (where γ is the constant in Ellison's interpolation formula for s) in the form of isoconcentration lines, profiles of vertical and lateral spreads of smoke and curves of ground concentration variation with distance. The detailed data obtained in the present investigation offers a good opportunity to test the validity of the form of K_y. The two ground source runs for u_∞ = 10 fps under neutral and stable stratification of flow are most suited for this purpose. $\alpha\ (\zeta_o')$ was determined by Yamamoto and Shimanuki through comparison with Project Prairie Grass data. α appears as an adjustable factor in the ground concentration curves and thus can be determined from the wind tunnel data. Figures 53 and 54 show this comparison and the values of α are

$$\begin{aligned} &\alpha \text{ (neutral)} = 10 \text{ (as compared to 13 given by Y \& S)} \\ &\alpha\ (\zeta_o' = -.001) = 13 \text{ (as compared to 7.2 given by Y \& S)} \end{aligned} \qquad (125)$$

The two sets of α values do not compare very well since α obtained by Y & S is monotonously increasing from extremely stable case to extremely unstable. The values obtained however do lie in the same range. The Y & S solution can now be compared with the experimental distributions for various α values. Figures 55 to 58 compare isoconcentration lines measured and those given by Y & S for ground source under neutral and stable stratifications. The theoretical lines have been drawn for various α values; including those given above, in order to facilitate comparison and to clearly see which α value would give best fit. It is obvious that the solutions for the α values given by Y & S and those calculated above are far from the observed concentrations. The value of α required lies between 1 and 3 if one attempts to fit the vertical concentration at $y = 0$ or the general shape of the contours. In this way, however, the lateral spreads given by theory are less than those observed in the wind tunnel. Moreover, it is not the same value of α which matches the contours near the plume centerline and those away from the centerline. The theoretical solution shows better agreement with the data only at short distances from the source. All of this points to the conclusion that α is not merely a function of ζ_o' but also depends on the position relative to the source. In other words the K_y formulation

$$K_y \alpha z$$

is inadequate. Unfortunately no alternative functional relationship is analytically apparent. It is suggested that one could use the wind tunnel data in non-dimensional form as in figures 55-58 in field applications.

5.5 Mass Diffusivity

The diffusion equation is known to give realistic results concerning the diffusion process if the diffusion coefficient is known fairly accurately. The solution of the two dimensional problem under neutral conditions of stability has been shown to satisfactorily represent the experimental results. The success in this direction has been mainly due to the fact that the equivalence of mass diffusivity with that of momentum holds in neutral stability and has been substantially confirmed by measurement. The same, however, is not ture for the diffusivities under thermal stratification. Arya (1968) achieved an experimental break through in that he measured the vertical turbulent fluxes in the stably stratified shear layer at a section about 40 ft. downwind of a step change in the boundary temperature. He was thus able to relate the diffusivities of heat and momentum. It is tempting to proceed inductively to probe the variation of vertical mass diffusity in order to extend the above stated work. The results may only be partially significant since the diffusion data was distributed over a 15 ft length of the wind tunnel test section while the flux measurements by

Arya were made at the end of this length, in addition the various fluxes were probably not in equilibrium. An attempt is worthwhile however, since it may stimulate further investigations on the same lines.

A number of methods have been used to recover the vertical mass transfer coefficient from the two-dimensional diffusion equation

$$u(z)\ \frac{\partial c}{\partial x} = \frac{\partial}{\partial z}\ (K_z\ \frac{\partial c}{\partial z}) \tag{126}$$

For example, Al Saffar (1964) Ellison and Turner (1960) etc., integrated this equation and recovered K_z as

$$K_z = \frac{\frac{\partial}{\partial x}\int_o^z ucdz}{\left.\frac{\partial c}{\partial z}\right|_z} \tag{127}$$

by graphically determining the derviatives. Poreh (1961) assumed a form for the concentration distribution and integrated the diffusion equation to relate K_z to some functions which required evaluation from experimental data. The scatter of the data has forbidden evaluation of these functions. A method which can take care of irregularities of data is, therefore, required. Perdreauville and Goodson (1966) have presented a method for identification of unknown parameters in partial differential equations. This reduces the higher order derivatives to the function itself

which is represented by the data (concentrations in this case). The method is as follows:

Assume that the concentration $c(x,z)$ data extends to a height h and to an axial distance L from the source. Multiply both sides of the diffusion equation 126 by a weighting function F (whose properties will be determined such that the derivatives of concentration are eliminated) and integrate w.r.t. x and z over the region of data.

$$\int_0^L \int_0^h Fu \frac{\partial c}{\partial x} \, dz dx = \int_0^L \int_0^h F \frac{\partial}{\partial z} \left(K_z \frac{\partial c}{\partial z}\right) dz dx \qquad (128)$$

If F is continuous in the range $\begin{matrix} 0 \leq x \leq L \\ 0 \leq z \leq h \end{matrix}$, $Fu \frac{\partial c}{\partial x}$ will be continuous and the order of integration may be changed on the left hand side. Integrating, then, by parts

$$\int_0^h u(z) \left[FC \Big|_0^L - \int_0^L c \frac{\partial F}{\partial x} \, dx\right] dz = \int_0^L \left[FK_z \frac{\partial c}{\partial z} \Big|_0^h - \right.$$

$$\left. \int_0^h K_z \frac{\partial c}{\partial z} \frac{\partial F}{\partial z} \, dz\right] dx \qquad (129)$$

If $F(x = 0,L) = 0$

$F(z = 0,h) = 0$

the above equation becomes;

$$- \int_0^h u(z) \int_0^L c \frac{\partial F}{\partial x} \, dxdz = - \int_0^L \int_0^h (K_z \frac{\partial F}{\partial z}) \frac{\partial c}{\partial z} \, dzdx$$

Integrating right hand side by parts again, one gets

$$- \int_0^h u(z) \int_0^L c \frac{\partial F}{\partial x} \, dxdz = - \int_0^L [K_z \frac{\partial F}{\partial z} c \Big|_0^h -$$

$$\int_0^h c \frac{\partial}{\partial z} (K_z \frac{\partial F}{\partial z}) \, dz] \, dx$$

If $\frac{\partial F}{\partial z} \Big|_{z=0,h} = 0$ (130)

The derivatives of concentration are eliminated and the equation reduces to

$$- \int_0^h u(z) \int_0^L c \frac{\partial F}{\partial z} \, dxdz = \int_0^L \int_0^h c \frac{\partial}{\partial z} (K_z \frac{\partial F}{\partial z}) \, dzdx \qquad (131)$$

subject to conditions in equations 129 and 130. A function satisfying these conditions is

$$f(x,z) = \sin^2 az \cdot \sin bx \qquad (132)$$

where $a = \frac{N_a \pi}{h}$, $(N_a = 1,2,...)$

$$b = \frac{N_b \pi}{L} , \quad (N_b = 1,2,...)$$

Letting $K_z = c_1 z + c_2 z^2 + c_3 z^3$ and substituting $F(x,z)$ in equation 131 one obtains,

$$c_1 \int_0^L \sin bx \left[\int_0^h \{(2a^2 \cos 2az)\ Z + (a \sin^2 az)\}\ c(x,z)dz\right]dx$$

$$+c_2 \int_0^L \sin bx \left[\int_0^h \{2a^2 \cos 2az)\ z^2 + (a \sin^2 az)2z\}c(x,z)dz\right]dx$$

$$+c_3 \int_0^L \sin bx \left[\int_0^h \{2a^2 \cos 2az)\ z^3 + (a \sin^2 az)3z^2\}c(x,z)dz\right]dx$$

$$= - \int_0^L \sin 2az\ u(z) \left[\int_0^h (b \cos bx)\ c\ (x,z)\ dx\right]\ dz \qquad (133)$$

Numerical integration in equation 133 yields a linear algebraic equation in c_1, c_2 and c_3. The numerical values of the integrals depend on the values assigned to a and b. If the integrals are denoted by I_1, I_2, I_3 and I_4 respectively equation 133 can be rewritten as

$$c_1 I_1(a,b) + c_2 I_2(a,b) + c_3 I_3(a,b) + I_4(a,b) = 0 \qquad (134)$$

At least three equations in three unknowns c_1, c_2 and c_3 would be necessary. However, a and b are assigned say, 3 and 4 values respectively giving 12 equations in c_1, c_2 and c_3. The method of least squares is used to reduce the number of equations to number of unknowns (3).

A computer program has been developed (see Appendix C) to solve equation 133 numerically. In order to improve the integrations and weighting in x direction additional points were generated. The evaluation of integrals was improved by fitting polynomials through the data. The

program was tested using data generated by Bosanquet and Pearson (1936) formula

$$c(x,z) = Q/K_1 x \cdot e^{-\frac{\bar{u}z}{K_1 x}} \qquad (135)$$

for linear variation of K_z as

$$K_z = K_1 z$$

the value of K_1 was recovered within 1% by use of this program.

The equivalent line source data for the point source at ground level under stable and neutral conditions of flow at same u_∞ has been used to evaluate the vertical diffusion coefficient. Figure 59 shows the mass diffusivity results for these two conditions of flow. The diffusivity for the neutral case rises twice as fast as that for the stable case. They reach a maximum around $z = 0.2$ ft and then start falling. The maximum occurs a little too early as compared to the boundary layer thickness. The explanation may be sought in the fact the diffusion near the source does not extend to the region of integration and the zero concentrations tend to produce $K_z = 0$ above the upper limit of the data. Hence if an averaged K_z variation over the diffusion field is computed it would incorporate the zero values and tend to cause the maximum to occur early. Figure 60 shows the mass diffusivity under neutral conditions in comparison with diffusivity of momentum

$K_M = ku_*z$ based on constancy of shear stress and that measured by Klebanoff. The computed K_z compares well with $K_M = ku_*z$ up to about 1" from the surface. It lends support to the generally made assumption of equivalence of the momentum and mass diffusivity within the surface layer (constant flux region) which extends up to only $zu_*/\nu =$ 200 according to Tieleman's (1967) measurements made in the wind tunnel which corresponds to 1". K_z tends to agree with the Klebanoff's measurement over a larger height increasing the region of K_z and K_M equivalence. Not much trust can be placed in K_z variation away from the wall for the reasons explained above. Figure 61 shows the mass diffusivity results for the stable case and the momentum diffusivity measured by Arya (1968). At first sight, the agreement looks very poor since K_z would be expected to be, at least, equal to K_M or less than it. A deeper examination, however, clarifies the situation. Measurements of K_M by Arya (1968) under stable stratification were made at 78 ft station while the diffusion coefficient K_z is computed from concentration measurements extending from the downwind 65 ft station. As discussed in section 4.2, although a plane homogeneity of flow may be approximately in order according to mean velocity and temperature fluctuations, momentum flux may still be adjusting itself at the 65 ft station from a neutral flow variation at the 40 ft station to the variation obtained by Arya at the 75 ft station. The computed diffusion coefficient is not drastically

different from K_M in Figure 61 and is of the same order. If the measurement of K_M were available around 65 ft station, a statement about K_z/K_M could be made.

5.6 Uncertainty Analysis

Efforts were made to eliminate the systematic errors by frequent calibrations and checks on the instruments and techniques. Experimental errors are analyzed here with regard to all the basic measurements made in this study. Errors in mean velocity measurement due to turbulence effects were corrected according to Goldstein's formula

$$U_{true} = U_m \left(1 - \frac{\overline{u^2}}{U}\right) \qquad (136)$$

where U_m is the measured velocity. Time lag errors during recording were eliminated by retraversing the carriage vertically. Probable error in velocity measurement due to positioning of the pitot static tube, reading the pressure head, etc., is estimated to be $\pm$2%. Probable error in temperature measurement is estimated also to be within $\pm$2%. Probable errors in sampling probe placement viz, x, y and z are within $\pm$2%, 1% and 1% respectively. Concentration are subject to random errors due to radiactive decay. Number of counts n observed in a given time obeys a poisson distribution which approaches a Gaussian distribution if n becomes large. The standard deviation for a single measured value (counts) in a set may be calculated quite simply as

$$\sigma_N = \sqrt{N} \quad . \tag{137}$$

For experimental error, small deviations are more probable than large ones, hence only one reading is usually made which is assumed to be near enough to the true N to be adequate for evaluation of standard deviation. Probable error for Gaussian distribution is about 67% of the standard deviation. The standard deviation of count rate is

$$\sigma_R = \frac{\sqrt{N}}{t} \tag{138}$$

where t is the counting time. If the background is present, the standard deviation of net count rate is

$$\sigma_R = \sqrt{\frac{N_s}{t_s^2} + \frac{N_B}{t_B^2}} \tag{139}$$

where N_s and N_B are number of sample and background counts and t_s and t_B the counting times. In the present analysis, an effort was made to keep the probable errors in concentration measurements less than 6%. For this reason the simple counting time and background counting time were constantly manipulated with this end in view. The propagation of errors of sampling probe placement into the concentration can be investigated according to the second power equation

$$\Delta c = \sqrt{\left(\frac{\partial c}{\partial x}\,\Delta x\right)^2 + \left(\frac{\partial c}{\partial z}\,\Delta z\right)^2 + \left(\frac{\partial c}{\partial y}\,\Delta y\right)^2} \tag{140}$$

The concentration gradients are strongest at $x = 1'$ in a given set of data. Moreover the vertical concentration gradients is greater than the lateral ones, the typical propagation of error is, therefore, studied at $z = 1/4"$ at the plume center line. From plotted data

$$\frac{\partial c}{\partial z} = 517{,}00 \quad \mu\mu ci/cc/ft$$

$$\frac{\partial c}{\partial x} = 55{,}00 \quad \mu\mu ci/cc/ft$$

$$\Delta x = .0025 \text{ ft}$$

$$\Delta z = .0002 \text{ ft}$$

$$\Delta c = \sqrt{(517{,}000 \times .0002)^2 + (55{,}000 \times .0025)^2}$$

$$= \pm 172 \quad \mu\mu ci/cc$$

$$\text{probable error} = \frac{172}{16{,}500} \times 100 \simeq 1\%$$

Thus the propagation of positioning error into the concentration data is about 1% near the source and should be expected to fall off rapidly at large distances.

The determination of propagation of error into the mass diffusivity is not as direct as has been done above. The program was however, checked against data generated from a known distribution and error was about 1%. The probable error in K_z values up to $z = 1\ 1/2"$ due to errors in concentration, velocity etc., may be about 5%.

Chapter VI

CONCLUSIONS

The theoretical analysis and the experimental results discussed earlier lead to the following significant conclusions:

(1) The Lagrangian statistics of a cloud of passive substance diffusing in diabatic atmosphere can be obtained from the Eulerian description of diffusion. Assuming a log-linear law velocity profile and a power law variation of vertical mass diffusivity, the diffusion equation may be solved to obtain,

$$\frac{d\bar{z}}{dt} = bu_* \phi\left(\frac{\bar{z}}{L}\right)$$

$$\frac{d\bar{x}}{dt} = \frac{u_*}{k}\left[\ln c\,\frac{\bar{z}}{z_o} + \frac{\beta}{L}(\bar{z}-z_o)\right]$$

which are known as a consequence of extended Lagrangian similarity hypothesis of Batchelor.

(2) The diffusion equation not only yields the same form for the statistics as those derived from Lagrangian consideration but also enables the unknown constants to be determined. The constants b and c under stable conditions of flow, are

$$b = 0.28$$

$$c = 0.608$$

It is shown that b should incorporate the stratification effect in form of the ratio K_H/K_M.

(3) The effect of stratification on $d\bar{z}/dt$ is shown to be a function of $\bar{z}/L$ alone even though the assumed vertical mass diffusivity was not a linear function of height. This serves to clarify some of the questions raised by Pasquill (1966) in regard to the effect of stratification.

(4) The diffusion characteristics obtained from experiments in the wind tunnel shear layer under various stability conditions agree well with those observed in the atmosphere. This agreement is excellent in the case of ground level concentrations. The index m describing a power law variation of this concentration with distance matches with the reliable field estimates. The length scales L and z_o correlate the data well and may be used as a means of transferring the wind tunnel data to the field.

(5) The data fits the similarity theory predictions very well. It appears that the parameters evaluated in the field by Klug (1968) hold also for the wind tunnel data in stable flow. The wind tunnel data supports the assumption of a Gaussian variation of ground level concentration with distance due to an elevated point source.

(6) Detailed diffusion patterns obtained from wind tunnel experiments may be preferrable over the numerical solutions for the three dimensional problem which require arbitrary specification of lateral diffusivity.

REFERENCES

Al-saffar, A. M. (1964), "Eddy diffusion and mass transfer in open channel flow." Ph.D. Dissertation, Civil Engineering Department, University of California, Berkley, California.

Arya, S. P. S. (1968), "Structure of stably stratified boundary layer." Ph.D. Dissertation, College of Engineering, Colorado State University, Fort Collins, Colorado.

Aris, R. (1956) "On dispersion of a solute in a fluid flowing through a tube." Proceedings Royal Society, vol. A 235, pp. 67-77.

Barad, M. L., and Haugen, D. A. (1959), "A preliminary analysis of Sutton's hypothesis for diffusion from a continuous point source," Journal of Meteorology, vol. 16, pp. 12-21.

Batchelor, G. K. (1959), "Note on diffusion from sources in a turbulent boundary layer." Unpublished.

Batchelor, G. K. (1964), "Diffusion from sources in a turbulent boundary layer."" Arch. Mech. Stosowanej, vol. 3, pp. 661-670

Bosanquet, C. H., and Pearson, J. L. (1936), "The spread of smoke and gases from chimneys." Trans. Faraday Society, vol. 32, pp. 1249-1264.

Calder, K. L. (1949), "Eddy diffusion and evaporation in flow over aerodynamically smooth and rough surfaces." Quarterly Journal of Mechanics and Applied Mathematics, vol. 2, pp. 153-176.

Calder, K. L. (1965), "On equation of atmospheric diffusion". Quarterly Journal of Royal Meteorological Society, vol. 91, pp. 514-517.

Cermak, J. E. (1963), "Lagrangian Similarity hypothesis applied to diffusion in turbulent shear flow." Journal of Fluid Mechanics, vol. 15, part 1, pp. 49-64.

Cermak, J. E., Sandborn, V. A., Plate, E. J., Binder, G. J., Chuang, H., Meroney, R. N., and Ito, S., (1966), "Simulation of atmospheric motion by wind tunnel flows." CER66-JEC-VAS-EJP-GJB-HC-RNM-SI17, College of Engineering, Colorado State University, Fort Collins, Colorado.

REFERENCES - Continued

Chandra, S. (1967), "Diffusion from an instantaneous point source into a turbulent boundary layer." Ph.D dissertation, College of Engineering, Colorado State University, Fort Collins, Colorado.

Chatwin, P. C. (1968), "The dispersion of a puff of passive contaminant in the constant stress region." Quarterly Journal of Royal Meteorological Society, vol. 94, pp. 401-411.

Cramer, H. E. (1957), "A practical method for estimating the dispersal of atmospheric contaminants." Proceeding of First National Conference on Applied Meteorology, pp. c33-c35.

Csanady, G. T. (1964), "Turbulent diffusion in a stratified fluid." Journal of Atmospheric Sciences, vol. 21, pp. 439-447.

Davar, K. S. (1961), "Diffusion from a point source within a turbulent boundary layer." Ph.D. Dissertation, College of Engineering, Colorado State University, Fort Collins, Colorado.

Davies, D. R. (1950a), "Three dimensional turbulence and evaporation in lower atmosphere I." Quarterly Journal of Mechanics and Applied Mathematics, Vol. 3, pp. 51-63.

Davies, D. R. (1950b), "Three dimensional turbulence and evaporation in lower atmosphere II." Quarterly Journal of Mechanics and Applied Mathematics, vol. 3, pp. 64-73.

Davies, D. R. (1952), "On diffusion from a continuous point source at ground level into a turbulent atmosphere." Quarterly Journal of Mechanics and Applied Mathematics, vol. 5, pp. 168-178.

Deacon, E. L. (1949), "Vertical diffusion in lower layers of atmosphere." Quarterly Journal of Royal Meteorological Society, vol. 75, pp. 89-103.

Ellison, T. H. (1957), "Turbulent transport of heat and momentum from an infinite rough plane." Journal of Fluid Mechanics, Vol. 2, pp. 456-466.

Ellison, T. H. (1959), "Turbulent diffusion," Scientific Progress, vol. 47, pp. 495-506.

REFERENCES - Continued

Ellison, T. H., and Turner, J. S. (1960), "Mixing of dense fluid in a turbulent pipe flow." Journal of Fluid Mechanics, vol. 8, part 4, 529-544.

Fischer, H. B. (1964), "Longitudinal dispersion by velocity gradients in open channel flow". Technical memo 64-4, W. M. Keck Laboratory, California Institute of Technology.

Frankiel, F. N. (1953) "Turbulent diffusion," Advances in Applied Mechanics, vol. 3, pp. 61-107.

Frost, R. (1946), "Turbulence and diffusion in lower atmosphere." Proceedings Royal Society, Series A, vol. 186, pp. 20-35.

Gifford, F. A. (1962), "Diffusion in a diabatic surface layer," Journal of Geophysical Research, vol. 67, pp. 3207-3212.

Haugen, D. A., Barad, M. L., and Antanaitis, P. (1961), "Values of parameters appearing in Sutton's diffusion models," Journal of Meteorology, vol. 18, pp. 368-372.

Holzman, B. (1943), "Influence of stability on evaporation." Annals New York Academy of Sciences, vol. 44, p. 13

Jordanov, D. L. (1966), "On diffusion from a point source in the atmospheric surface layer." Izv. Atmospheric and Oceanic Physics, vol. 2, pp. 576-584.

Kao, S. K., and Cermak, J. E. (1966), "Turbulent diffusion in the neutral surface layer" Unpublished, Fluid Dynamics and Diffusion Laboratory, Colorado State University, Fort Collins, Colorado

Kesic, D. (1967), "Diffusion of heat from an instantaneous point source in a turbulent boundary layer," M.S. Thesis, College of Engineering, Colorado State University, Fort Collins, Colorado.

Klug, W. (1968), "Diffusion in atmospheric surface layer: comparison of similarity theory with observations," Quarterly Journal of Royal Meteorological Society, vol. 94, pp. 555-562.

Koehler, S. (1967), "Turbulent diffusion in a stably stratified boundary layer." Ph.D. Dissertation, College of Engineering, Colorado State University, Fort Collins, Colorado.

REFERENCES - Continued

Laikhtman, D. L. (1961), "Physics of the atmospheric boundary layer," Israel Program for Scientific Translations, Israel.

Malhotra, R. C. (1962), "Diffusion from a point source in a turbulent boundary layer with unstable stratification." Ph.D. Dissertation, College of Engineering, Colorado State University, Fort Collins, Colorado.

Malhotra, R. C., and Cermak, J. E. (1963), "Wind tunnel modelling of atmospheric diffusion," J. Geophysical Research, vol 68, pp. 2181-2184.

Monin, A. S. (1959a), "Smoke propagation in surface layer of atmosphere," Advances in Geophysics, vol. 6, pp. 331-343.

Monin, A. S. (1959b), "Survey of atmospheric diffusion," Advances in Geophysics, vol. 6, pp. 29-40.

Monin, A. S., and Obukhov, A. M. (1954), "Basic relationships for turbulent mixing in the atmospheric ground layer," Transactions Geophysics Institute, Academy of Sciences, U. S. S. R., vol. 24, pp. 225-259.

Monin, A. S., and Yaglom, A. M. (1965), "Statistical Hydromechanics," Nauka Press, Moscow (English Translation by Joint Publications Research Service, U. S. Department of Commerce).

Panofsky, H. A. (1968), "A survey of current thought on wind properties relevant for diffusion in the lowest 100 M." Symposium on Atmospheric Turbulence and Diffusion in the Planetary Boundary Layer, Albuquerque N. M. , Dec. 1967.

Panofsky, H. A., and Prasad, B. (1965), "Similarity theories and diffusion," International Journal of Air and Water Pollution, vol. 9, pp. 419-430.

Pasquill, F. (1949), "Eddy diffusion of water vapor and heat near ground," Proceedings Royal Society of London, Series A, vol. 198, p. 116

Pasquill, F. (1966), "Lagrangia similarity and vertical diffusion from a source at ground level," Quarterly Journal of Royal Meteorological Society, vol. 92, pp. 185-195.

Perdreauville, F. J., and Goodson, R. E. (1966), "Identification of systems described by partial differential equations," Transactions American Society of Mechanical Engineers, Journal of Basic Engineering, pp. 463-468.

REFERENCES - Continued

Plate, E. J., and Zin, C. W. (1966), "Investigations of the thermally stratified boundary layer," Fluid Mechanics Paper No. 5, Fluid Dynamics and Diffusion Laboratory, Colorado State University, Fort Collins, Colorado.

Poreh, M. (1961), "Diffusion from a line source in a turbulent boundary layer," Ph.D. Dissertation, College of Engineering, Colorado State University, Fort Collins, Colorado.

Quraishi, A. A. (1963), "Diffusion in a turbulent boundary layer," Ph.D. Dissertation, College of Engineering, Colorado State University, Fort Collins, Colorado.

Rider, N. E. (1954), "Eddy diffusion of momentum, water vapor and heat near the ground," Philosophical Transactions, Royal Society, vol. A246, p. 481.

Roberts, O. F. T. (1923), "The theoretical scattering of smoke in a turbulent atmosphere," Proceedings Royal Society of London, Series A, vol. 104, pp. 640-654.

Rossby, C. G., and Montgomery, R. B. (1935), "The layer of frictional influence in wind and ocean currents," Papers in Physical Oceanography, vol. 3, p. 17.

Rounds, W. (1955), "Solutions of the two-dimensional diffusion equations," Transactions American Geophysical Union, vol. 36, pp. 395-405.

Saffman, P. G. (1962), "The effect of wind shear on horizontal spread from an instantaneous ground source," Quarterly Journal of Royal Meteorological Society, vol. 88, pp. 382-393.

Sayre, W. M. (1967), "Dispersion of mass in open channel flow," Ph.D. dissertation, College of Engineering, Colorado State University, Fort Collins, Colorado.

Schmidt, W. (1925), "Der Massenaustansel in freier luft and verwandte erscheinungen," Probleme der Kosmischen physik, Hamberg, vol. 7.

Shih, C., (1966), "Continuous point source diffusion in a turbulent shear layer," M. S. Dissertation, College of Engineering, Colorado State University, Fort Collins, Colorado.

Smith, F. B. (1957), "The diffusion of smoke from a continuous elevated point source into a turbulent atmosphere," Journal of Fluid Mechanics, vol. 2, pp. 49-76.

REFERENCES - Continued

Sutton, O. G. (1932), "A theory of eddy diffusion in the atmosphere," Proceedings Royal Society, Series A, vol. 135, pp. 143-165.

Sutton, O. G. (1934), "Wind structure and evaporation in a turbulent atmosphere," Proceedings Royal Society, Series A, Vol. 146, pp. 701-722.

Sutton, O. G. (1936), "The logrithmic law of wind structure near the ground." Quarterly Journal of Royal Meteorological Society, vol. 62, pp. 124-126.

Sutton, O. G. (1937), "The logrithmic law of wind structure near the ground," Quarterly Journal of Royal Meteorological Society, vol. 63, pp. 105-107.

Sutton, O. G. (1947), "The problem of diffusion in lower atmosphere," Quarterly Journal of Royal Meteorological Society, vol. 73, pp. 257-274.

Sutton, O. G. (1953), "Micrometeorology," McGraw-Hill Book Co., New York.

Taylor, G. I. (1921), "Diffusion by continuous movements," Proceeding London Mathematical Society, Series 2, vol. 20, pp. 196-202

Taylor, G. I. (1954a), "The dispersion of matter in turbulence flow through a pipe," Proceedings Royal Society, Series A, Vol. 223, pp. 446-468.

Taylor, G. I. (1954b), "Conditions under which dispersion of a solute in a stream of solvent can be used to measure molecular diffusion,"" Proceedings Royal Society, Series A, vol. 225, pp. 473-477.

Tyldesley, J. B., and Wellington, C. E. (1965), "The effect of wind shear and vertical diffusion on horizontal dispersion," Quarterly Journal of Royal Meteorological Society, Vol. 91, pp. 158-174.

Veenhuizen, S. (1969), "Secondary flow in a boundary layer," M.S. Thesis, College of Engineering, Colorado State University, Fort Collins, Colorado.

Yano, M. (1966), "The turbulent diffusion in a simulated vegetative cover," Ph.D. Dissertation, College of Engineering, Colorado State University, Fort Collins, Colorado.

REFERENCES - Continued

Yamamoto, G. and Shimanuki, A., (1960), "Numerical solution of the equation of the atmospheric diffusion," Scientific Report, Tohoku University, Series 5, vol. 14, pp. 24-35.

Yamamoto, G. and Shimanuki, A. (1964), "The determination of lateral diffusivity in diabatic conditions near the ground from diffusion experiments," Journal of Atmospheric Sciences, vol. 11, pp. 187-196.

Yotsukura, N., and Fiering, M. B. (1964) "Numerical solution to a dispersion equation," Proceedings American Society of Civil Engineers, vol. 90, pp. 83-104.

APPENDICES

Appendix A

EQUIPMENT SPECIFICATIONS

Manufacturers specifications of various commercial instruments and appliances used in this study are listed below.

Pressure Meter

Trans-Sonics Type 120 B Equibar Pressure Meter--Serial 44801--Differential Capacitance.

D. C. Output: 0-30 millivolts $\pm$ 2%, proportional to pressure.

Accuracy of meter reading: $\pm$ 3% full-scale of selected range.

Response time: 10 milliseconds to 63% of a step change in pressure at atmospheric pressure.

Range: 0.001 mm Hg. to 3 mm Hg. full-scale in 7 steps.

Scaler

Nuclear-Chicago Corp. Model 192A "ultrascaler"

Input sensitivity: variable from 1 to 800 mv. separate position provides 0.25 v input sensitivity for G.M. or Scintillation detectors

Range: Four direct reading decade unit with scale selection of 10, 40, 100 400 1,000, 4,000 and 10,000.

Register: A four digit register following the decades allows storage up to 10^8 counts.

Resolution time: Choice of one or five- microsecond resolution time of first decade, which is essentially resolution time of the scaler.

Timer: Odometer type, indicates elapsed time up to 999.99 minutes with accuracy of about .005 min.

Predetermined count and time: Preset time and count circuits can stop the scaler automatically for count values 100 to 10,000,000.

Amplifier: Useful frequency response extends beyond 2 megacycles, allowing high-speed counting.

High voltage supply: Continuously variable from 500 to 5,000.

Voltmeter

Hewlett-Packard 340A Digital Voltmeter and 3443A High Gain Auto Range Unit.

Sample rate: 5 samples per second to 1 per 5 seconds.

Range: 4-digit representation in four steps from 99.99 millivolts to 999.9 volts full scale.

Accuracy: $\pm$ 0.05% of reading $\pm$ 1 digit in volt range to $\pm$ 0.1% of reading $\pm$ 1 digit in millivolt range.

Input impedance: 10.2 M ohms.

G. M. Tube

Tracerlab Type 1106 Halogen Quenched thin metal wall Beta-Gamma counters.

Operating voltage: 900 volts.

Plateau Length: >200 v.

Plateau slope/100v: 8%

Dead time approximately: 100 μ seconds.

Background: 20 counts/min.

Wall Metal: Stainless steel.

Cathode wall thickness: 30 to 40 mg/cm^2

Cathode wall I. D.: 0.6 inch

Cathode wall length: 3.0 inches.

Flow Meters

Fischer and Porter Co., Model 10A103 multiple tube panel.

Metering tube: Glas, FP-1/8-14-G-6 3/4.

Range: 40 to 90 cc/min of air at s.t.p.

Scale: Graduated in cc/min of air

Accuracy: $\pm$ 2% of maximum scale reading.

Maximum temperature and pressure: 200°F and 200 psig.

Appendix B

Source Strength Q

The extent of dilution of Krypton-85 before release in the wind tunnel is determined from the assumed detectable levels of the gas near the plume boundaries at a position about 15 ft downwind from the source. Theoretically the G.M. tube can measure, on the average, about 2.5 μμcuries/cc equivalent one count per minute but the statistical error involved limits such an estimation. If the concentration at the edges of the plume is to be, say, 20 μμcuries/cc, then the maximum concentration at the ground may be 200 μμcuries/cc. To find the dilution involved in the 15 ft travel from the source, an approximate method like that of similarity theory by Ellison (1959) may be used.

Assume: $u_\infty = 10$ fps

$u_* = .4$ fps

$z_o = .00008$

then: $$\frac{x}{z_o} = \frac{15}{.00008} = 2 \times 10^5$$

Solving $$\frac{x}{z_o} = \frac{1}{kb}\left[\frac{z}{z_o}\left(\ln \frac{\bar{z}}{z_o} - 1\right)\right] \qquad (A)$$

$$\frac{\bar{z}}{z_o} = 4{,}800$$

then, $$\frac{C_{max}\ (15')}{Q} = A \frac{1}{\bar{z}^2 \frac{u_*}{k}\left(\ln \frac{\bar{z}}{z_o}\right)} \qquad (B)$$

The constant of proportionality may be estimated by comparing of equation (B) to that obtained from Gaussian plume model viz.,

$$\frac{C_{max}}{Q} \simeq \frac{1}{\pi \sigma_y \sigma_z \bar{u}}$$

Taking $\sigma_z \simeq \bar{z}$

$$\frac{\sigma_y}{\sigma_z} \simeq 1$$

$$\bar{u} \simeq \frac{u_*}{k}(\ln \frac{\bar{z}}{z_o}).$$

One obtains $A \simeq \frac{1}{\pi}$

$$\frac{C_{max}(15')}{Q} \simeq \frac{1}{\pi \bar{z}^2 \frac{u_*}{k}(\ln \frac{z}{z_o})}$$

$$\simeq .267 \frac{\text{sec}}{\text{ft}^3}$$

$$Q \simeq \frac{200}{.267} \times 28{,}300 \ \mu\mu\text{curies/sec}$$

$$\simeq 20 \ \mu\text{curies/sec}$$

Dilution of Kr-85

Source diameter ≈ 0.1"

Approximate local velocity ≈ 5 fps.

Average release rate = $5 \times \frac{\pi}{4} (0.1)^2 (\frac{1}{12})^2 \times 28{,}300 \times 60$ cc/min.

≈ 500 cc/min

Concentration of Kr-85 at the source ≈ $\frac{20\ \mu\text{curies/sec}}{500\ \text{cc/min}}$

≈ 2.4 μcuries/cc

Concentration of Kr-85 supplied = 67 mcuries/cc

The gas is therefore, required to be diluted about 30,000 times before use. The dilution of the gas supplied for this investigation was done keeping the above estimates in view. Compressed air was used for the dilution.

Calibration of diluted gas

Volume of the planchet = 8.15 cc

Activity of the standard = 8 μcuries

Average count rate for the standard = 9,670 cpm

Corrected count rate for the standard = 9,850 cpm
(Dead time correction)

Corrected sample count rate = 18,350 cpm

Concentration of sample = $\frac{8\ \mu\text{curies} \times 18{,}350\ \text{cpm}}{9{,}850\ \text{cpm} \times 8.15\ \text{cc}}$

= 1.76 μcuries/cc

This concentration is nearly the same as approximated above.

Sampling rate and sampling time

Sampling tube diameter = 1/16"

Sampling rate in free stream = $10 \times 60 \times [\frac{\pi}{4} \times (\frac{1}{16})^2 \times (\frac{1}{12})^2 \times 28{,}3000$ cc/min

$\simeq$ 360 cc/min.

An average sampling rate of 250 cc/min was used throughout this investigation.

A test was made to determine the minimum sampling time. For the same sampling rate, count rate was recorded using different sampling intervals. This count rate first increased with increase in the sampling interval but leveled off at about 2.5 minutes interval. Three minutes sampling interval was, therefore, used throughout in order to obtain consistent results.

Background concentration

Average release rate = 500 cc/min

Period of release $\simeq$ 3 min

Volume of recirculating system $\simeq$ 60,000 cu. ft.

Background concentration after one run

$$\simeq \frac{500 \times 1.76 \times 3}{60{,}000 \times (30.48)^3} = 1.5 \times 10^6 \ \mu\text{curies/cc}$$

This concentration is much lower than the maximum permissible concentration (M.P.C.) of Kr-85 and thus posed no hazard.

Appendix C

```
      PROGRAM COEFFT                                                  06/16/69
      DIMENSION C(8,60),U(60),X(80),Z(80),FSINT(80),COFINT(5),PRODZ(80),
     1AZ(10),AX(10),A(40,4),AC(10,10),BC(3),AI(10,10),AK(3),XV(80),PRODX
     2V(80),CC(80,80),DATA(10)
      DIMENSION CK1(20),CK2(20),CK3(20),CKZ(20)
C     FOR FIRST THREE INTEGRALS ESTABLISH A STATEMENT FUNCTION
      WT(Y,AA,N)=2.*(AA**2)*COS(2.*AA*Y)*(Y**N)+AA*N*SIN(2.*AA*Y)*(Y**(N
     1-1))
C     READ PARAMETERS
      READ (5,1) NZMAX,NXMAX,NAMAX,NBMAX,M,DELZ,DELX,EPS,XX,Z0
      J=1
   50 READ (5,2) (C(I,J),I=1, NXMAX),U(J)
      J=J+1
      IF (J.LE.NZMAX) GO TO 50
      WRITE(6,73)
      WRITE (6,89)
C     COMPUTE PARAMETERS
      XL=(2*NXMAX-1)
      H=(NZMAX-1)*DELZ
C     GENERATE DATA IN X DIRECTION AT 0.25 FT INTERVALS
      NXGEN=61
      DO 85 J=1,NZMAX
      Z(J)=(J-1)*DELZ
      WRITE(6,77) Z(J)
      X(1)=0
      DATA(1)=0
C     FIT A POLYNOMIAL THROUGH DATA AT SAME LEVEL
      NXMAX1=NXMAX+1
      DO 86 I=2,NXMAX1
      X(I)=2*(I-1)-1
      DATA(I)=C(I-1,J)
   86 CONTINUE
      CALL LSTSQ(X,DATA,M,NXMAX1,XX,XL,VALUE,AX,1)
      XV(1)=0
      CC(1,J)=0
      DO 87 K=2,NXGEN
      XV(K)=(K-1)*0.25
      CC(K,J)=AX(1)+AX(2)*XV(K)+AX(3)*XV(K)**2+AX(4)*XV(K)**3+AX(5)*XV(K
     1)**4+AX(6)*XV(K)**5+AX(7)*XV(K)**6+AX(8)*XV(K)**7+AX(9)*XV(K)**8
      IF (CC(K,J).LT.0.0) CC(K,J)=0.0
   87 CONTINUE
      IF (J.LE.7) GO TO 841
      IZERO=5
      IF (J.LE.12) GO TO 83
      DO 81 IX=13,61,8
      IF (CC(IX,J)-0.005)81,81,82
   81 CONTINUE
   82 IZERO=IX-8
   83 DO 84 K=1,IZERO
      CC(K,J)=0.0
   84 CONTINUE
  841 WRITE(6,88) (CC(K,J),K=1,NXGEN)
   85 CONTINUE
      WRITE (6,70)
C     START COMPUTATION OF INTEGRALS FOR DIFFERENT VALUES OF A AND B
      DO 30 NA=1,NAMAX
      DO 30 NB=1,NBMAX
      A1=NA*3.14159/H
      B=NB*3.14159/XL
      N=NB+(NA-1)*NBMAX
      NE=NAMAX*NBMAX
C     COMPUTE FIRST THREE INTEGRALS
      DO 20 L=1,3
      DO 10 I=1, NXGEN
      XV(I)=(I-1)*0.25
      Z(1)=0
      PRODZ(1)=0
      DO 5 J=2,NZMAX
      Z(J)=(J-1)*DELZ
      PRODZ(J)=WT(Z(J),A1,L)*CC(I,J)
    5 CONTINUE
```

```
C      FIRST INTEGRATION
       CALL LSTSQ (Z,PRODZ,M,NZMAX,Z0,H,VALUE,AZ,0)
       FSINT(I)=VALUE
       PRODXV(I)=SIN(B*XV(I))*FSINT(I)
    10 CONTINUE
C      SECOND INTEGRATION
       CALL LSTSQ (XV,PRODXV,M,NXGEN,XX,XL,VALUE,AX,0)
       COFINT(L)=(VALUE/(12.0**L))*12.0
       A(N,L)=COFINT(L)
    20 CONTINUE
C      COMPUTE LAST INTEGRAL
       DO 25 J=1,NZMAX
       Z(J)=(J-1)*DELZ
       DO 26 I=1,NXGEN
       XV(I)=(I-1)*0.25
       PRODXV(I)=B*COS(B*XV(I))*CC(I,J)
    26 CONTINUE
       CALL LSTSQ (XV,PRODXV,M,NXGEN,XX,XL,VALUE,AX,0)
       FSINT(J)=VALUE
       PRODZ(J)=(SIN(A1*Z(J))**2)*U(J)*FSINT(J)
    25 CONTINUE
       CALL LSTSQ (Z,PRODZ,M,NZMAX,Z0,H,VALUE,AZ,0)
       COFINT4=VALUE/12.0
       A(N,4)=-COFINT4
       WRITE (6,71) NA,NB,(COFINT(L),L=1,3),COFINT4
    30 CONTINUE
       WRITE (6,75)
    75 FORMAT(1H1,4X,*CONSTANTS K1,K2,K3 IN*,/,*K(Z)=K1*Z+K2*Z**2+K3*Z**
      13*)
C      REDUCE NO. OF EQUATIONS TO NO. OF UNKNOWNS
       DO 31 NT=3,NE,1
       DO 15 I=1,3
       DO 15 J=1,3
       BC(J)=0
       AC(I,J)=0
    15 CONTINUE
       DO 41 N=1,NT
       DO 41 J=1,3
       BC(J)=BC(J)+A(N,J)*A(N,4)
       DO 41 K=1,3
       AC(J,K)=AC(J,K)+A(N,J)*A(N,K)
    41 CONTINUE
       CALL INVERSE (AC,AI,3)
       DO52 I=1,3
       AK(I)=0
       DO51 J=1,3
       AK(I)=AK(I)+AI(I,J)*BC(J)
    51 CONTINUE
    52 CONTINUE
       WRITE (6,76) NT
       WRITE (6,72) (AK(I),I=1,3)
       CK1(NT)=AK(1)
       CK2(NT)=AK(2)
       CK3(NT)=AK(3)
    31 CONTINUE
       DO 22 J=1,41
       HT=(J-1)*0.025
       DO 21 I=3,NE
       CKZ(I)=CK1(I)*HT+CK2(I)*HT**2+CK3(I)*HT**3
    21 CONTINUE
       WRITE (6,9) HT,(CKZ(I),I=3,NE)
     9 FORMAT (4X,F8.3,10F11.7)
    22 CONTINUE
     1 FORMAT (5I3,5F12.6)
     2 FORMAT (8F9.3,F8.3)
    70 FORMAT (1H1,////,4X,*NA*,13X,*NB*,8X,*COEFF INTEGRAL 1*,3X,*COEFF
     1 INTEGRAL 2*,3X,*COEFF INTEGRAL 3*,3X,*COEFF INTEGRAL 4*)
    71 FORMAT (/ , 4X,I2,13X,I2,4X,4(5X,F14.6))
    89 FORMAT(5X,*DATA GENERATED BY CURVE FITTING AT 0.25 FT INTERVALS IN
      1 X DIRECTION*)
    73 FORMAT(1H1,4X,*U=10 FPS,STABLE STRATIFICATION*)
    77 FORMAT(/,2X,*Z=*,F5.2)
    88 FORMAT(16F8.3)
    76 FORMAT(/,4X,*NO. OF EQUATIONS SOLVED=*,I2)
    72 FORMAT(4X,*K1=*,F10.6,2X,*K2=*,F10.6,2X,*K3=*,F10.6)
   100 CALL EXIT
       END
```

```
      SUBROUTINE LSTSQ(X,Y,M,NP1,P,Q,VALUE,A,SIG)
      DIMENSION X(30),Y(30),XC(20),YX(10),A(10),B(10),C(10,10),D(10,10)
      MP1=M-1
      M2=2*M
C     FORM SUMS OF POWERS OF X(I)
      DO 20 K=1,M2
      XC(K)=0.0
      DO 15 I =1,NP1
   15 XC(K)=XC(K) + X(I)**K
   20 CONTINUE
C     FORM SUM OF Y(I)
      YC=0.0
      DO 22 I=1,NP1
   22 YC=YC+Y(I)
C     FORM SUMS OF PRODUCTS Y(I) * X(I)**K
      DO 30 K=1,M
      YX(K) = 0.0
      DO 25 I=1,NP1
   25 YX(K) =YX(K) + Y(I)*X(I)**K
   30 CONTINUE
C     GENERATE NORMAL MATRIX C USING SUMS OF POWERS OF X(I)
      DO 40 I=1,MP1
      DO 35 J=1,MP1
      IPJM2=I+J-2
      IF(IPJM2)33,31,33
   31 C(1,1)=FLOAT(NP1)
      GO TO 35
   33 C(I,J)=XC(IPJM2)
   35 CONTINUE
   40 CONTINUE
      B(1)=YC
      DO 45 I=2,MP1
   45 B(I)=YX(I-1)
C     INVERT NORMAL MATRIX C
      CALL INVERSE (C,D,MP1)
      DO 55 I=1,MP1
      A(I)=0.0
      DO 54 J=1,MP1
   54 A(I)=A(I)+D(I,J)*B(J)
   55 CONTINUE
      IF(SIG.EQ.1) GO TO 80
      VALUE=0.0
      DO 56 I=1,MP1
      IF(P.EQ.0.0) GO TO 58
      VALUE=VALUE+A(I)*(Q**I-P**I)/I
      GO TO 56
   58 VALUE=VALUE+A(I)*(Q**I)/I
   56 CONTINUE
   80 RETURN
      END
```

```
      SUBROUTINE INVERSE (A,B,N)
      DIMENSION A(10,10),B(10,10)
      EPS=0.0000001
      DO 6 I=1,N
      DO 5 J=1,N
      IF (I-J)4,3,4
    3 B(I,J)=1.0
      GO TO 5
    4 B(I,J)=0
    5 CONTINUE
    6 CONTINUE
      DEL=1.0
      DO 45 K=1,N
      IF(K-N)12,30,30
   12 IMAX=K
      AMAX=ABS(A(K,K))
      KP1=K+1
      DO 20 I=KP1,N
      IF(AMAX-ABS(A(I,K)))15,20,20
   15 IMAX=I
      AMAX=ABS(A(I,K))
   20 CONTINUE
      IF(IMAX-K)25,30,25
   25 DO 29 J=1,N
      ATMP=A(IMAX,J)
      A(IMAX,J)=A(K,J)
      A(K,J)=ATMP
      BTMP=B(IMAX,J)
      B(IMAX,J)=B(K,J)
   29 B(K,J)=BTMP
      DEL=-DEL
   30 CONTINUE
      IF(ABS(A(K,K))-EPS)93,93,35
   35 DEL=A(K,K)*DEL
      DIV=A(K,K)
      DO 38 J=1,N
      A(K,J)=A(K,J)/DIV
   38 B(K,J)=B(K,J)/DIV
      DO 43 I=1,N
      AMULT=A(I,K)
      IF(I-K)39,43,39
   39 DO 42 J=1,N
      A(I,J)=A(I,J)-AMULT*A(K,J)
   42 B(I,J)=B(I,J)-AMULT*B(K,J)
   43 CONTINUE
   45 CONTINUE
      RETURN
   93 WRITE (6,113)K
  113 FORMAT (25H SINGULAR MATRIX FOR K=,I2)
      RETURN
      END
```

TABLES

TABLE I SUMMARY OF WIND TUNNEL DIFFUSION EXPERIMENTS

Experiments Reported By:	Wind Tunnel Test Section and Type	Type and Position of the Source	Height and Type of Release	Maximum Sampling Distance	Nature of Surface	Stratification	Tracer	Diffusion Measurements
K.S. Davar (1961)	6'x 6'x 28' Recirculating	Point source x_o = 6 ft	Ground and elevated continuous	7 ft	Smooth aluminum	Neutral	Anhydrous ammonia	Complete mapping of concentration field
M. Poreh (1961)	6'x 6'x 80' Open circuit	Line source x_o = 15½, 33½ ft	Ground continuous	21 ft, 43½ ft	Smooth	Neutral	"	Vertical concentration profiles
R.C. Malhotra (1962)	6'x 6'x 28' Recirculating	Point source x_o = 6 ft	Ground continuous	7½ ft	Smooth aluminum	Neutral and unstable	"	Complete mapping of concentration field
A.A. Quraishi (1963)	6'x 6'x 80' Open circuit	Line source x_o = 46 ft	Ground and elevated continuous	12 ft	Plastic roughness element on wooden planks	Neutral	"	Vertical Concentration profiles
S. Bhaduri (1963)	6'x 6'x 28'	Point source x_o = 6 ft	Ground and elevated continuous	6½ ft	Two dimensional roughness elements ¼" high at 3" apart	Neutral	"	Complete mapping of concentration field
D. Kesic (1967)	6'x 6'x 28' Recirculating	Point source x_o = 27 ft	Elevated Instantaneous	5 inches	Smooth wooden	Neutral	Heat	Axial vertical and horizontal temperature profiles
M. Yano (1966)	6'x 6'x 80' Recirculating Micro-met w.t.	Point source x_o = 40, 55, 65 ft	Ground and elevated continuous	20 inches	Pegs	Unstable, Neutral and stable	Pure helium	Axial vertical and horizontal concentration profiles
S. Koehler (1967)	"	Point source x_o = 65 ft	Ground continuous	10 ft	Smooth aluminum	Stable	"	Vertical and Ground level concentration profiles
C. Shih (1966)	"	Point source x_o = 2,7,13, 20,40, & 60 ft	Ground continuous	15 ft	Smooth wooden & aluminum	Neutral	"	Free stream roughness changed
S. Chandra (1967)	"	Point source	Elevated Instantaneous	4 ft	Smooth	Neutral	"	Complete mapping

TABLE II RUN SUMMARY

Run	Position	Thermal Stratification	U_∞ ft/sec	ΔT °F	$Q_{\mu ci/sec}$
NG	Ground	Neutral	10	0	16.4
SG 1	Ground	Stable	10	80	16.4
SG 2	Ground	Stable	20	80	16.4
SE 1	Elevated H=2"	Stable	10	80	16.4
SE 2	Elevated H=4"	Stable	10	80	24.2
SE 3	Elevated H=8"	Stable	10	80	24.2

TABLE III FLOW PARAMETERS

Run	U_∞ ft/sec	δ ft	u* ft/sec	L ft	Z_o ft
NG	10	2.4	.406	∞	.00008
SG 2	20	2.3	.58	8.02	.00008
SG 1					
SE 1					
SE 2	10	2.37	.241	1.6	.00008
SE 3					

TABLE IV. POINT SOURCE CONCENTRATIONS (μμ ci/cc)

Run	x	z/y	0	0.25	0.5	0.75	1.0	1.5	2.0	2.5
NG	1	0	24,300	22,300	19,250	15,400	12,000	5,300	1,250	0
		0.25	13,600	12,750	10,600	8,550	6,500	2,950	750	0
		0.5	6,820	6,450	5,500	4,500	3,510	1,740	375	0
		0.75	3,280	3,200	2,820	2,340	1,850	960	240	0
		1.0	1,560	1,490	1,300	1,110	890	500	100	0
		1.5	190	190	180	130	120	90	0	0

Run	x	z/y	0	0.5	1.0	1.5	2.5	3.5	4.5	5.5
	3	0	2,770	2,662	2,420	2,045	1,236	638	282	61
		0.5	2,180	2,117	1,920	1,588	900	376	85	35
		1.0	1,320	1,250	1,103	950	619	300	57	25
		1.5	850	815	733	636	412	192	50	15
		2.0	467	447	398	345	231	122	41	8
		3.0	112	110	101	90	60	34	8	0
		4.0	17	16	15	13	8	0	0	0

Run	x	z/y	0	1.0	2.0	3.0	4.5	6.0	7.5	9
	7	0	670	634	535	411	237	117	55	5
		1.0	512	485	414	334	200	103	36	0
		2.0	375	345	287	233	159	93	40	0
		3.0	188	180	158	135	94	53	18	0
		4.0	118	101	82	64	44	29	18	0
		5.0	62	56	46	36	25	15	7	0
		6.0	29	27	23	20	14	8	3	0

Run	x	z/y	0	2.0	4.0	6.0	8.0	10.0	12.0	14.0
	11	0	327	285	208	134	72	31	10	5
		1.0	267	245	180	118	78	27	7	0
		2.5	215	187	128	80	43	15	3	0
		4.0	130	118	87	55	31	12	0	0
		6.0	47	44	34	24	15	7	0	0
		8.0	20	20	16	11	6	3	0	0

Run	x	z/y	0	2.0	4.0	6.0	8.0	10.0	12.0	14.0
	15	0	216	210	153	82	47	25	8	0
		1.5	177	166	130	78	49	32	20	12
		3.0	137	117	89	65	44	28	17	8
		5.0	85	78	66	50	32	19	10	3
		7.0	43	42	38	28	20	15	9	3
		9.0	20	20	17	12	5	1	0	0

Run	x	z/y	0	0.5	1.0	1.5	2.0	2.5	3.0	3.5
NG	2	0	6,055	5,340	4,520	3,240	2,100	1,135	480	95
		0.25	4,600	4,370	3,700	2,700	1,725	965	445	100
		0.5	3,590	3,350	2,775	2,000	1,265	680	300	90
		1.0	1,800	1,695	1,400	1,020	695	415	185	50
		1.5	750	670	515	353	245	165	97	0
		2.0	225	220	210	165	120	90	40	0

Run	x	z/y	0	1.0	2.0	3.0	4.0	5.0	6.5	8.0
	5	0	1,230	1,100	835	561	350	211	88	34
		0.5	943	898	709	472	281	156	53	12
		1.0	713	677	573	425	263	125	28	0
		2.0	422	393	335	245	152	85	15	0
		3.0	198	187	156	107	62	30	9	0
		4.0	80	72	58	42	27	15	7	0
		5.0	25	23	18	12	7	3	0	0

Run	x	z/y	0	1.0	2.0	3.0	5.0	7.0	9.0	11.0
	9	0	423	417	374	325	198	97	26	0
		1.0	355	344	315	272	165	80	30	7
		2.0	280	267	239	203	129	65	20	6
		3.0	180	175	163	142	91	46	14	6
		4.0	115	113	106	93	58	31	15	5
		5.5	55	52	46	39	27	17	10	3
		7.0	22	22	21	20	16	10	6	0

Run	x	z/y	0	2.0	4.0	6.0	8.0	10.0	12.0	14.0
	13	0	243	220	171	118	73	38	17	9
		1.5	198	180	143	103	68	38	19	9
		3.0	140	130	105	75	48	27	9	3
		5.0	80	70	52	37	25	15	7	3
		7.0	32	29	24	17	10	5	1	0
		9.0	5	4	2	0	0	0	0	0

TABLE IV. POINT SOURCE CONCENTRATIONS (μμ ci/cc) (Continued)

Run	x	z/y	0	0.25	0.5	0.75	1.0	1.5	2.0	2.5
SG1	1	0	32,500	29,950	24,850	18,400	12,300	4,375	1,125	300
		0.25	16,750	15,050	11,625	8,625	6,125	2,450	450	0
		0.5	9,250	8,300	7,000	5,575	4,250	1,800	200	0
		0.75	4,375	4,050	3,500	2,875	2,250	1,050	150	0
		1.0	1,750	1,700	1,500	1,220	880	300	50	0
		1.5	250	205	180	153	125	55	30	0

Run	x	z/y	0	0.5	1.0	1.5	2.0	3.0	4.0	5.0
	3	0	4,770	4,483	3,455	2,515	1,750	750	200	40
		0.5	3,060	2,946	2,590	2,070	1,500	660	180	50
		1.0	2,028	1,930	1,700	1,396	1,070	520	150	50
		1.5	1,100	1,045	885	704	530	232	100	30
		2.0	505	485	430	357	280	159	60	25
		3.0	77	77	74	68	60	38	17	7

Run	x	z/y	0	1.0	2.0	3.0	4.0	5.0	6.0	8.0
	7	0	1,118	1,058	900	701	500	311	171	41
		1.0	740	680	542	411	294	198	125	26
		2.0	425	398	339	278	216	155	100	17
		3.0	230	220	190	152	113	79	46	10
		4.0	101	96	84	68	49	32	20	7
		5.0	55	47	34	23	15	8	3	0

Run	x	z/y	0	1.0	2.0	3.0	4.0	6.0	8.0	10.0
	11	0	545	532	490	420	318	154	55	8
		1.0	454	440	399	337	262	134	48	5
		2.0	295	286	261	229	190	111	41	0
		3.0	172	166	153	136	116	74	30	0
		4.0	125	119	104	85	64	27	7	0
		5.0	62	59	50	41	32	10	0	0

Run	x	z/y	0	1.0	2.0	4.0	6.0	8.0	10.0	12.0
	15	0	369	355	319	221	130	59	14	0
		1.0	345	334	295	196	107	45	10	0
		2.0	270	260	331	149	81	34	7	0
		3.0	225	220	198	130	70	25	0	0
		5.0	95	92	85	61	34	9	0	0
		7.0	20	20	18	10	4	0	0	0

Run	x	z/y	0	0.5	1.0	1.5	2.0	2.5	3.0	3.5
	2	0	9,500	8,500	6,385	4,090	2,200	985	290	150
		0.5	5,300	4,630	3,500	2,350	1,300	595	160	50
		1.0	2,250	2,040	1,620	1,205	797	375	90	40
		1.5	922	880	733	515	312	165	80	35
		2	292	273	223	154	100	64	40	15
		3	30	25	20	20	10	7	5	0

Run	x	z/y	0	0.5	1.0	2.0	3.0	4.0	5.0	6.0
	5	0	1,820	1,762	1,575	1,128	728	411	202	75
		0.5	1,563	1,512	1,368	1,025	699	431	213	81
		1.0	1,130	1,097	1,010	777	522	301	135	34
		2.0	531	513	478	370	254	151	65	13
		3.0	206	200	190	152	102	53	17	0
		5.0	22	22	21	15	4	0	0	0

Run	x	z/y	0	1.0	2.0	3.0	4.0	6.0	8.0	10.0
	9	0	744	728	663	541	410	166	59	17
		1.0	625	595	511	400	277	120	50	20
		2.0	385	365	316	258	205	104	41	12
		3.0	220	211	186	159	130	76	30	5
		4.0	125	119	106	92	77	47	24	3
		5.0	58	55	50	35	21	5	0	0

Run	x	z/y	0	1.0	2.0	4.0	6.0	8.0	10.0	12.0
	13	0	380	372	346	264	151	70	31	15
		1.0	340	330	304	220	122	55	22	5
		2.0	255	246	226	165	97	48	19	0
		3.0	172	168	157	120	71	34	7	0
		4.0	111	109	104	84	57	27	3	0
		6.0	38	38	37	25	11	3	0	0

TABLE IV. POINT SOURCE CONCENTRATIONS (μμ ci/cc)(Continued)

Run	x	z/y	0	0.5	1.0	1.5	2.0	3.0	4.0	5.0
SG2	3	0	1,675	1,635	1,450	1,094	753	294	50	0
		0.5	1,125	1,332	1,131	906	675	294	87	10
		1.0	875	850	730	544	397	183	35	0
		1.5	547	528	473	374	273	120	35	0
		2.0	290	275	240	200	154	72	15	0
		3.0	62	62	53	43	29	4	0	0

	x	z/y	0	1.0	2.0	3.0	4.0	5.0	6.0	7.0
	5	0	538	484	360	224	116	49	12	2
		1.0	511	462	361	246	142	68	24	5
		2.0	301	265	200	134	70	26	2	0
		3.0	120	110	85	55	26	4	0	0
		4.0	50	42	28	12	1	0	0	0
		6.0	5	4	3	0	0	0	0	0

	x	z/y	0	1.0	2.0	3.0	4.0	5.0	6.0	7.0
	7	0	420	386	304	208	125	71	32	3
		1.0	318	298	257	200	136	79	40	12
		2.0	221	209	172	125	78	36	8	0
		3.0	144	140	120	90	56	27	5	0
		4.0	79	73	59	41	26	12	0	0
		6.0	25	23	15	10	5	3	0	0

	x	z/y	0	1.0	2.0	3.0	4.0	5.0	6.0	7.0
	9	0	262	246	214	169	118	72	40	18
		1.0	226	214	185	146	111	71	45	25
		2.0	173	167	145	112	79	48	23	18
		3.5	97	93	82	65	46	29	18	10
		5.0	48	47	38	29	22	16	10	5
		7.0	16	15	13	12	10	7	4	2

	x	z/y	0	1.0	2.0	3.0	4.0	5.5	7.0	8.5
	11	0	218	199	167	133	104	64	29	9
		1.0	188	175	151	121	94	53	25	8
		2.0	129	126	115	98	77	44	20	7
		3.5	102	98	84	67	52	33	17	5
		5.0	53	52	48	40	32	20	10	2
		7.0	20	18	13	8	2	0	0	0

	x	z/y	0	1.5	3.0	4.5	6.0	7.5	9.0	10.5
	13	0	160	138	103	69	43	24	12	4
		1.0	149	128	95	62	39	24	14	5
		2.0	114	105	78	50	29	14	5	0
		3.5	82	76	62	44	25	12	4	0
		5.0	60	53	39	26	14	6	2	0
		7.0	32	27	21	14	9	4	0	0
		9.0	16	15	12	9	5	2	0	0

		z/y	0	1.5	3.0	5.0	7.0	9.0	11.0	13.0
		0	127	120	95	61	35	18	2	0
		1.0	115	102	82	57	33	12	6	0
		2.0	98	92	77	56	33	5	0	0
		4.0	65	61	52	35	17	4	0	0
		6.0	45	41	34	23	11	1	0	0
		8.0	15	15	11	8	4	0	0	0

TABLE V. EQUIVALENT LINE SOURCE CONCENTRATIONS ($\mu\mu$ ci/cc x 10^{-3})

Q = 252.0μci/sec ft

Run	x	z	c	x	z	c	x	z	c	x	z	c	x	z	c	x	z	c
NG	1	0	44.0	2	0	20.49	3	0	13.9	5	0	8.0	7	0	5.74	9	0	4.36
		0.25	24.0		0.25	16.56		0.5	9.63		0.5	6.35		1.0	4.32		1.0	3.66
		0.5	14.4		0.5	12.41		1.0	6.69		1.0	5.05		2.0	2.85		2.0	2.775
		0.75	7.8		1.0	6.6		1.5	4.35		2.0	2.88		3.0	1.70		3.0	1.995
		1.0	3.8		1.5	2.57		2.0	2.45		3.0	1.35		4.0	0.93		4.0	1.280
		1.25	1.4		2.0	0.94		3.0	0.62		4.0	0.56		5.0	0.50		5.5	0.615
		1.5	0		3.0	0.09		4.0	0		5.0	0.16		6.0	0.25		7.0	0.305
	11	0	3.54	13	0	3.02	15	0	2.53									
		1.0	3.15		1.5	2.65		1.5	2.32									
		2.5	2.285		3.0	1.93		3.0	1.796									
		4.0	1.515		5.0	1.04		5.0	1.22									
		6.0	0.630		7.0	0.49		7.0	0.73									
		8.0	0.300		9.0	0.19		9.0	0.27									
SG	1	0	59.3	2	0	27.8	3	0	19.0	5	0	11.5	7	0	8.35	9	0	6.71
		0.25	29.6		0.5	14.98		0.5	13.1		0.5	9.15		1.0	5.50		1.0	5.23
		0.5	17.95		1.0	7.4		1.0	8.64		1.0	6.74		2.0	3.50		2.0	3.40
		0.75	9.4		1.5	2.68		1.5	4.46		1.5	4.9		3.0	1.93		3.0	2.19
		1.0	3.5		2.0	0.88		2.0	1.85		2.0	3.22		4.0	0.90		4.0	1.25
		1.5	0		3.0	0		3.0	0		3.0	1.25		5.0	0.29		5.0	0.46
											5.0	0						
	11	0	5.27	13	0	4.32	15	0	3.78									
		1.0	4.36		1.0	3.65		1.0	3.51									
		2.0	3.03		2.0	2.795		2.0	2.70									
		3.0	1.86		3.0	1.95		3.0	1.975									
		4.0	1.07		4.0	1.30		4.0	1.435									
		5.0	0.505		5.0	0.75		5.0	0.97									
					6.0	0.39		7.0	0.20									
SG2	3	0	6.79	5	0	3.80	7	0	2.80	9	0	2.04	11	0	1.775	13	0	1.49
		0.5	5.70		1.0	3.00		1.0	2.19		1.0	1.832		1.0	1.61		1.0	1.32
		1.0	3.80		2.0	1.68		2.0	1.50		2.0	1.338		2.0	1.25		2.0	1.10
		1.5	2.40		3.0	0.61		3.0	0.92		3.5	0.782		3.5	0.80		3.5	0.77
		2.0	1.23		4.0	0.21		4.0	0.52		5.0	0.392		5.0	0.47		5.0	0.52
		3.0	0.25		6.0	0		6.0	0.13		7.0	0.120		7.0	0.18		7.0	0.28
																	9.0	0.10
	15	0	1.33															
		1.0	1.28															
		2.0	1.13															
		3.0	0.92															
		4.0	0.72															
		5.0	0.55															
		6.0	0.4															
		8.0	0.28															

FIGURES

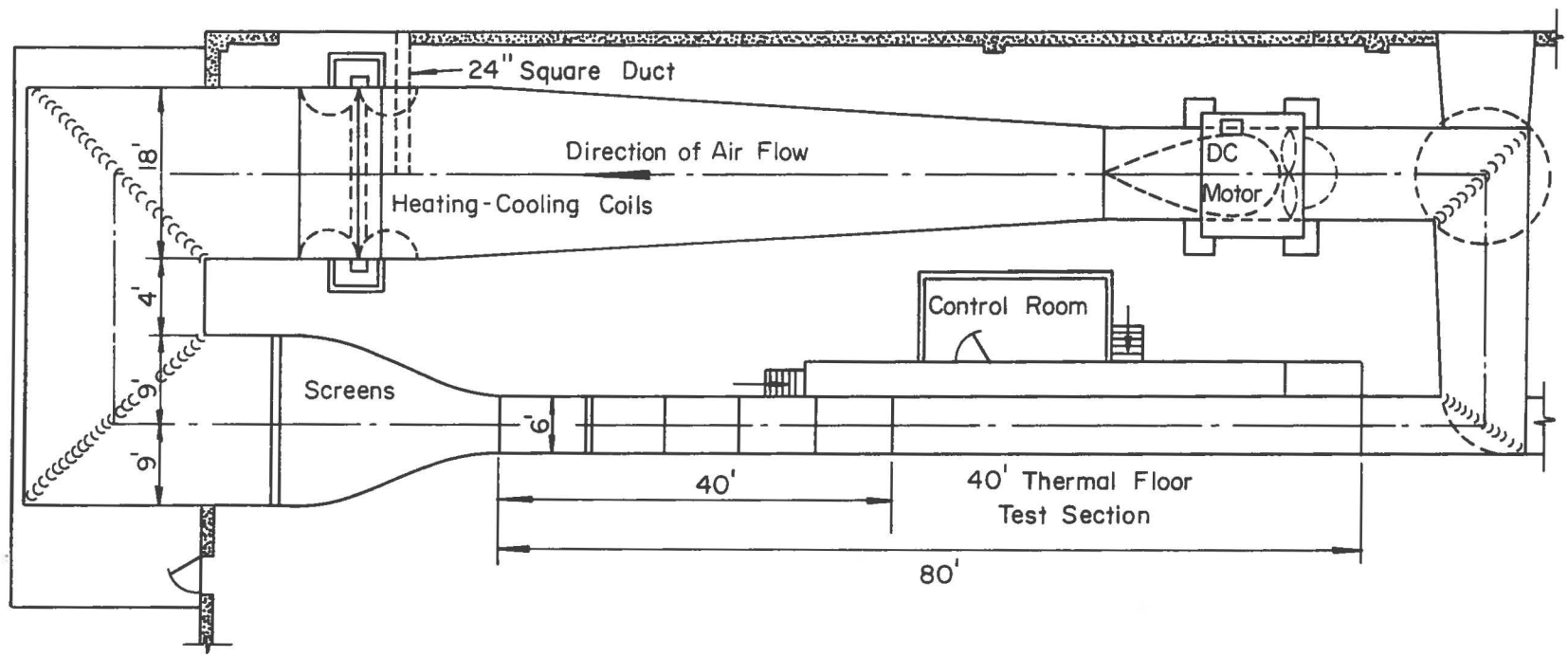

Fig. 1. Wind Tunnel

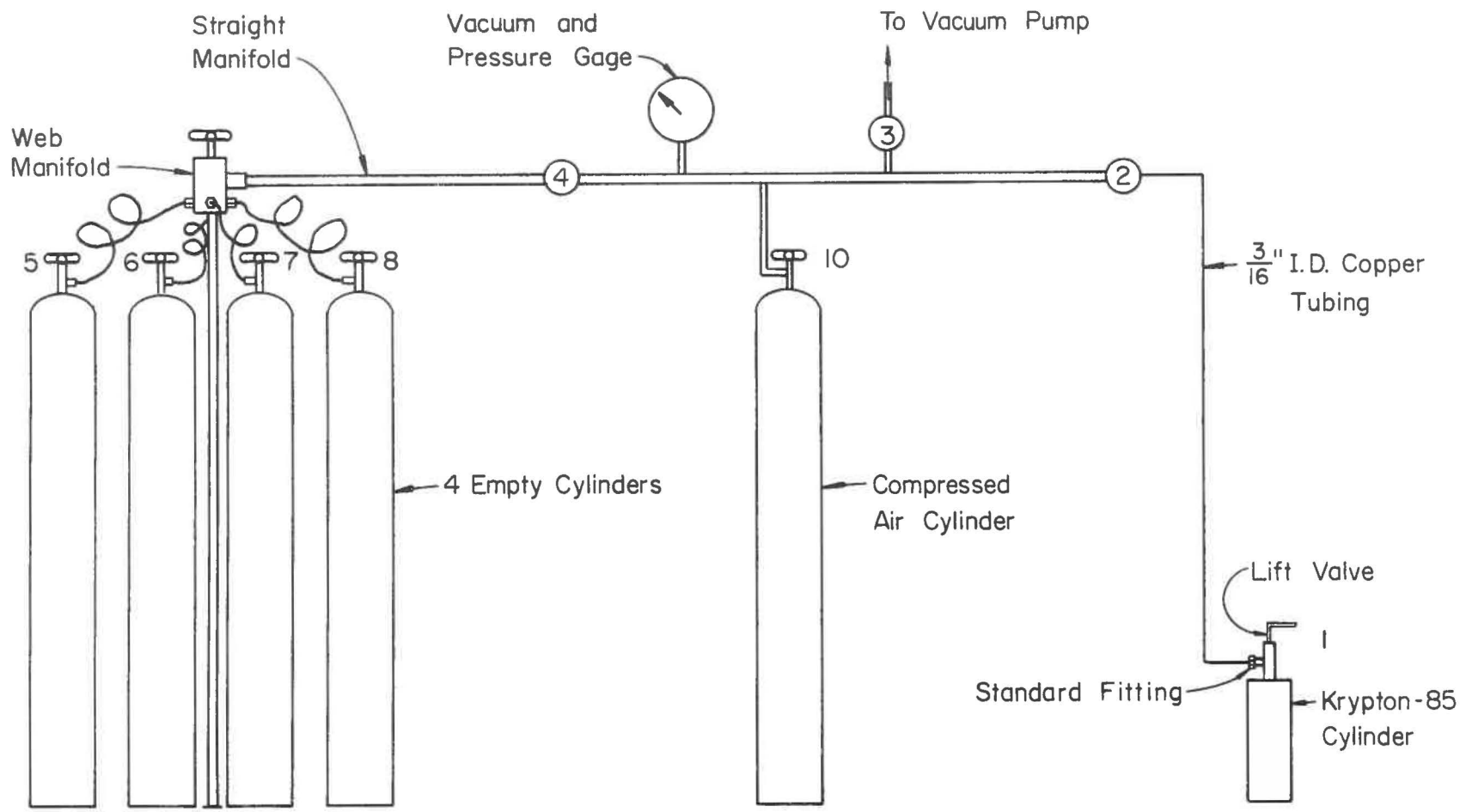

Fig. 2. Transfer and dilution arrangement

Fig. 3. Krypton-85 calibration arrangement

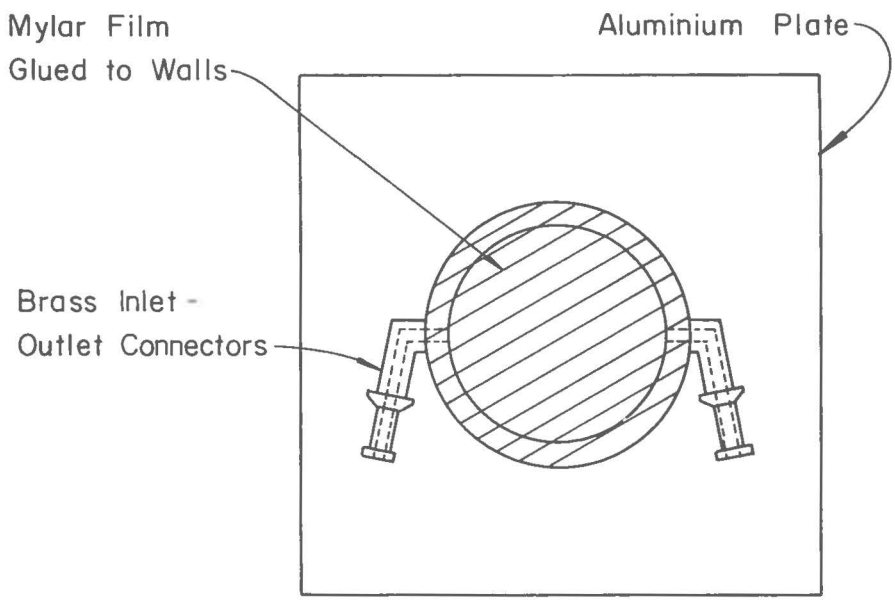

Fig. 4. The gas planchet

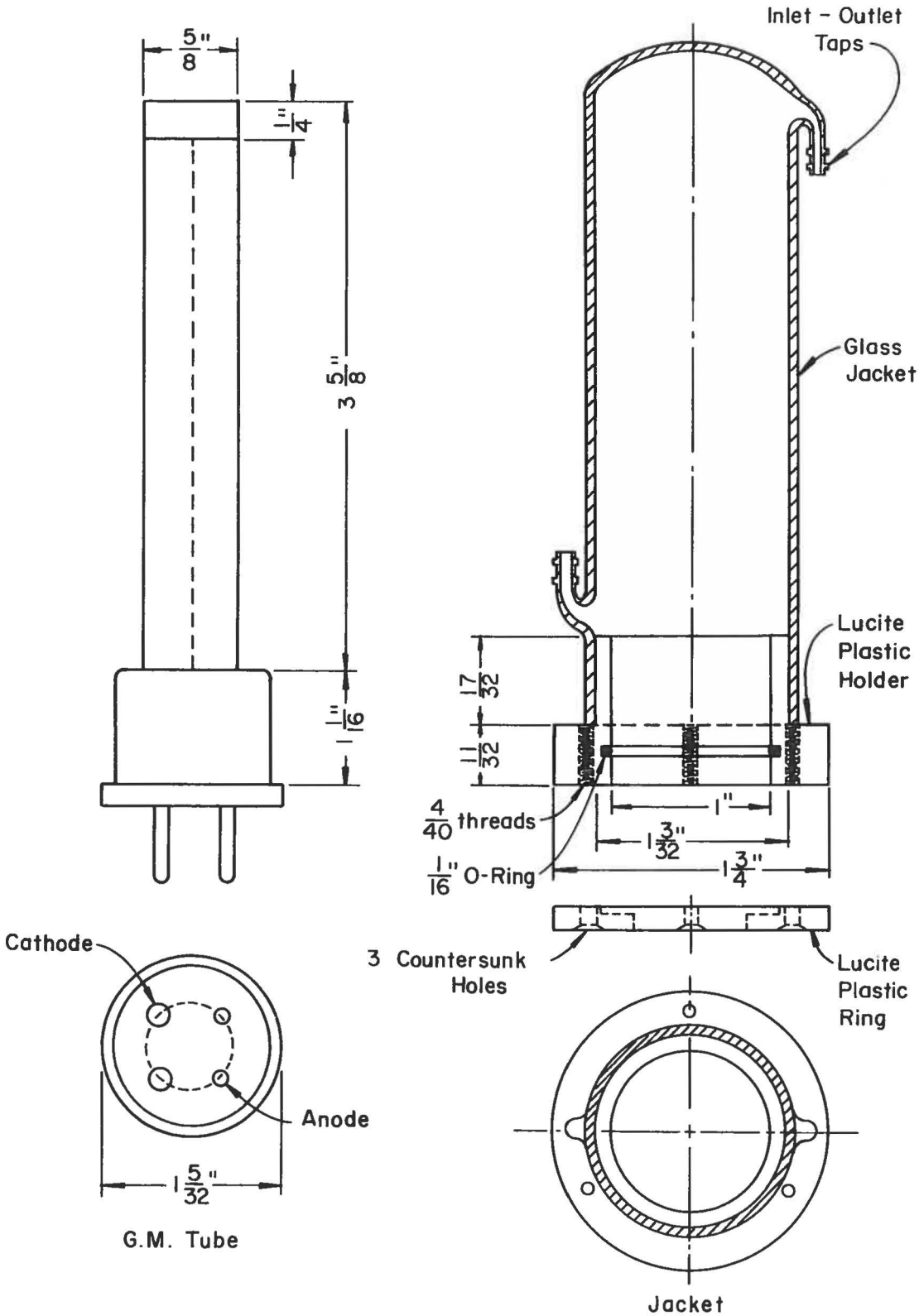

Fig. 5. The G.M. tube and the glass jacket

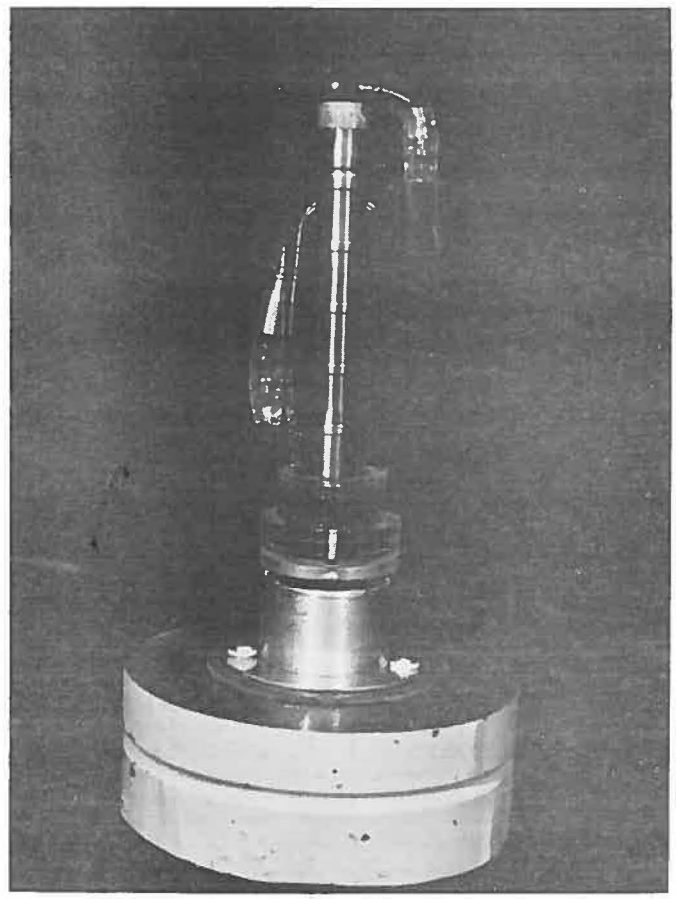

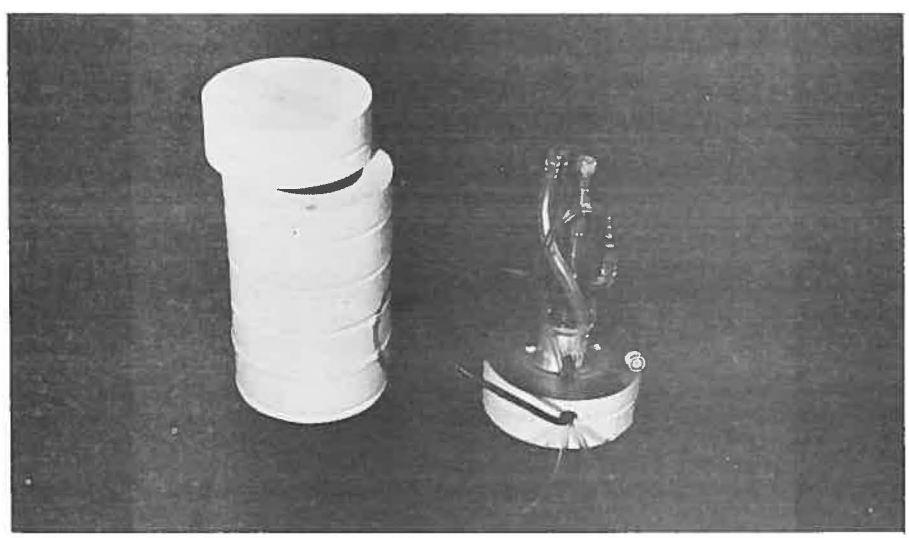

Fig. 6. The G.M. tube holder and shield

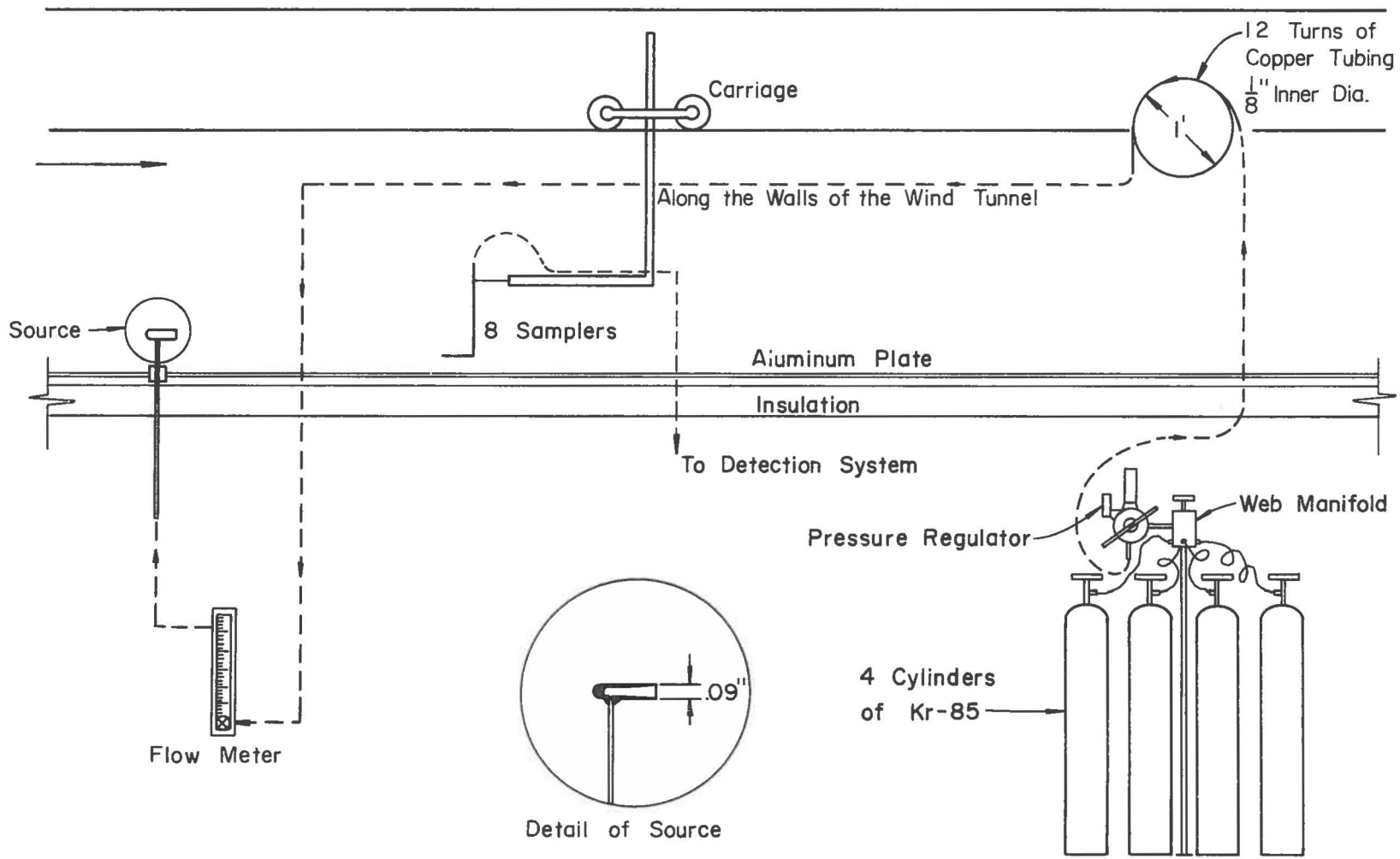

Fig. 7. Release system

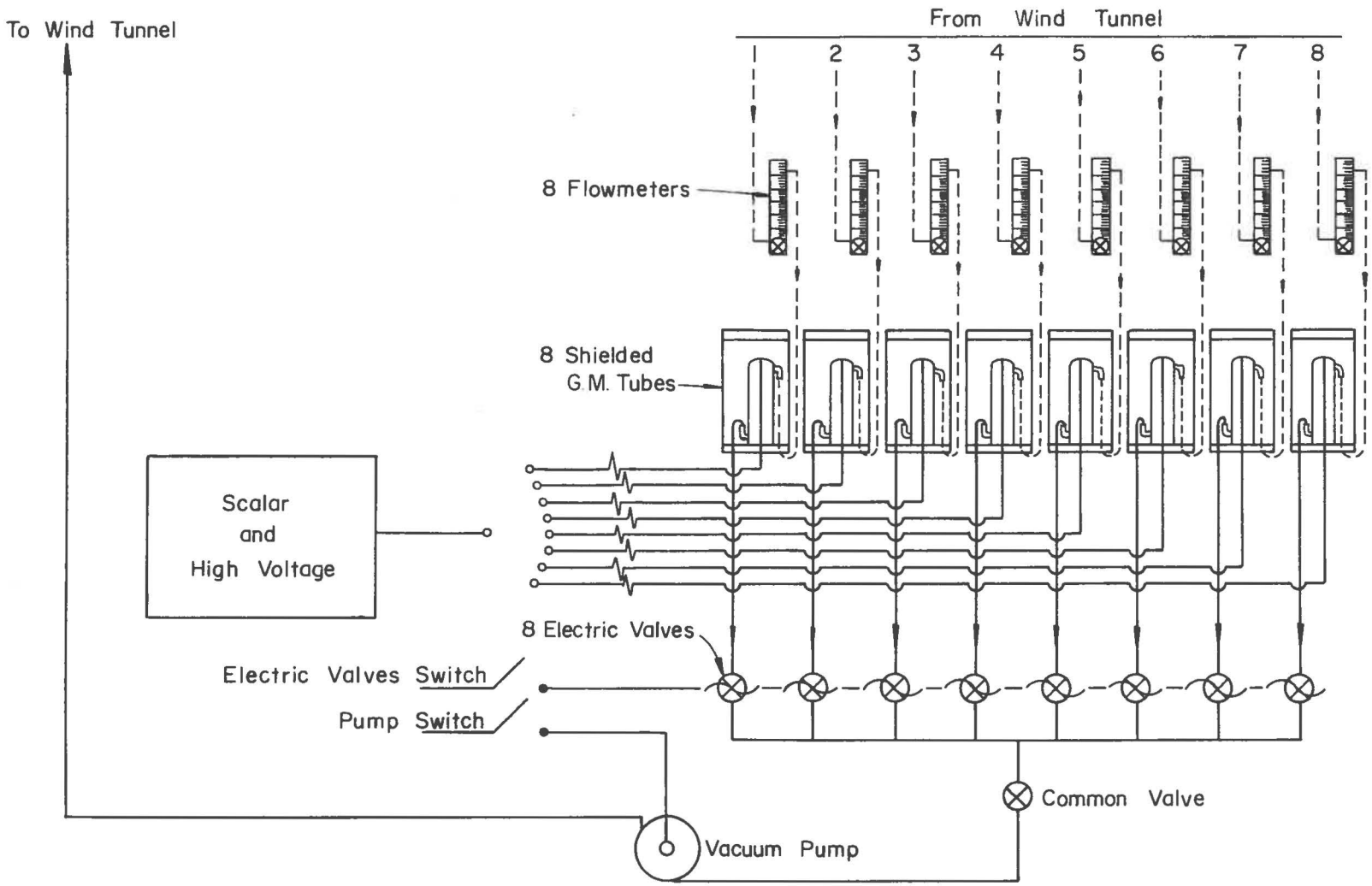

Fig. 8. Detection system

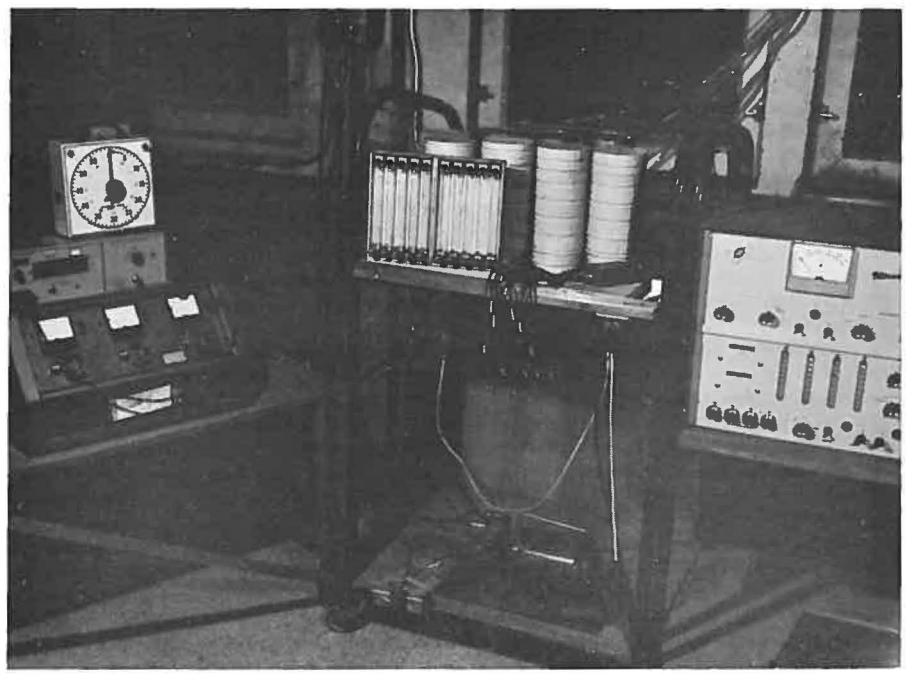

Fig. 9. Instruments

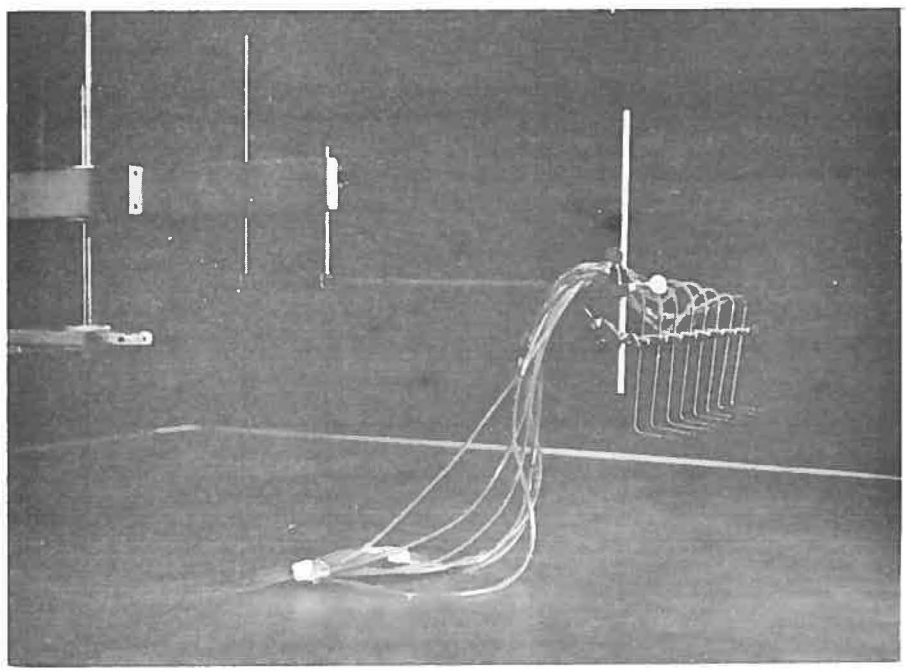

Fig. 10. Sampling rake

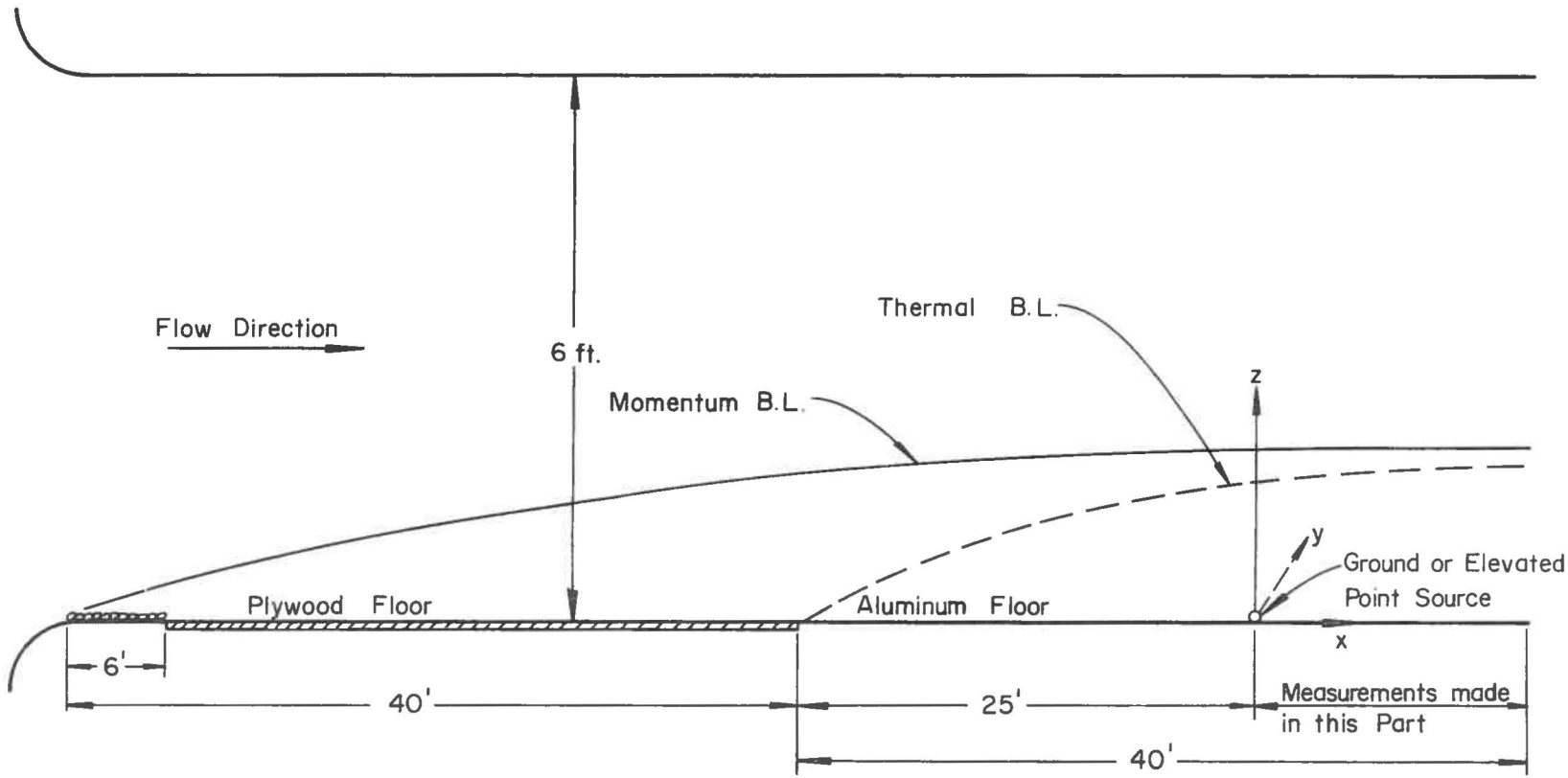

Fig. 11. Test section and the coordinate system

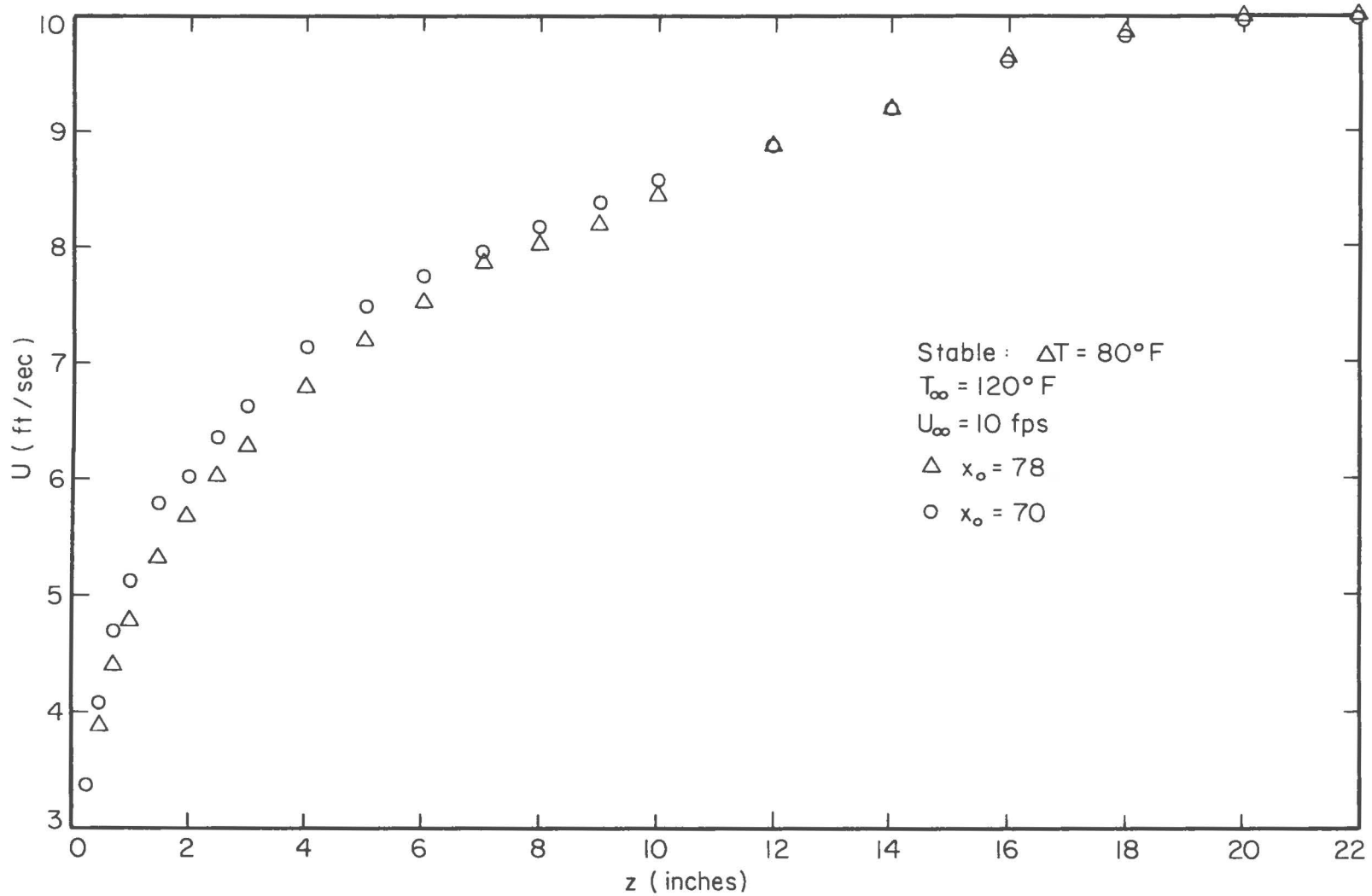

Fig. 12. Comparison of velocity profiles at 70 ft and 78 ft sections

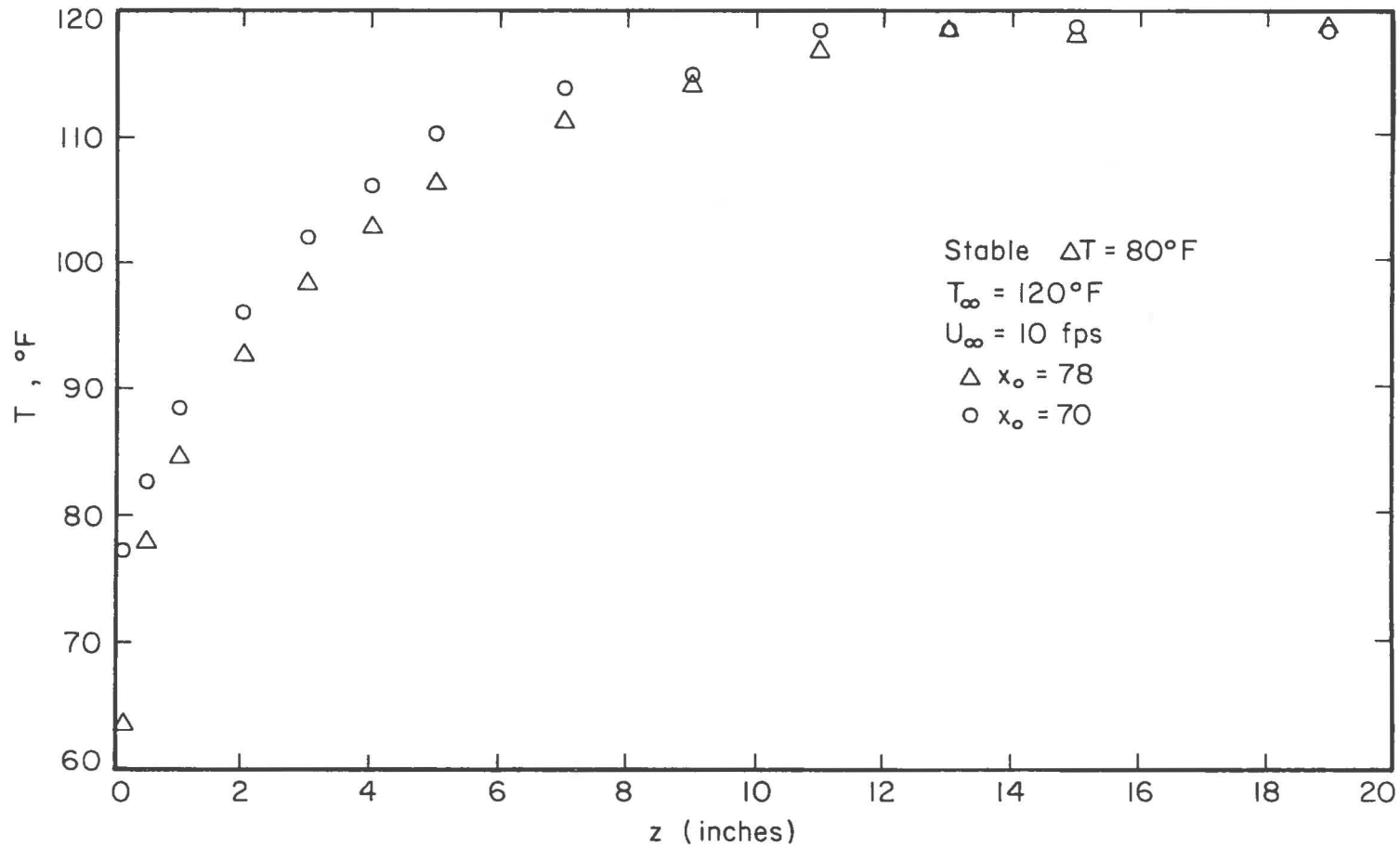

Fig. 13. Comparison temperature profiles at 70 ft and 78 ft sections

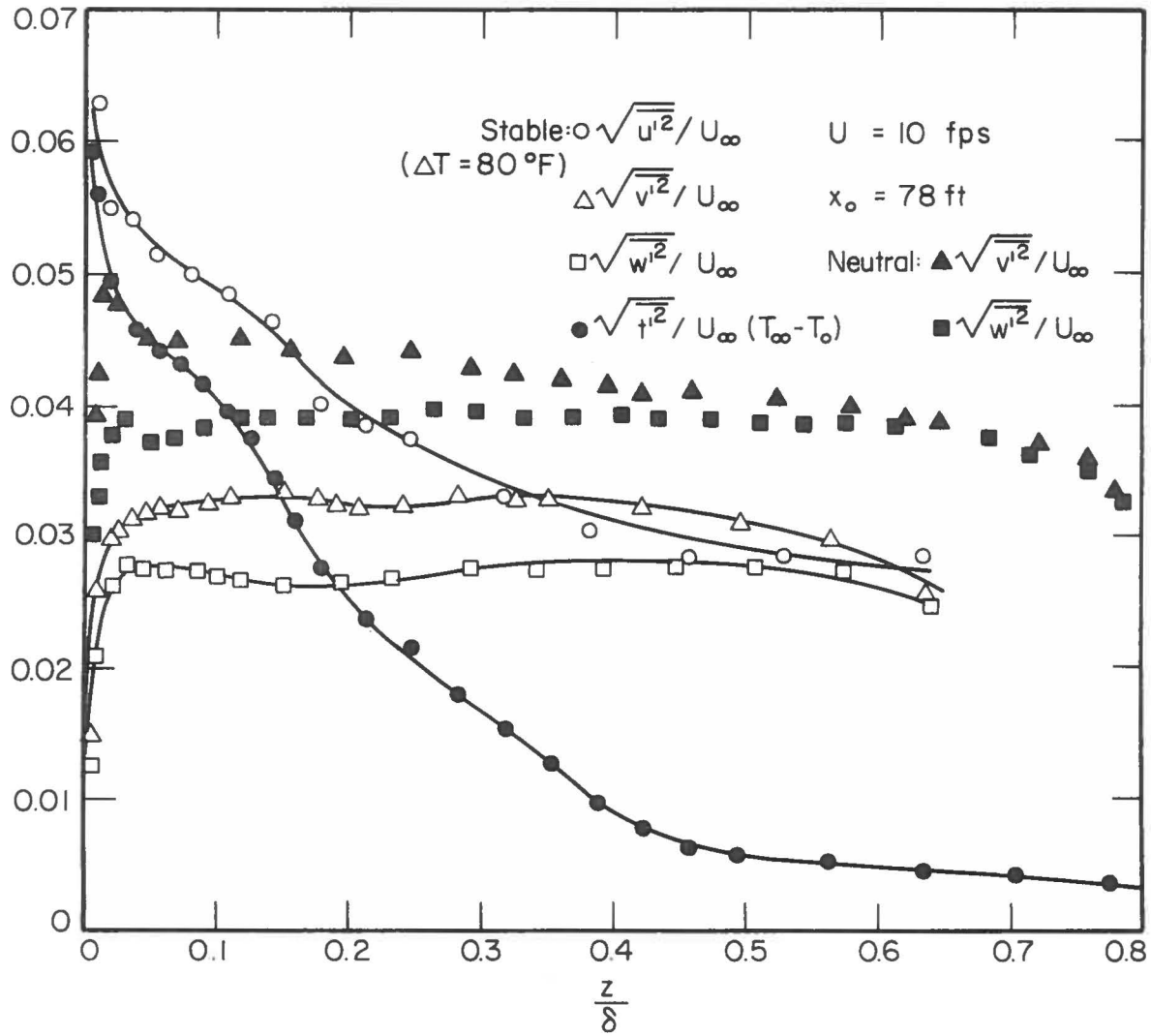

Fig. 14. Distribution of momentum flux (after Arya (1968))

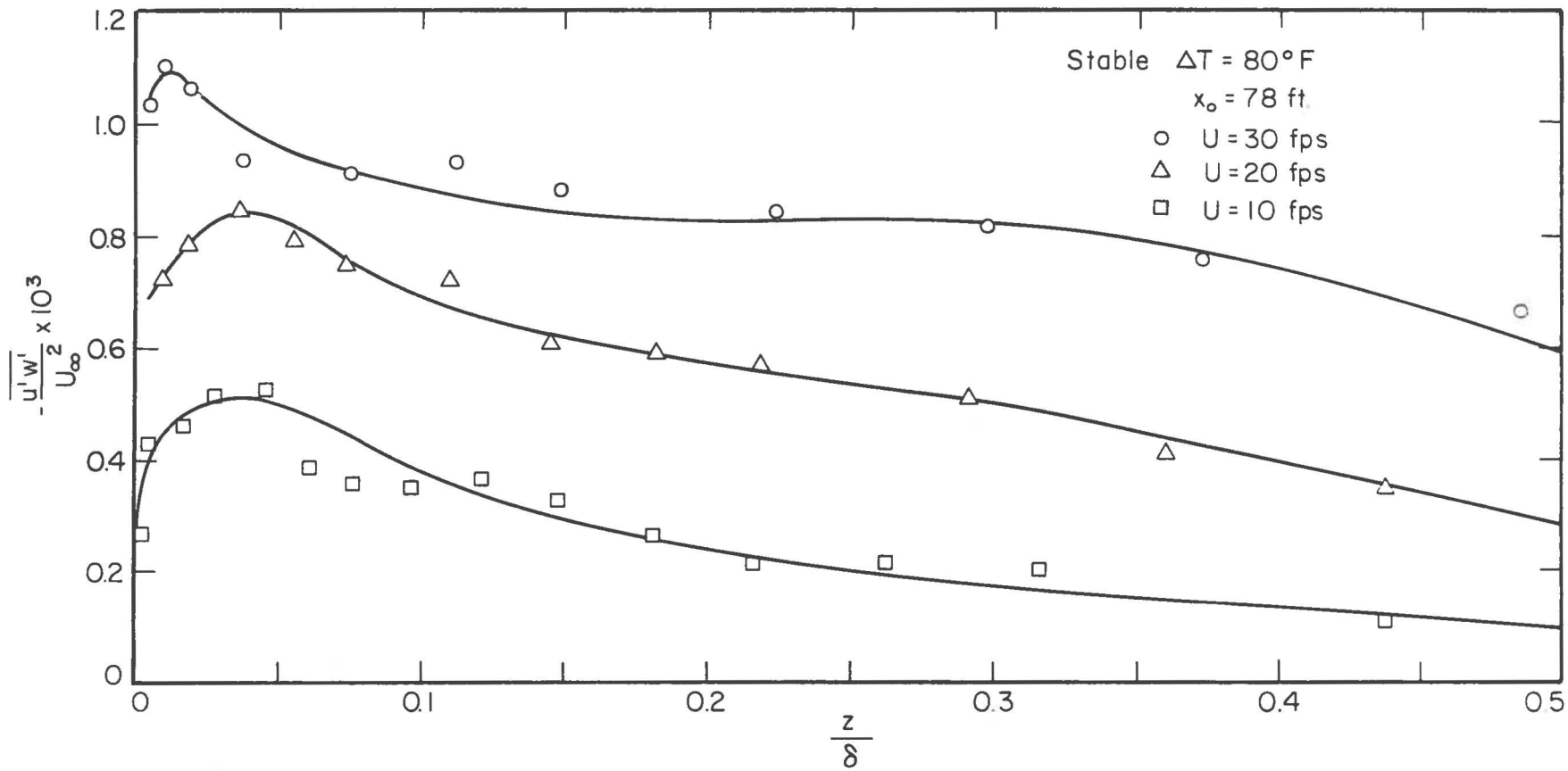

Fig. 15. Vertical secondary flow component $\frac{w}{u_\infty}$ vs $\frac{z}{d}$ (after Arya (1968))

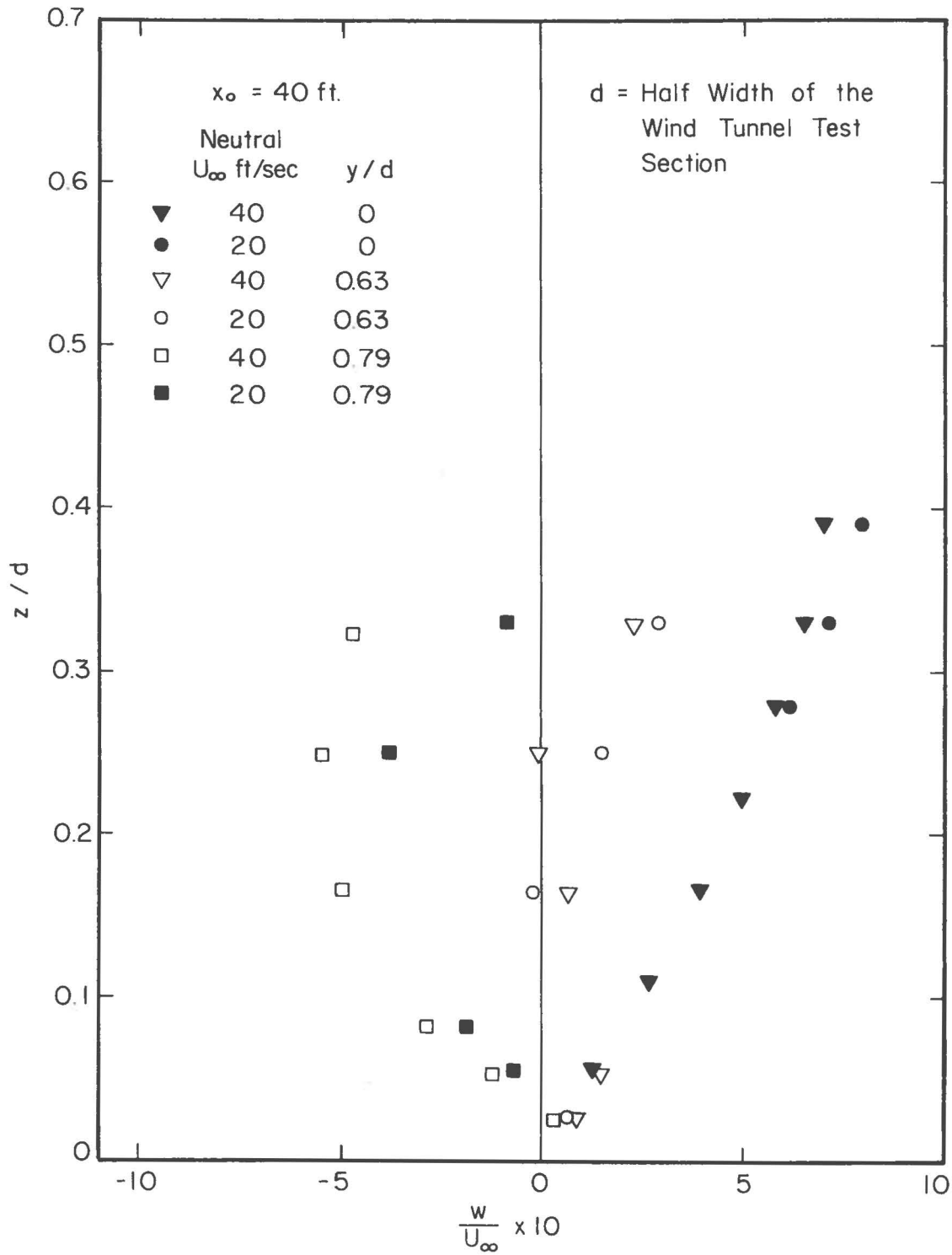

Fig. 16. Distribution of turbulent intensities;
u_∞ = 10 fps T = 80°F (after Veenhuizen (1969))

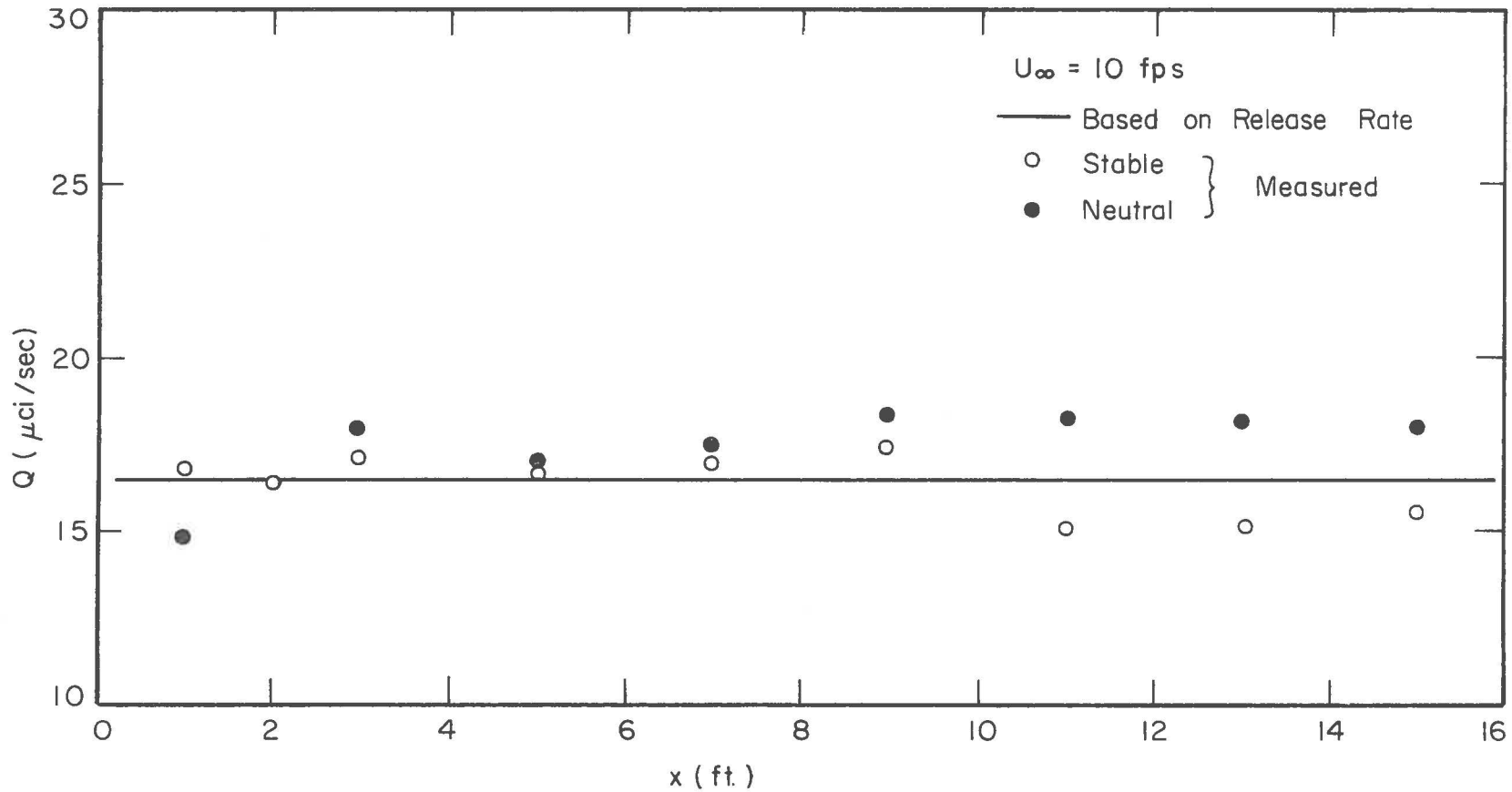

Fig. 17. Comparison of source strength Q with values calculated from concentration data from x = 1' to x = 15'

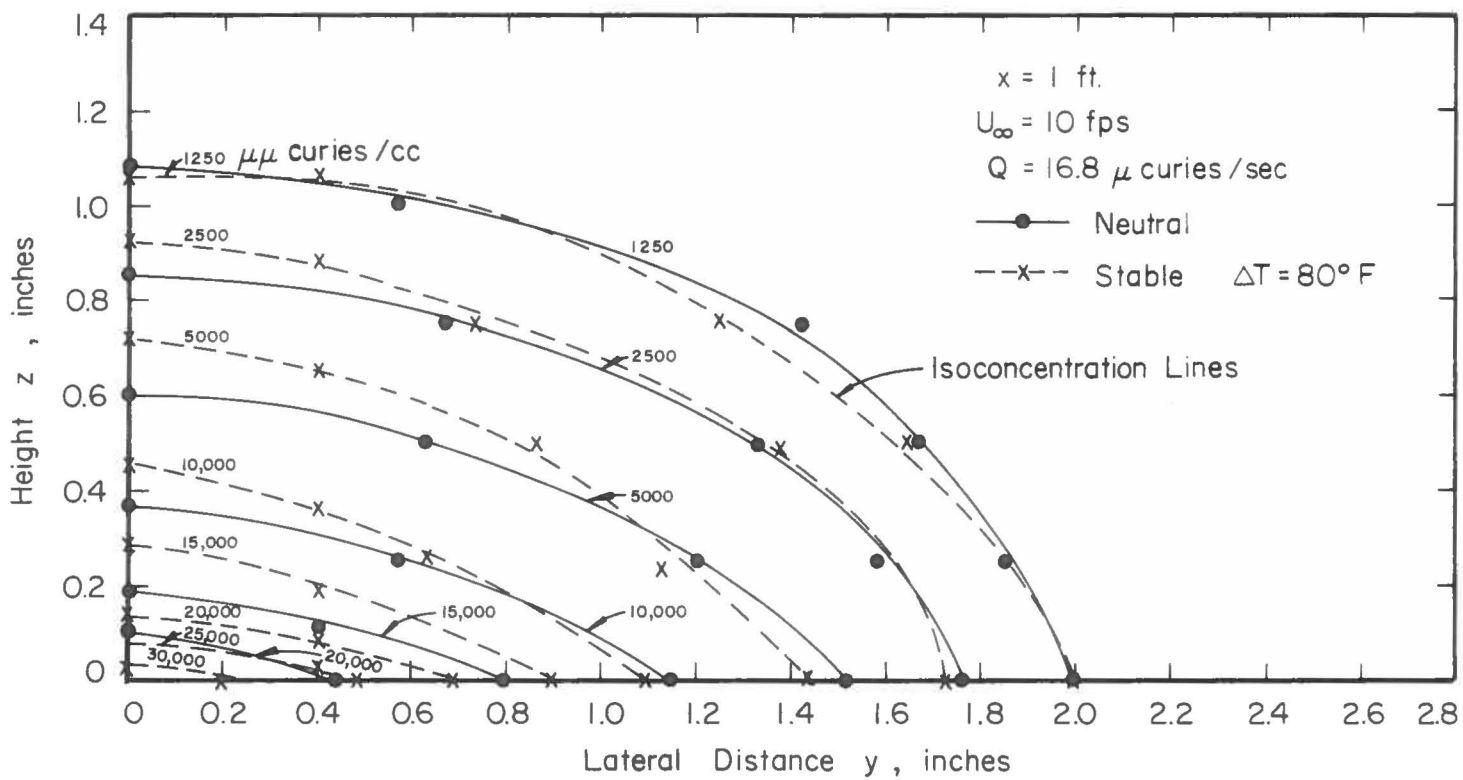

Fig. 18. Isopleths of Kr-85 concentration, in a vertical plane across the wind, at x = 1' under stable and neutral conditions

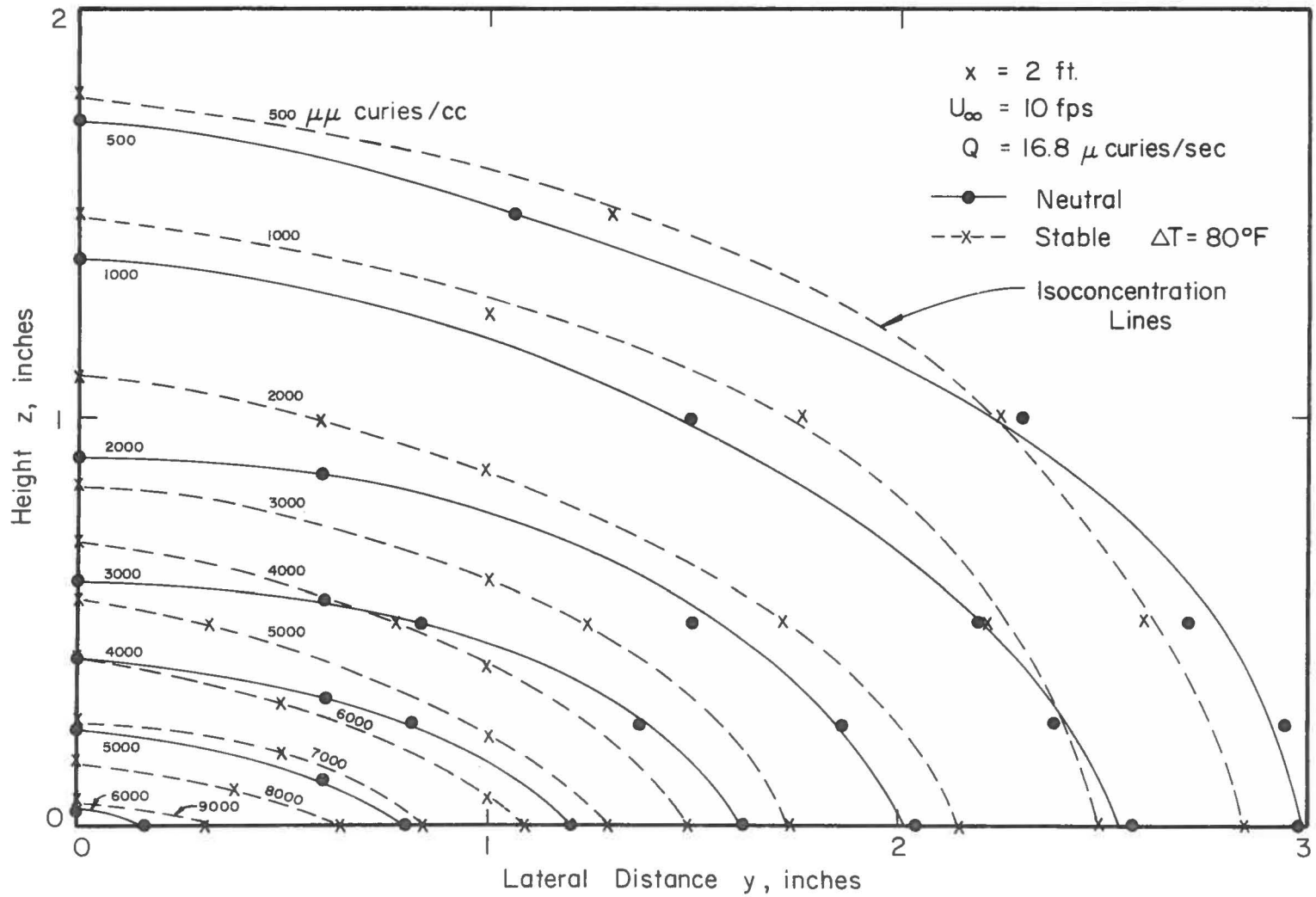

Fig. 19. Isopleths of Kr-85 concentration, in a vertical plane across the wind, at x = 2' under stable and neutral conditions

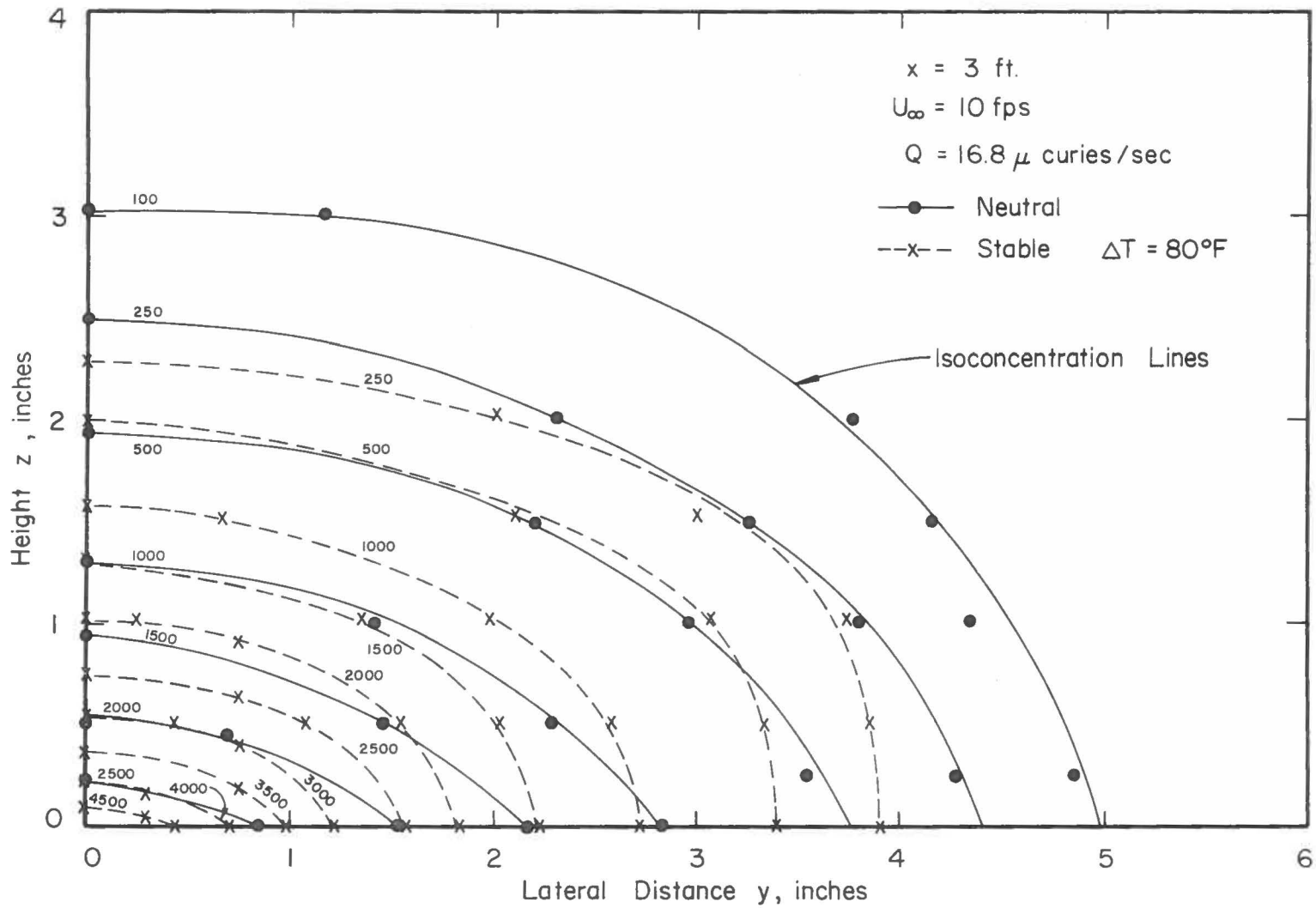

Fig. 20. Isopleths of Kr-85 concentration, in a vertical plane across the wind, at x = 3' under stable and neutral conditions

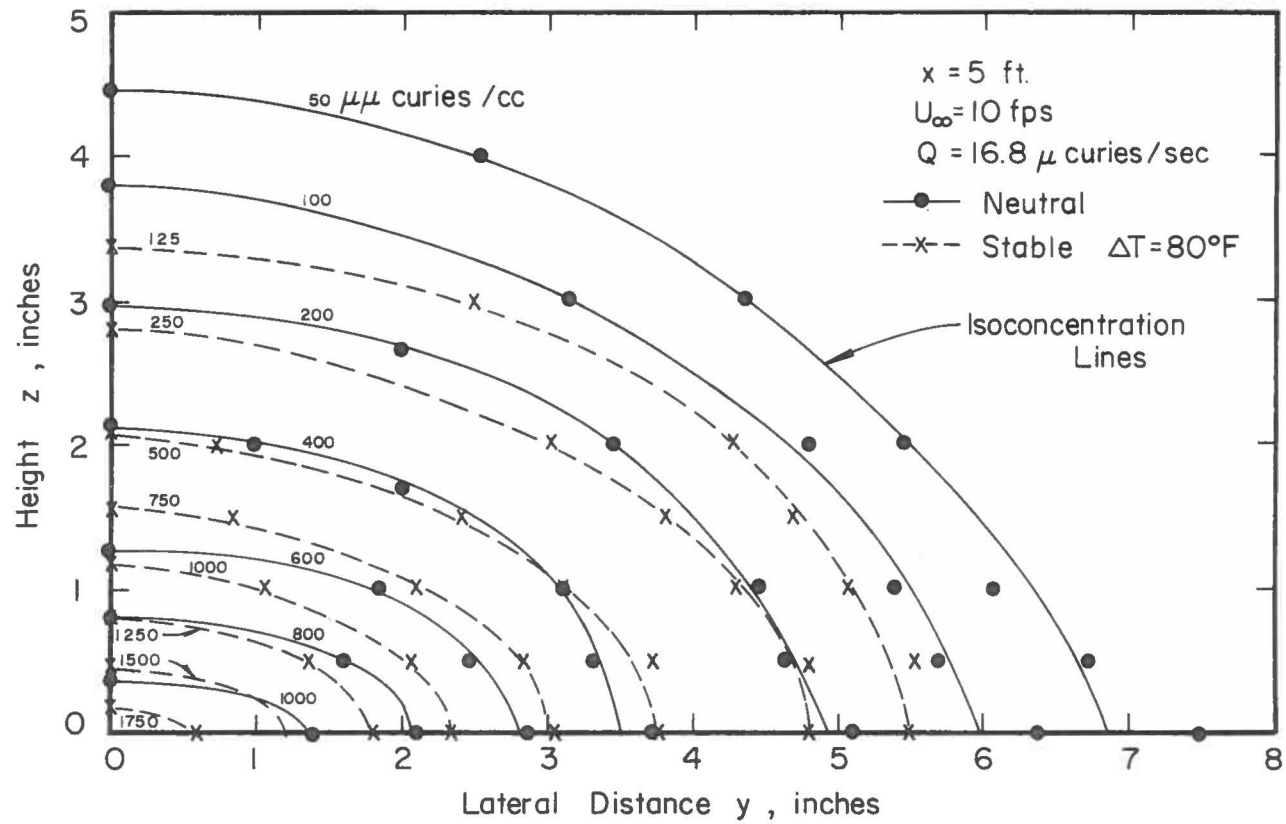

Fig. 21. Isopleths of Kr-85 concentration, in a vertical plane across the wind, at x = 4' under stable and neutral conditions

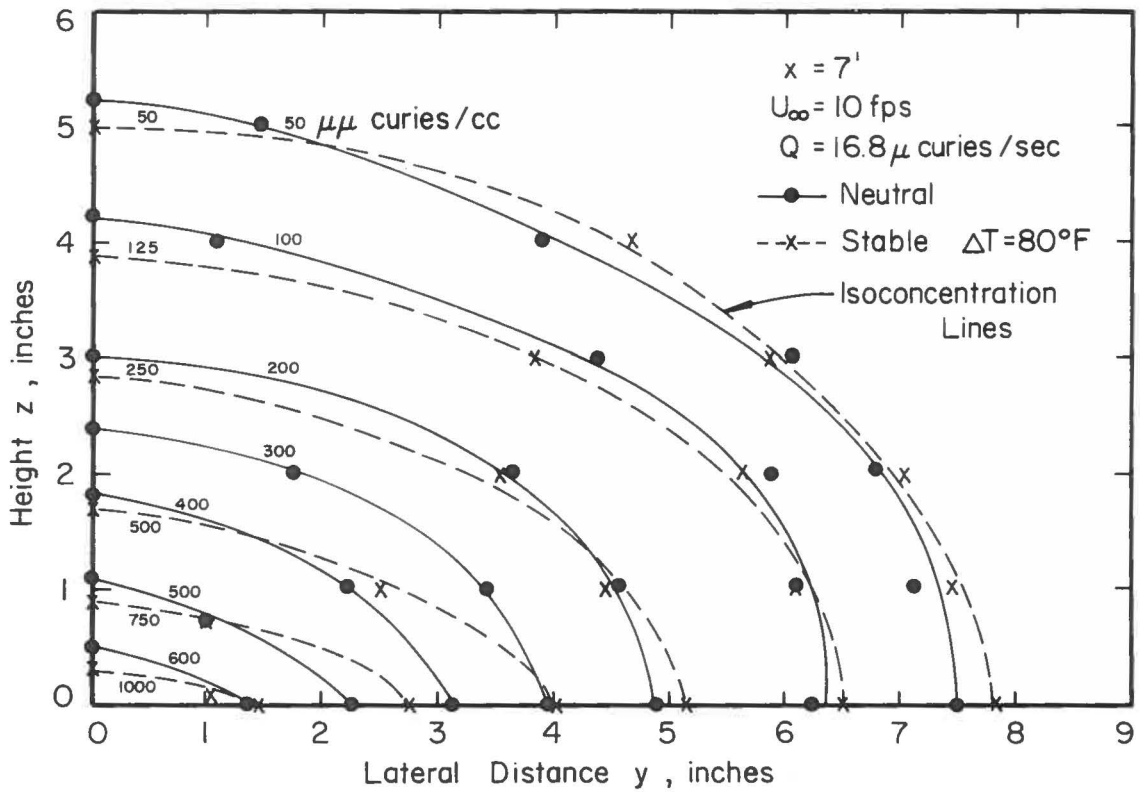

Fig. 22. Isopleths of Kr-85 concentration, in a vertical plane across the wind, at x = 5' under stable and neutral conditions

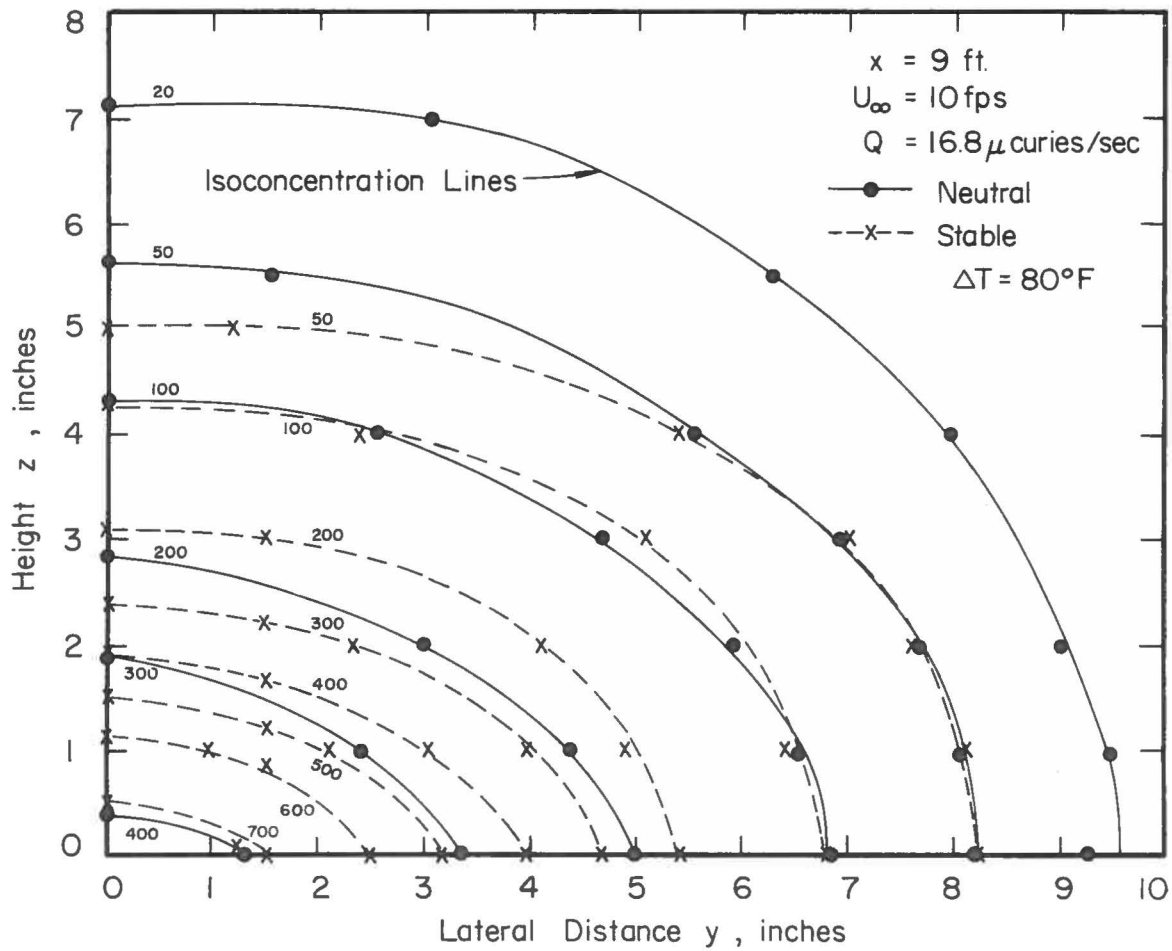

Fig. 23. Isopleths of Kr-85 concentration, in a vertical plane across the wind, at x = 9' under stable and neutral conditions

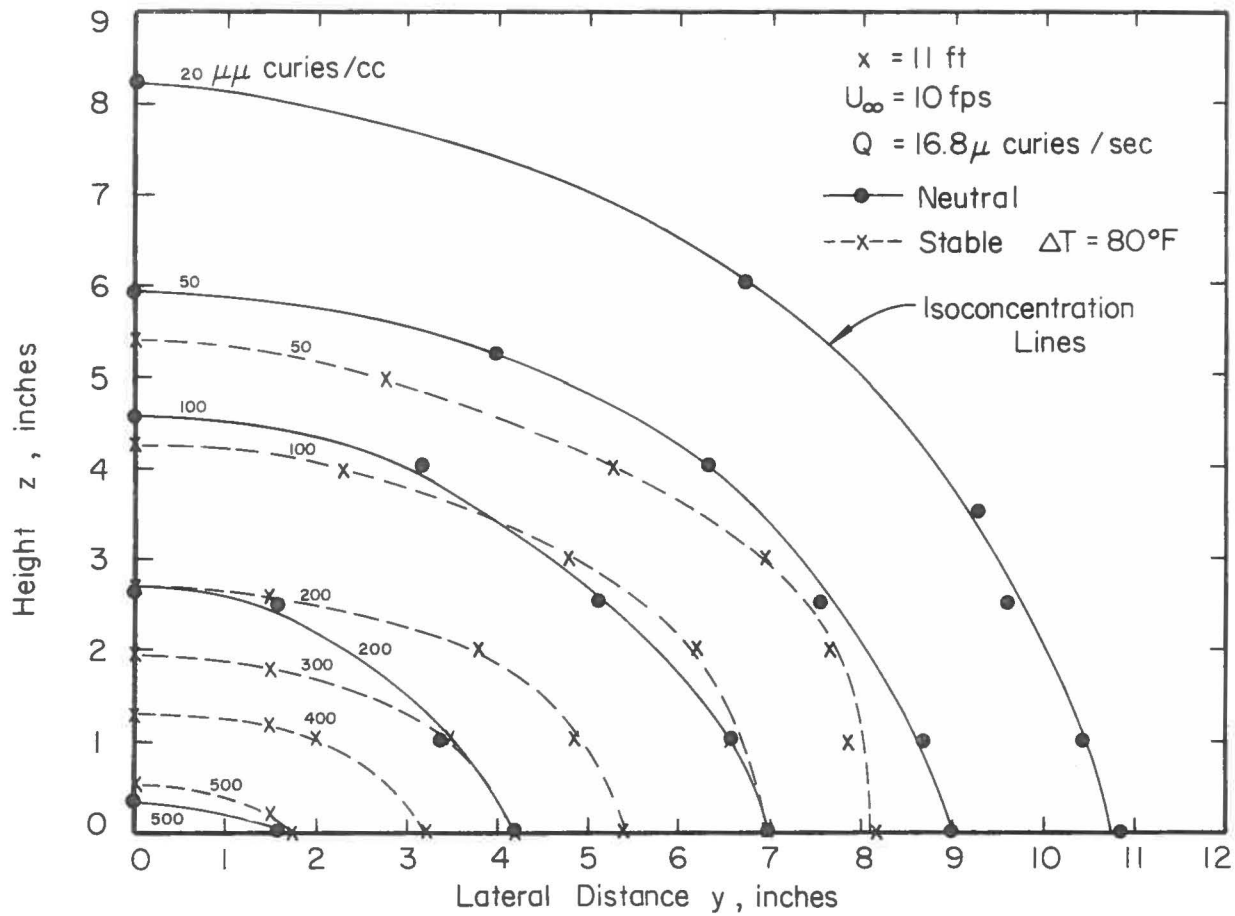

Fig. 24. Isopleths of Kr-85 concentration, in a vertical plane across the wind, at x = 11' under stable and neutral conditions

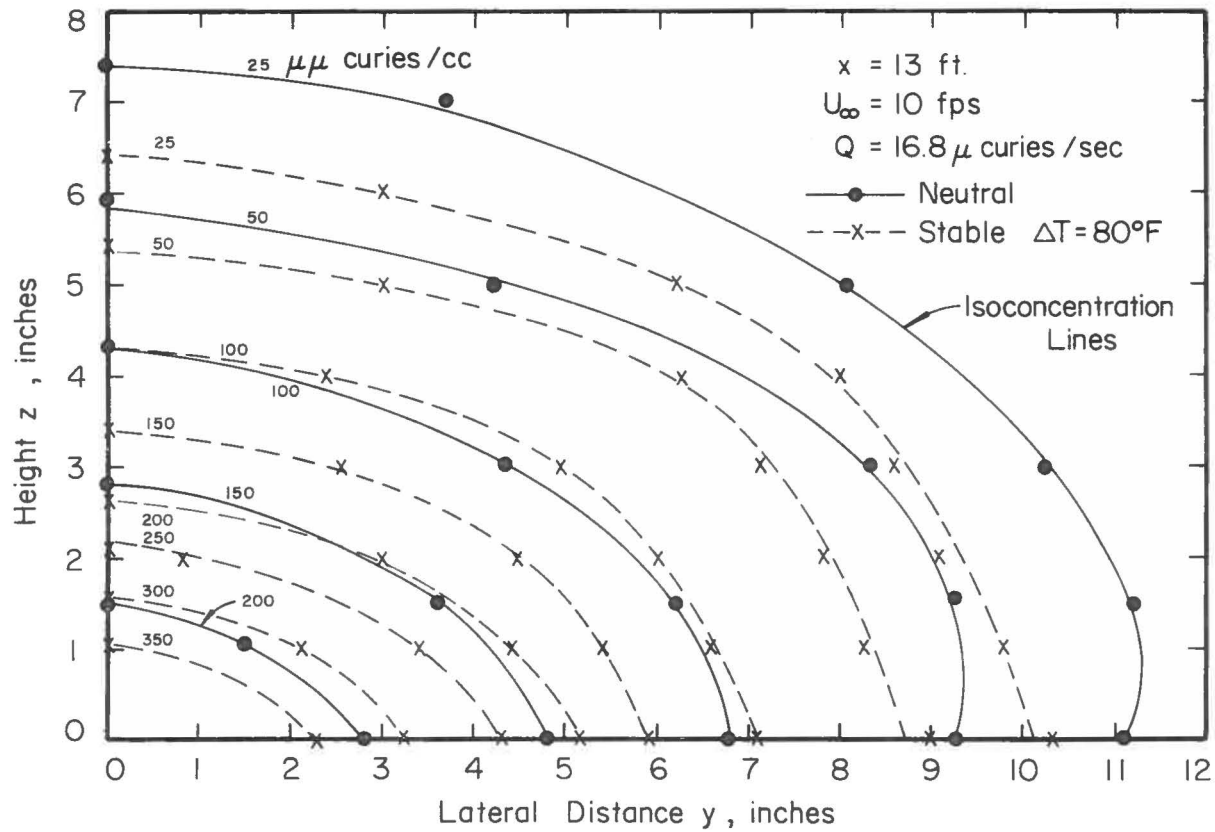

Fig. 25. Isopleths of Kr-85 concentration, in a vertical plane across the wind, at x = 13' under stable and neutral conditions

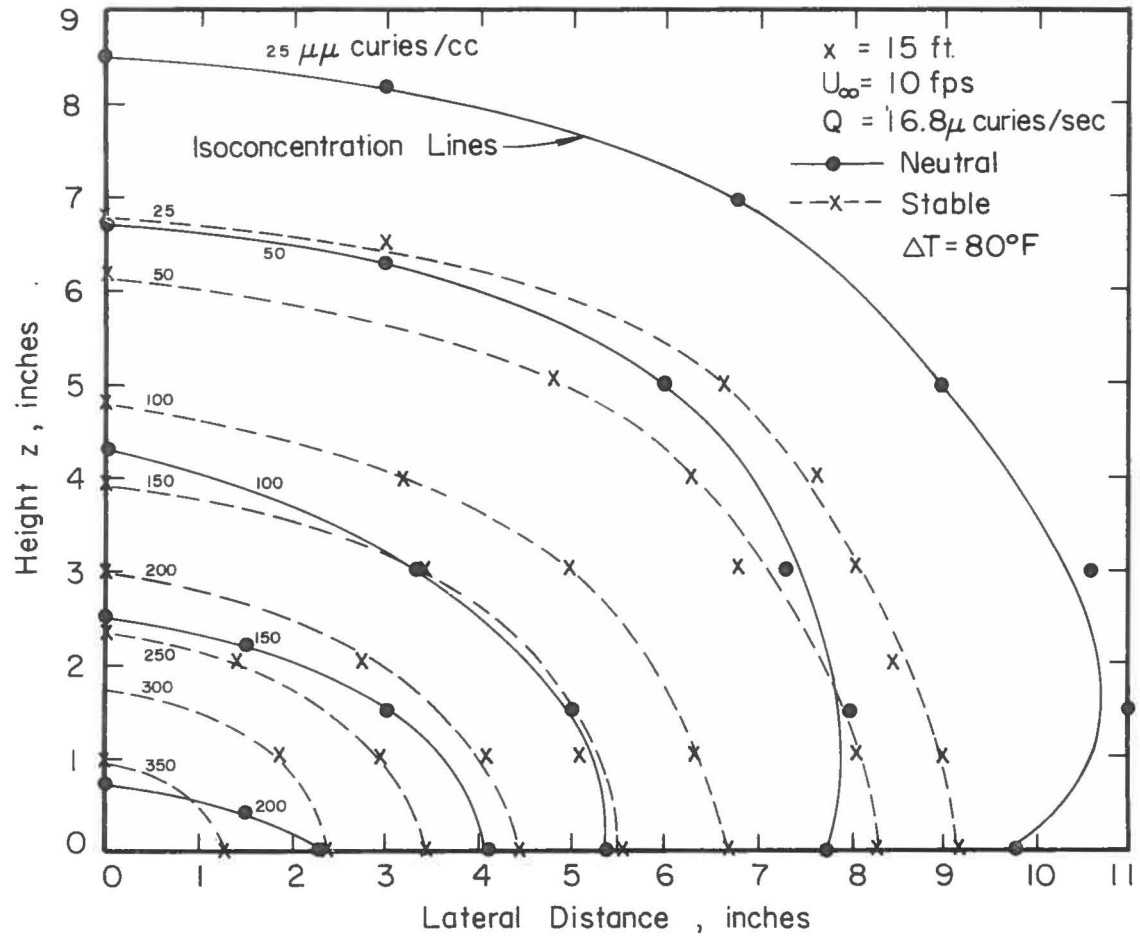

Fig. 26. Isopleths of Kr-85 concentration, in a vertical plane across the wind, at x = 15' under stable and neutral conditions

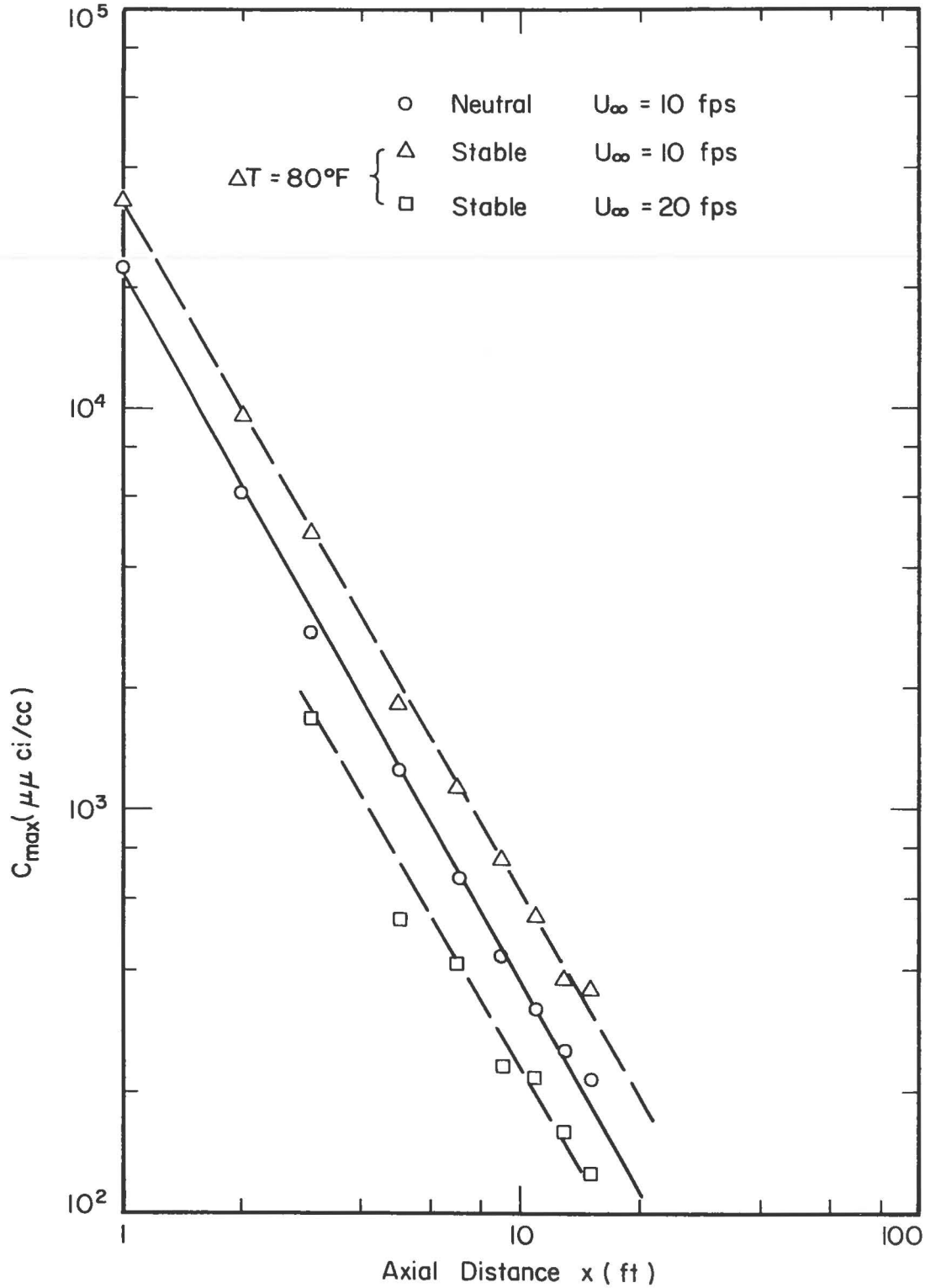

Fig. 27. The variation of maximum concentration with axial distance for ground source under various stability conditions

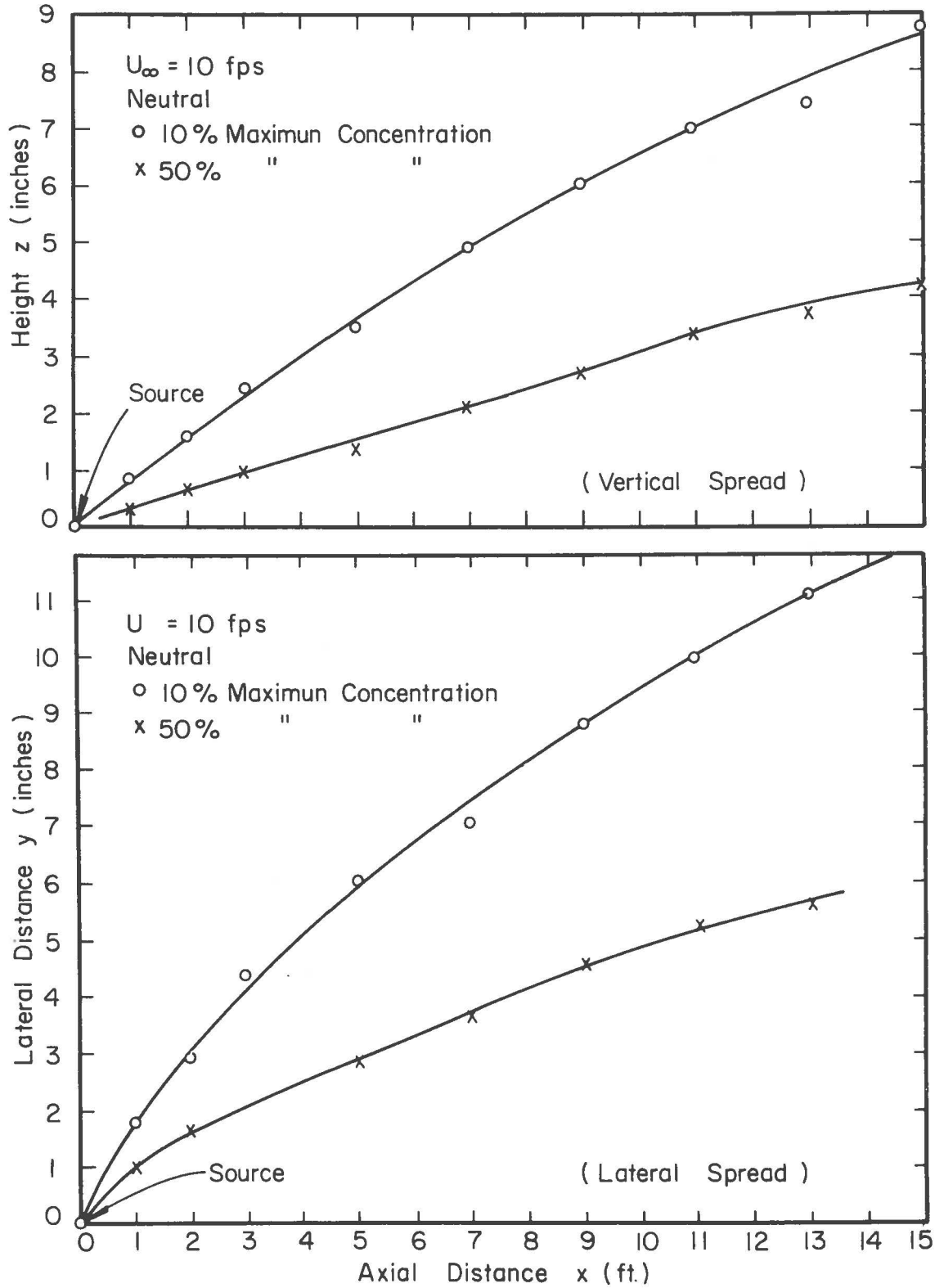

Fig. 28. Vertical and lateral spreads of the ground source plume; u_∞ = 10 fps ΔT = 0

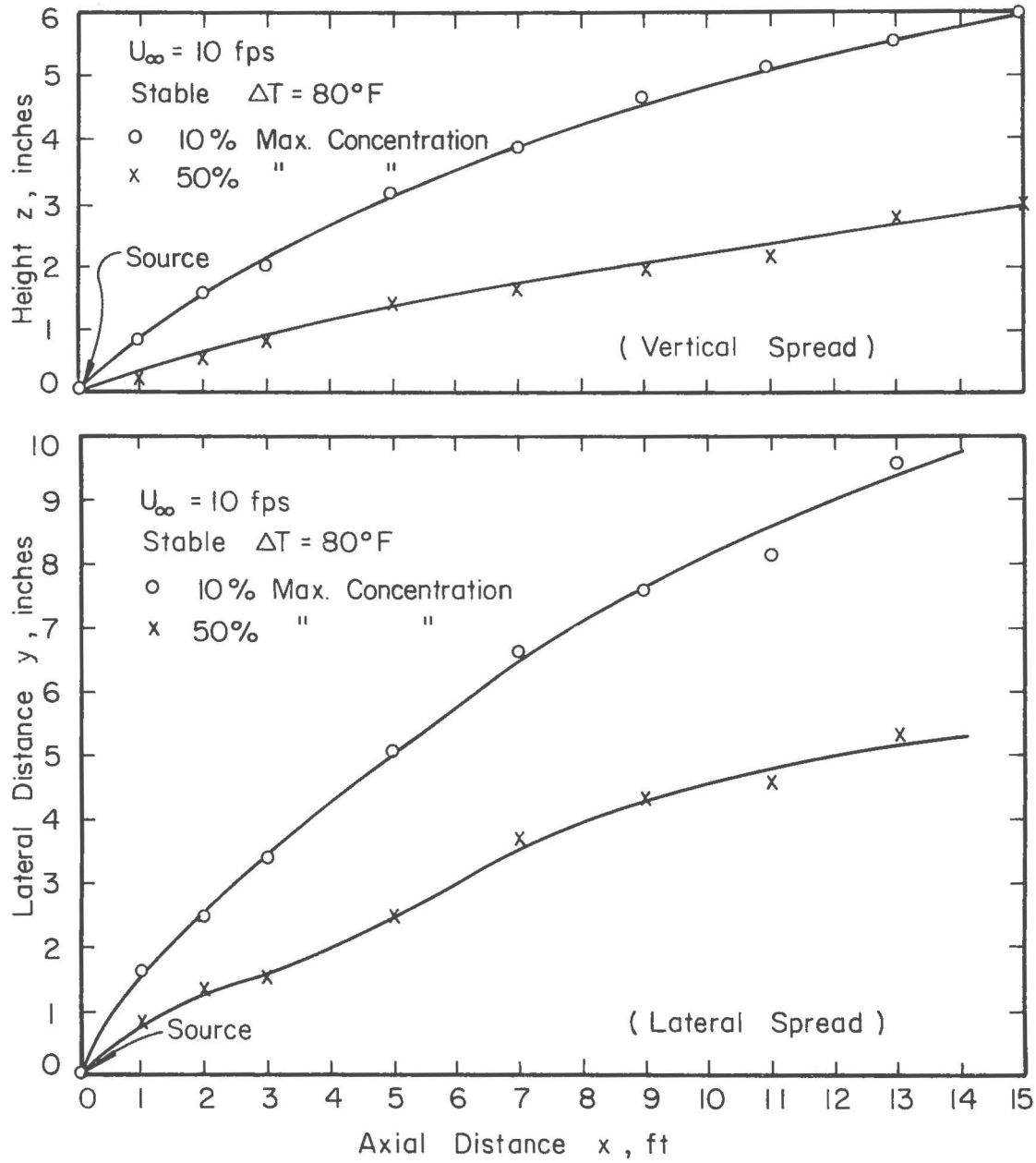

Fig. 29. Vertical and lateral spreads of the ground source plume; u_∞ = 10 fps stable, ΔT = 80°F

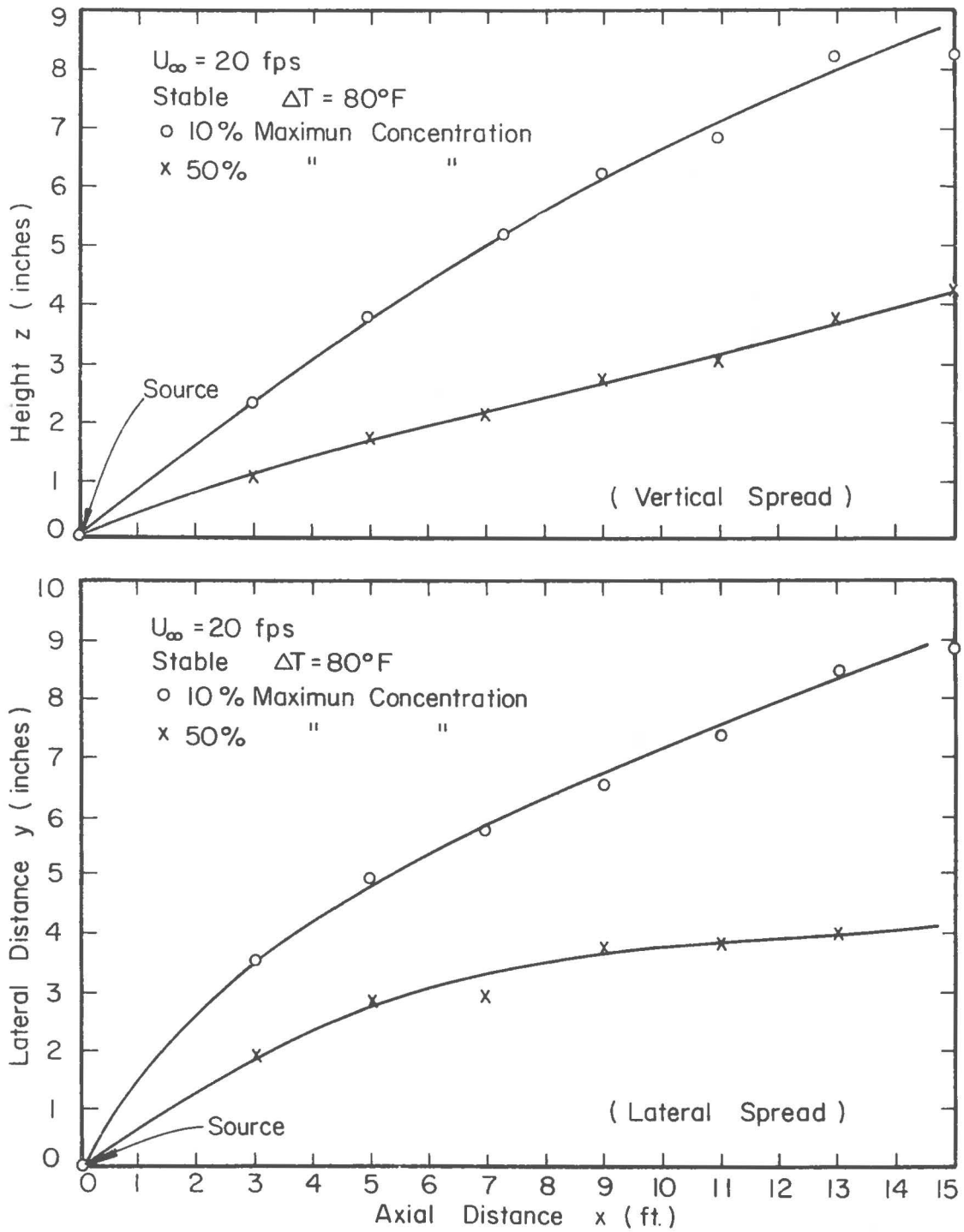

Fig. 30. Vertical and lateral spreads of the ground source plume; u_∞ = 20 fps stable, ΔT = 80°F

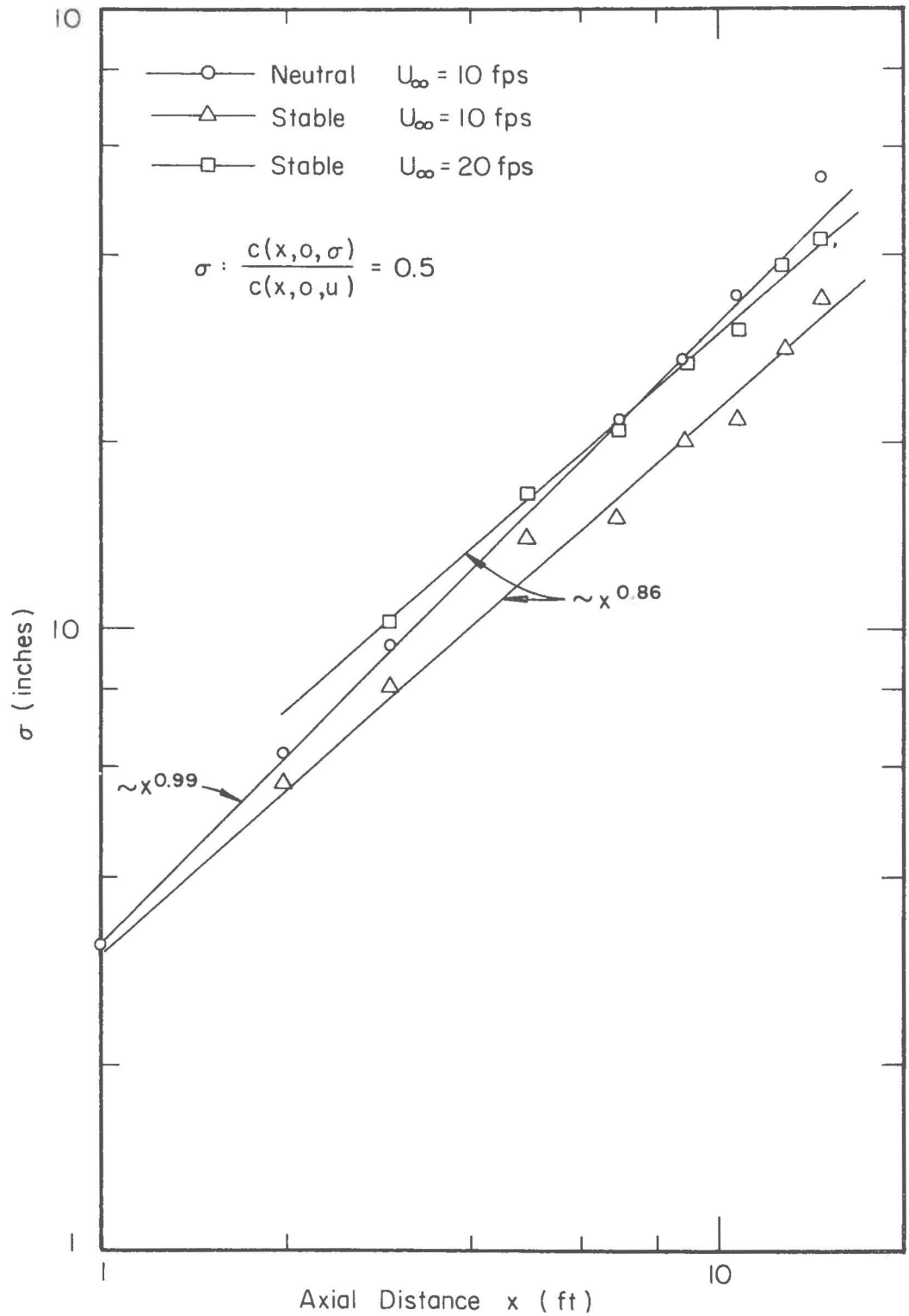

Fig. 31. Vertical spreads of the ground source plumes in terms of 50% height σ

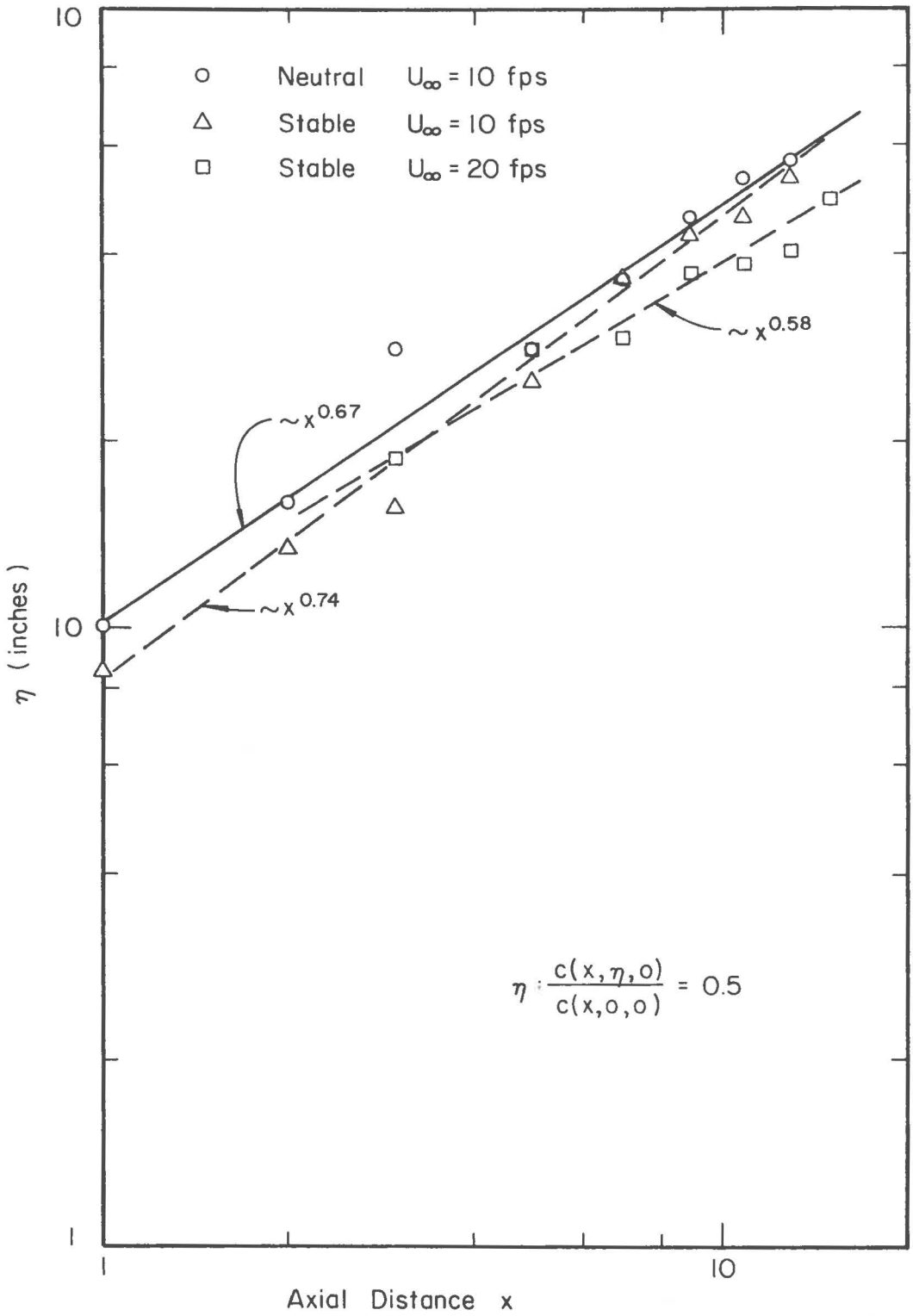

Fig. 32. Lateral spreads of the ground source plumes in terms of 50% width η

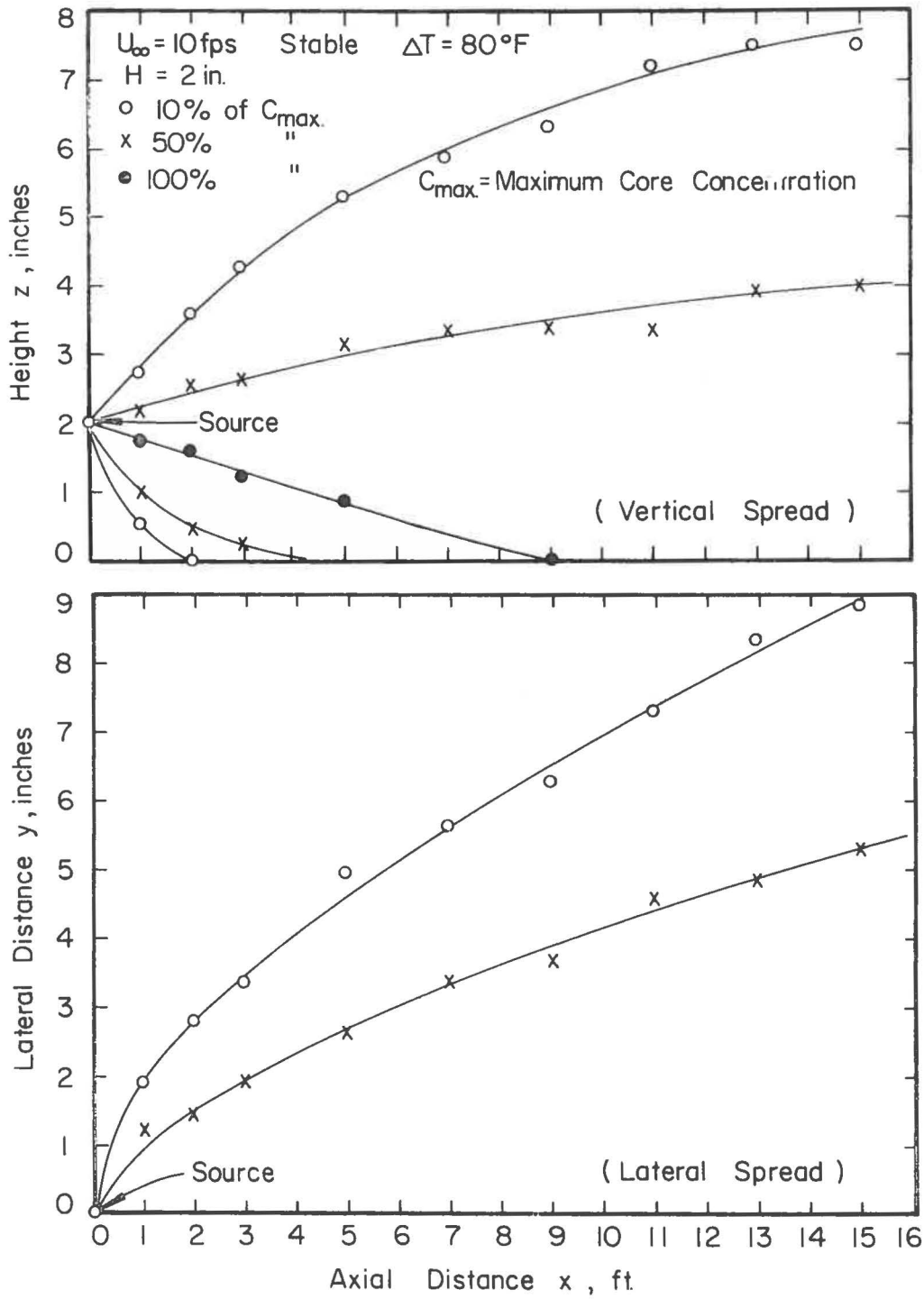

Fig. 33. Vertical and lateral spreads of the elevated point source plume, H = 2" u_∞ = 10 fps stable, ΔT = 80°F

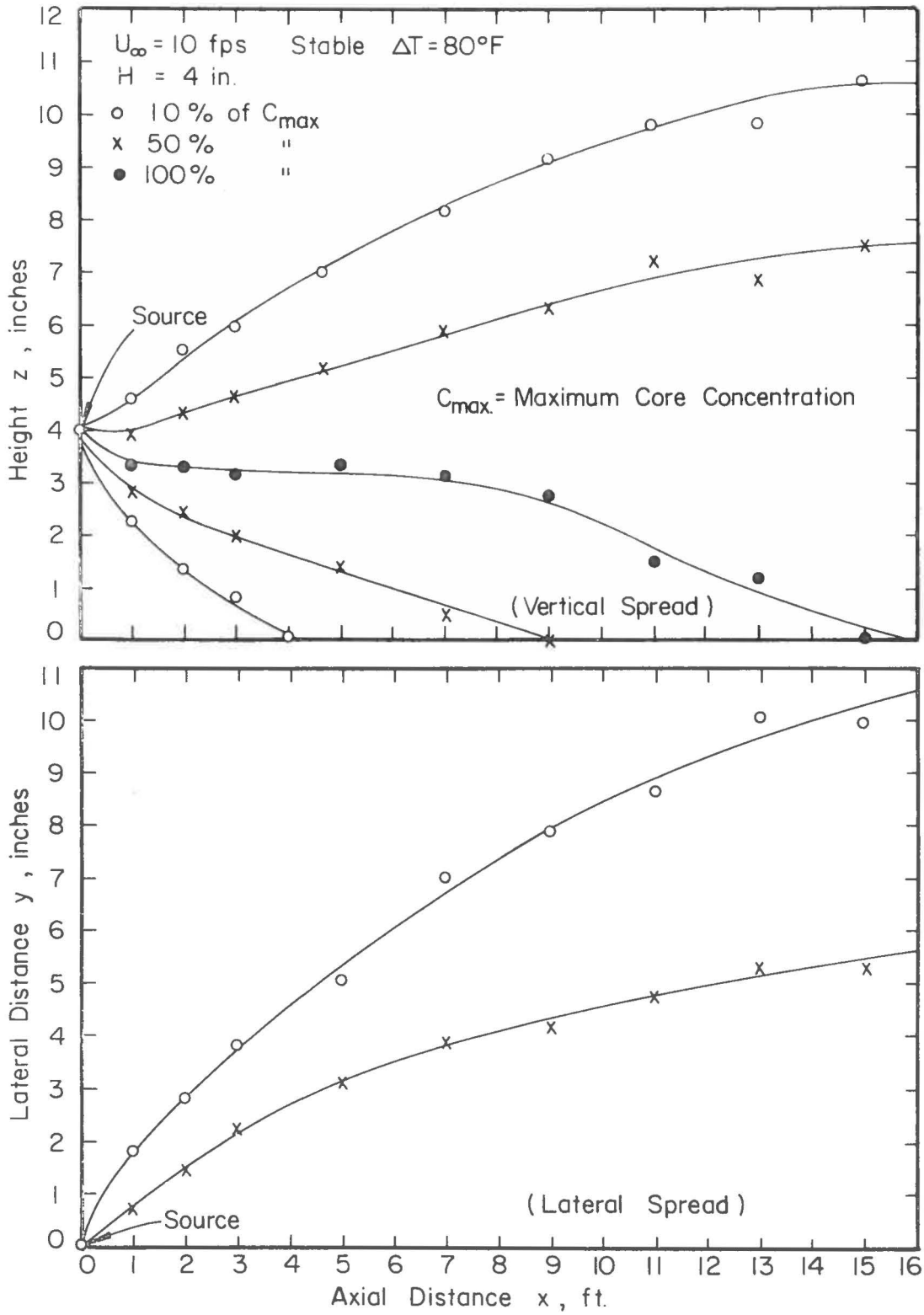

Fig. 34. Vertical and lateral spreads of the elevated point source plume, H = 4" u_∞ = 10 fps stable, ΔT = 80°F

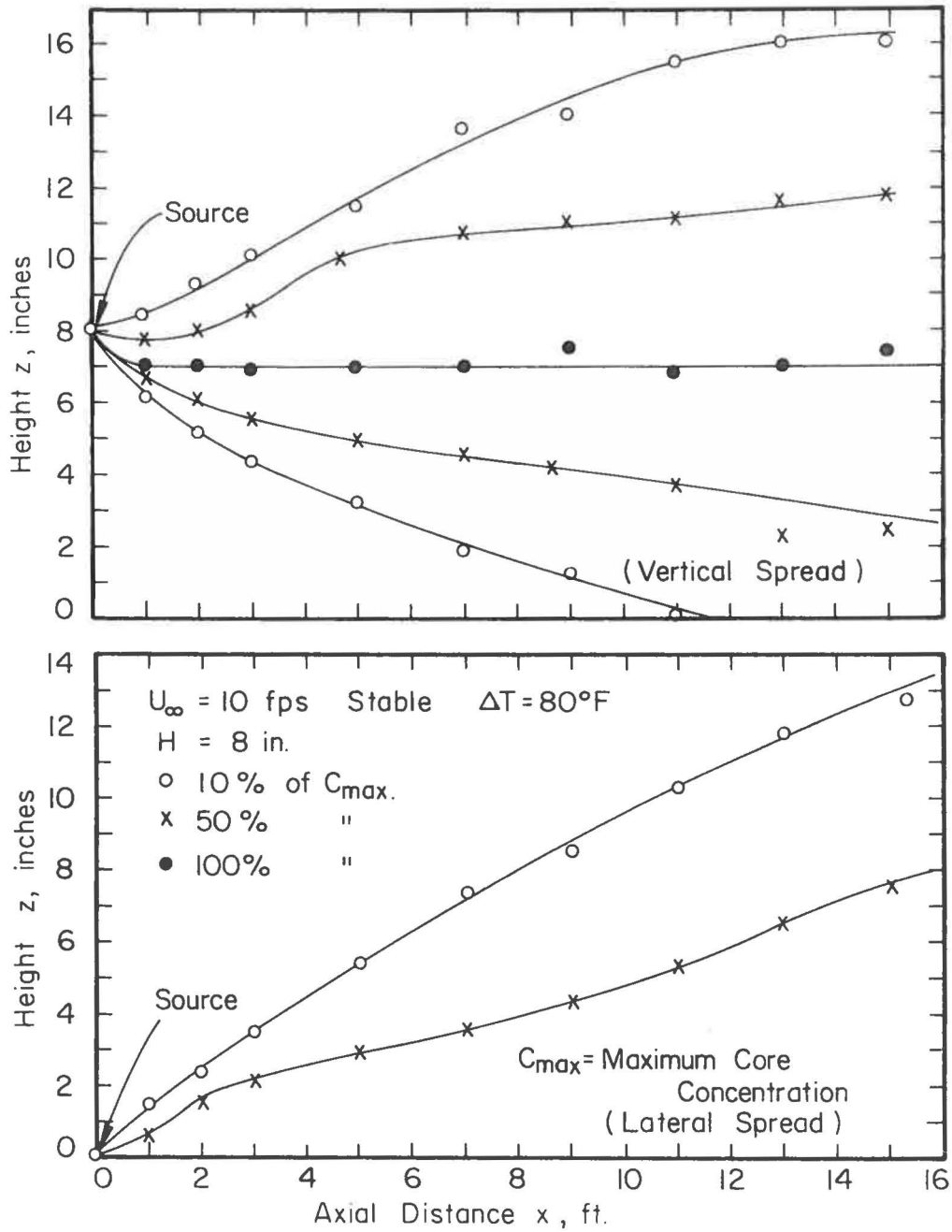

Fig. 35. Vertical and lateral spreads of the elevated point source plume, H = 8" u_∞ = 10 fps stable, ΔT = 80°F

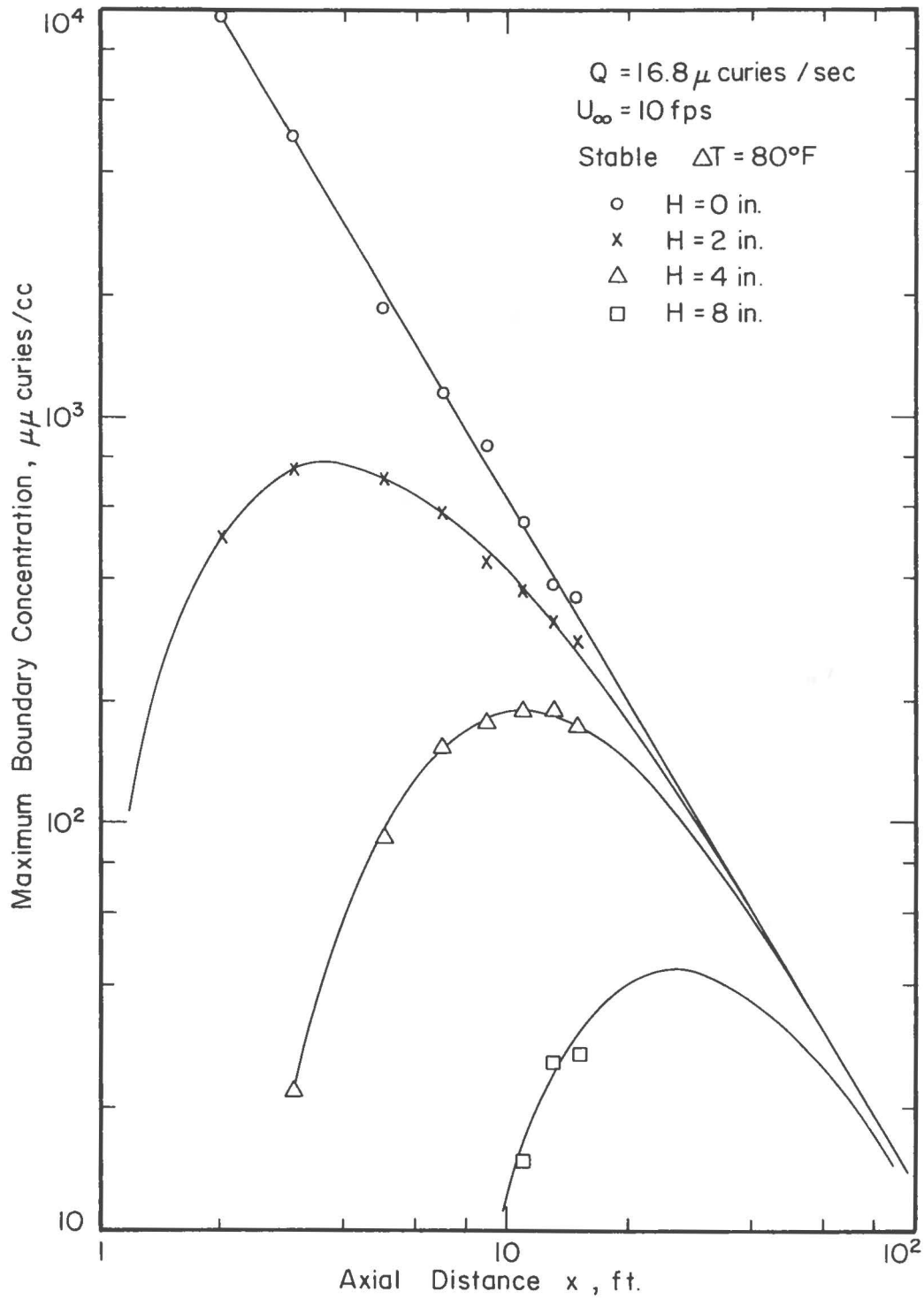

Fig. 36. The variation of maximum ground level concentration for various elevated sources; u_∞ = 10 fps stable ΔT = 80°F

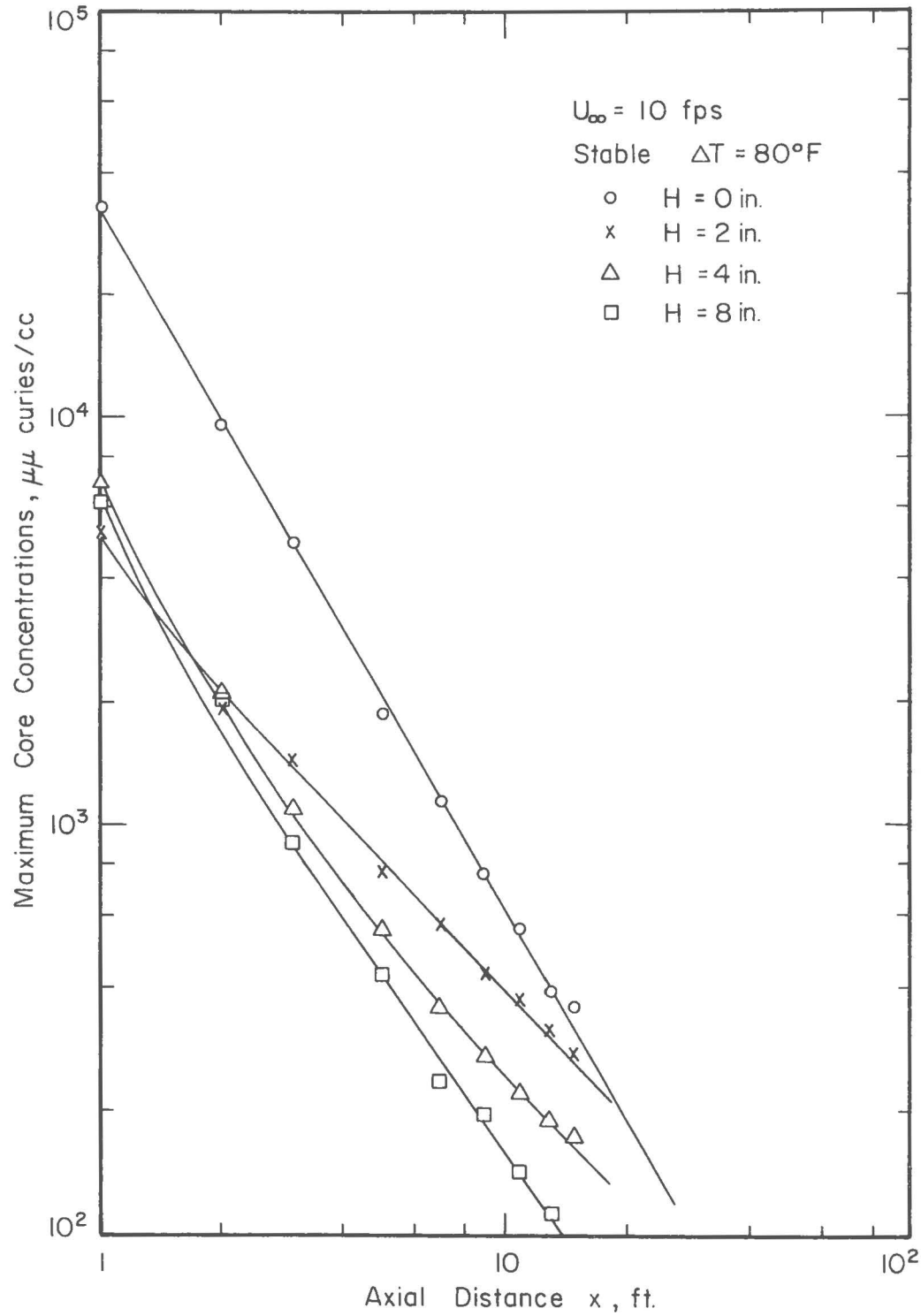

Fig. 37. The variation of maximum core concentration with axial distance for various elevated sources; u_∞ = 10 fps stable, ΔT = 80°F

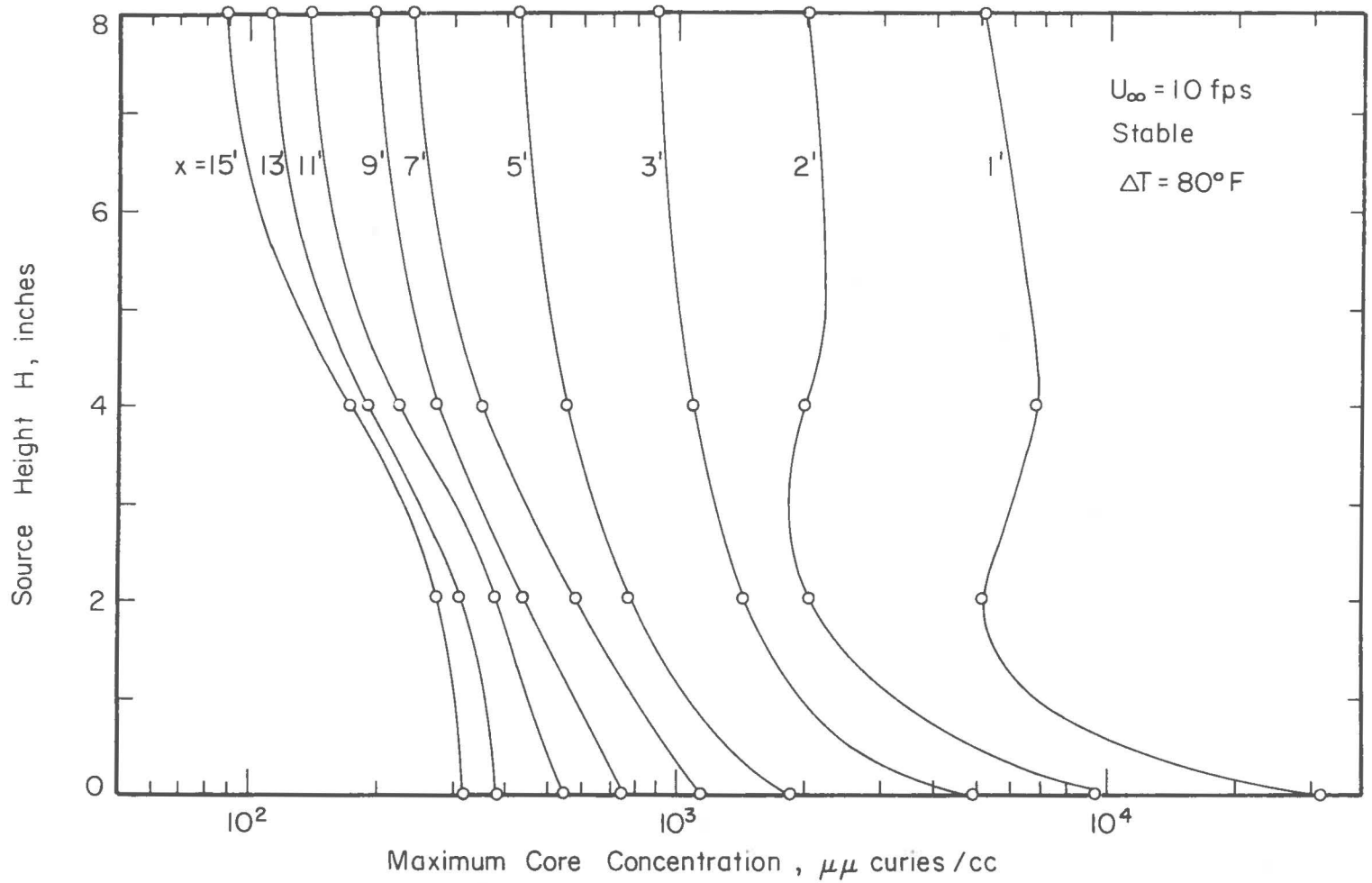

Fig. 38. The effect of source elevation on the maximum concentration at various distances; u_∞ = 10 fps stable ΔT = 80°F

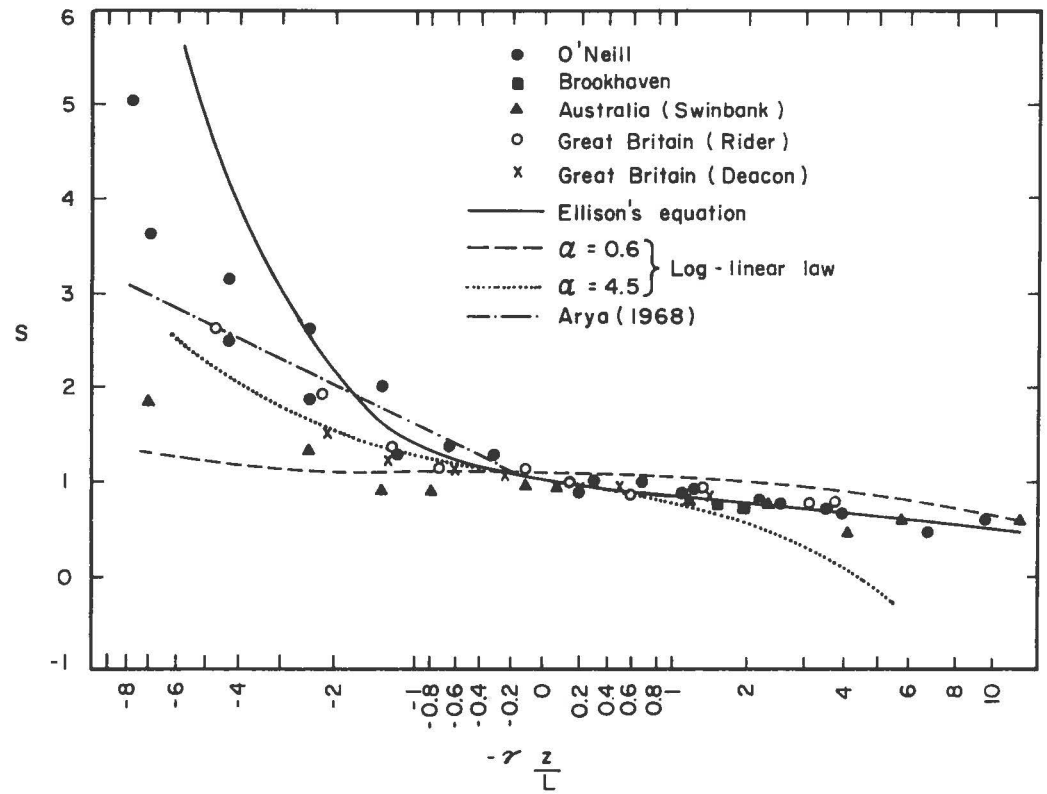

Fig. 39. "universal" relation between the non-dimensional wind shear s and the non-dimensional height z/L (according to Panofsky et al, 1960)

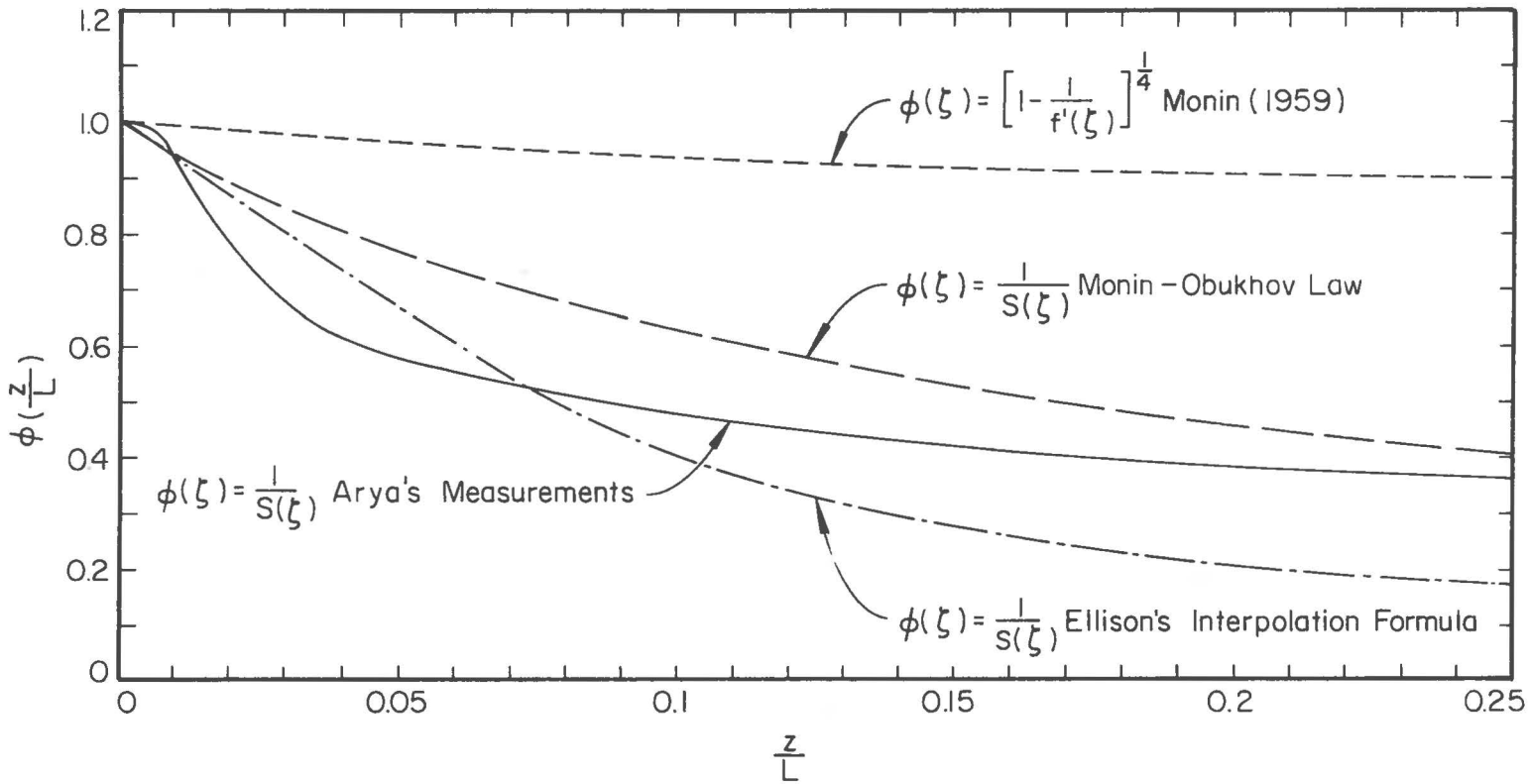

Fig. 40. Function $\phi(\zeta)$ according to different formulas

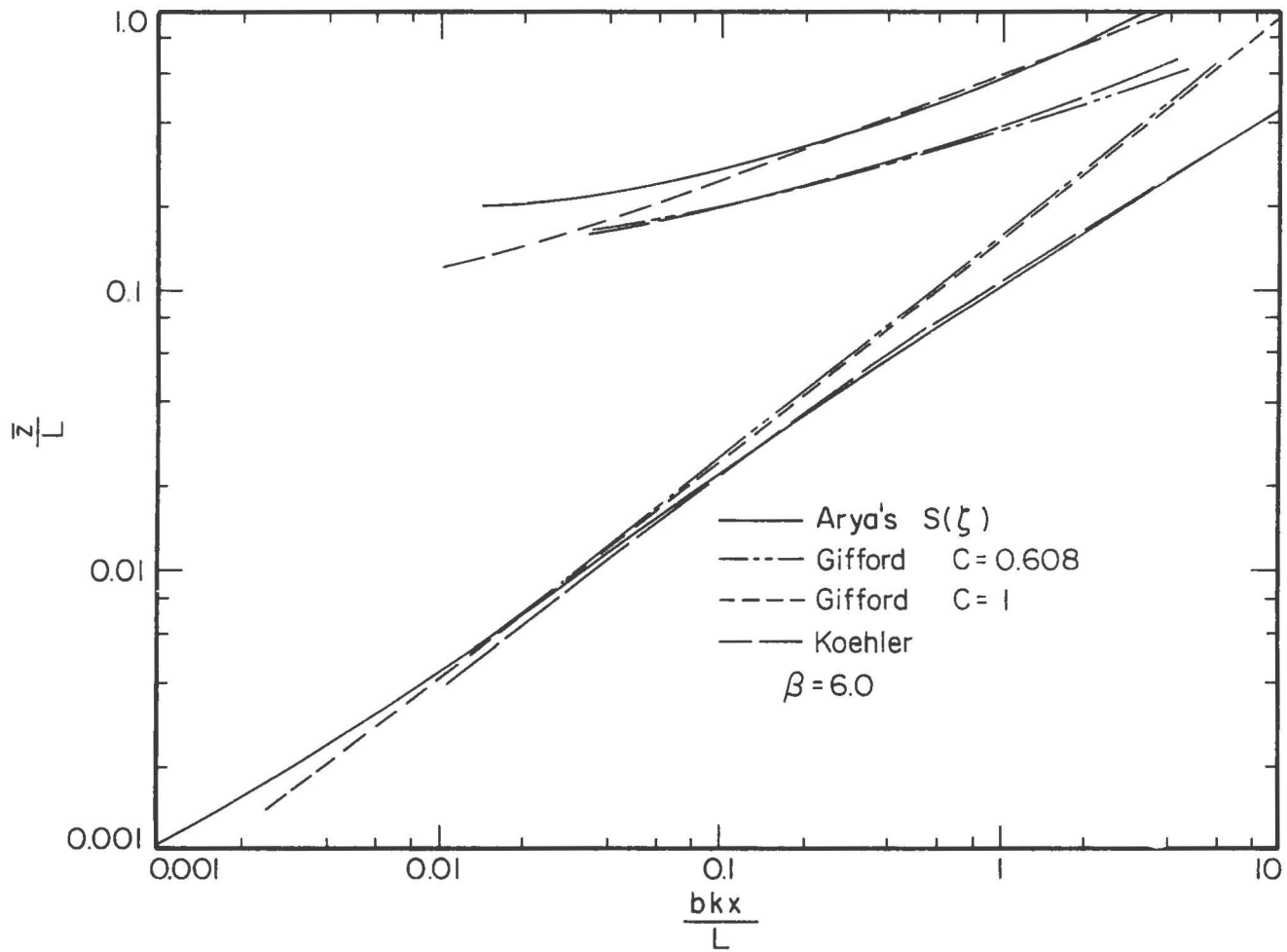

Fig. 41. Average non-dimensional plume rise z/L vs $bk\bar{x}/L$ for various $\phi(\zeta)$

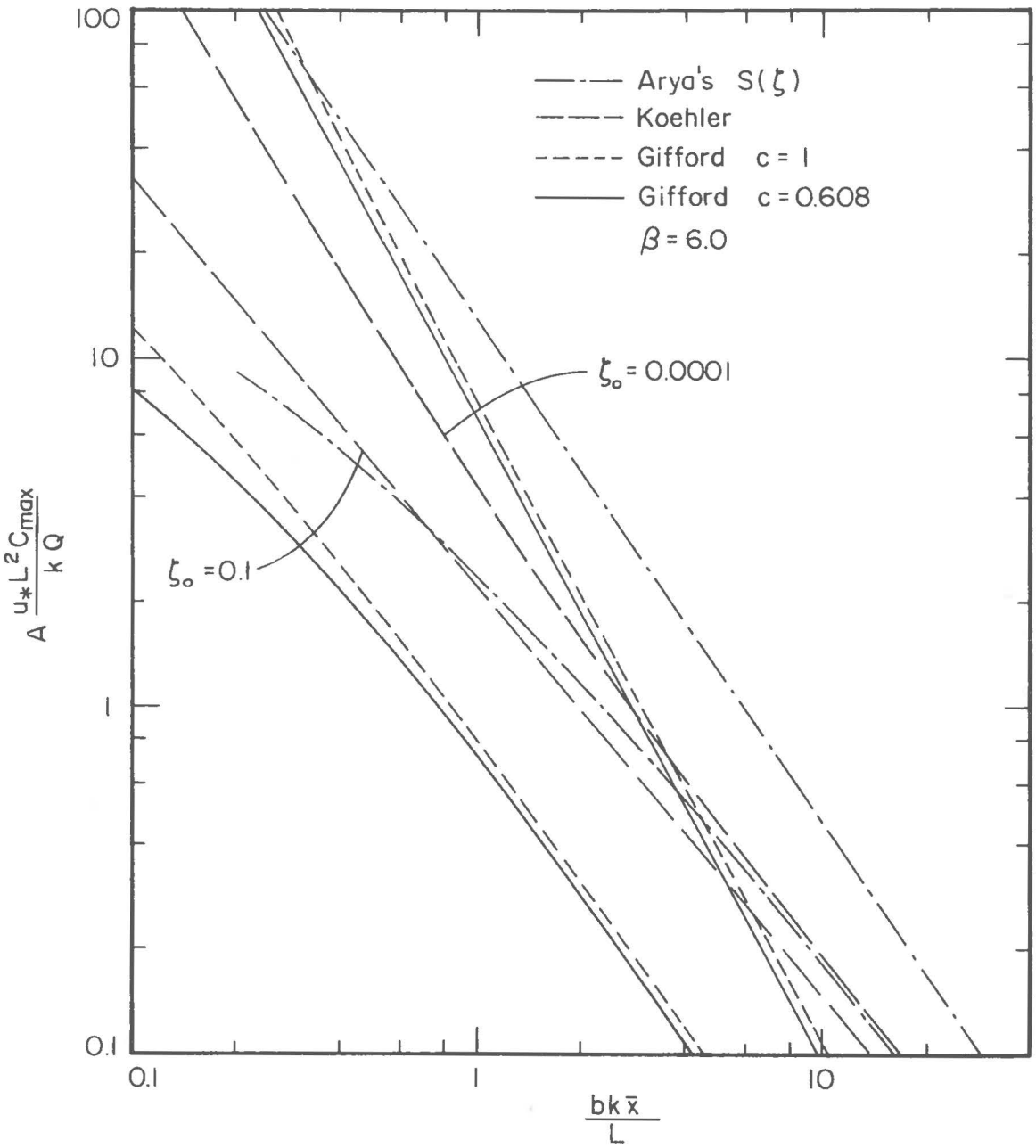

Fig. 42. Maximum ground level concentration $u_* L^2 c_{max}/AkQ$ vs $bk\bar{x}/L$ for various $\phi(\zeta)$

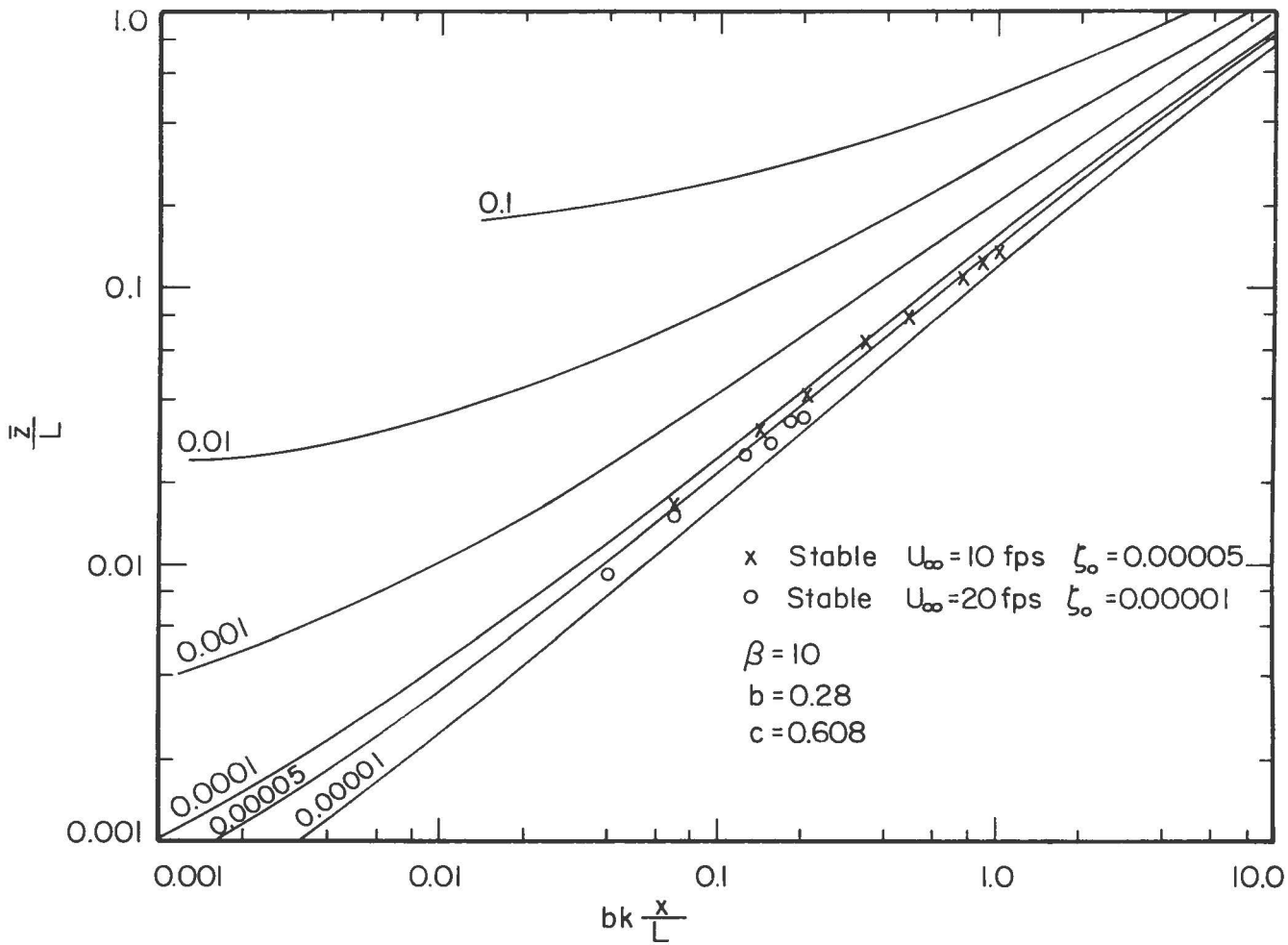

Fig. 43. Comparison of average non-dimensional plume rise data with similarity theory

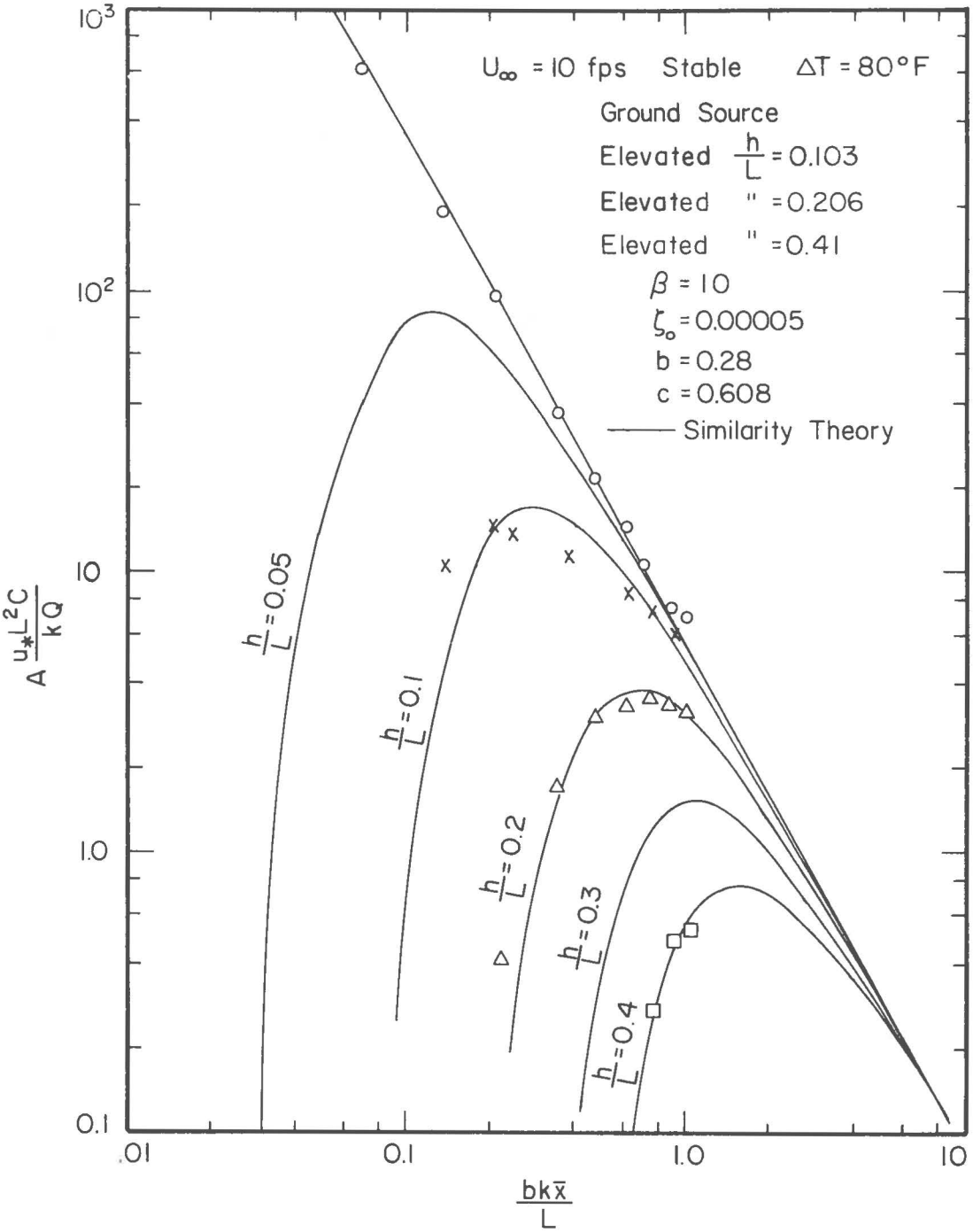

Fig. 44. Comparison of maximum boundary concentration due to various ground and elevated sources with similarity theory; u_∞ = 10 fps stable, ΔT = 80°F

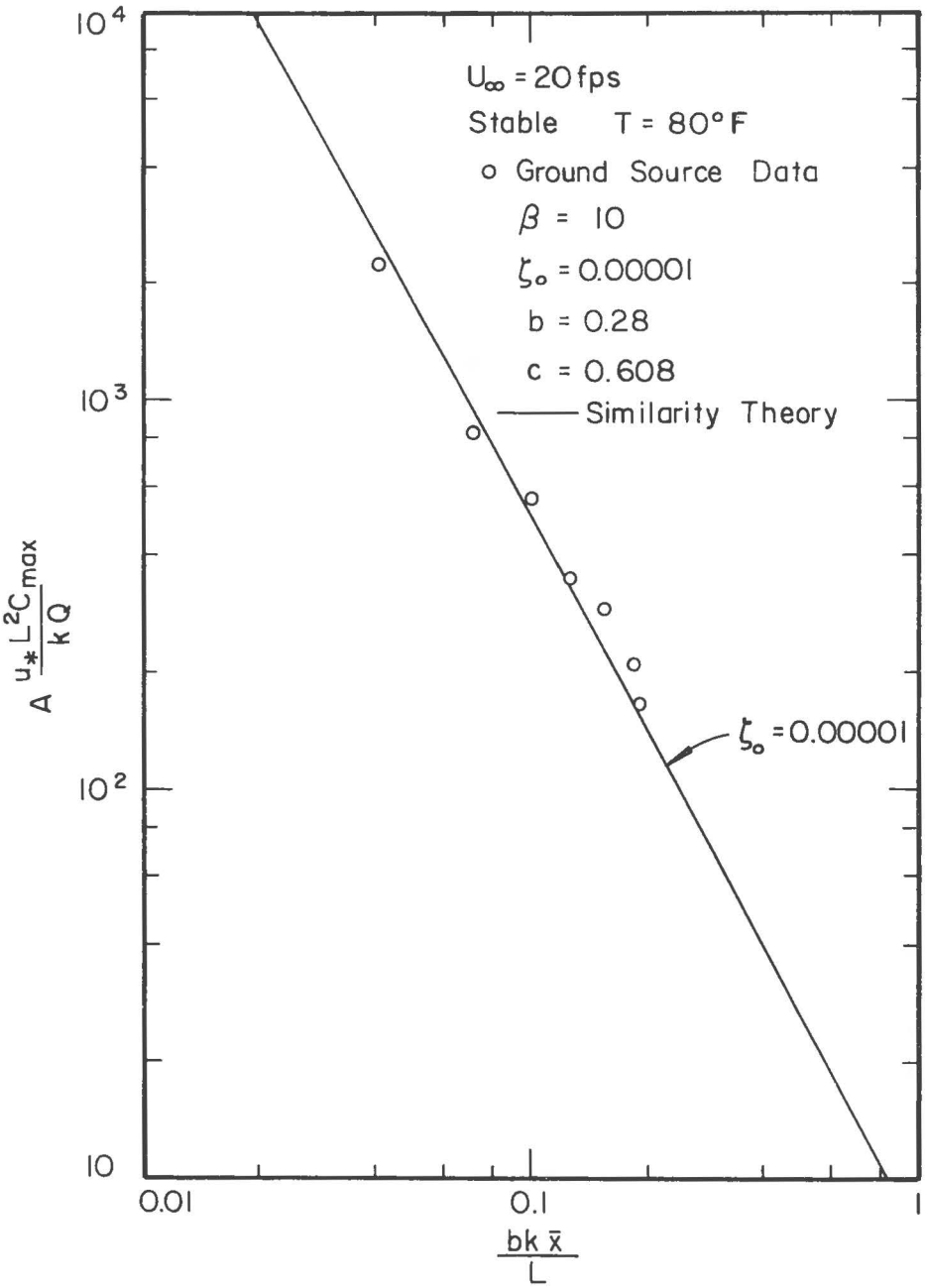

Fig. 45. Comparison of maximum ground concentration for ground source with similarity theory; u_∞ = 20 fps stable, ΔT = 80°F

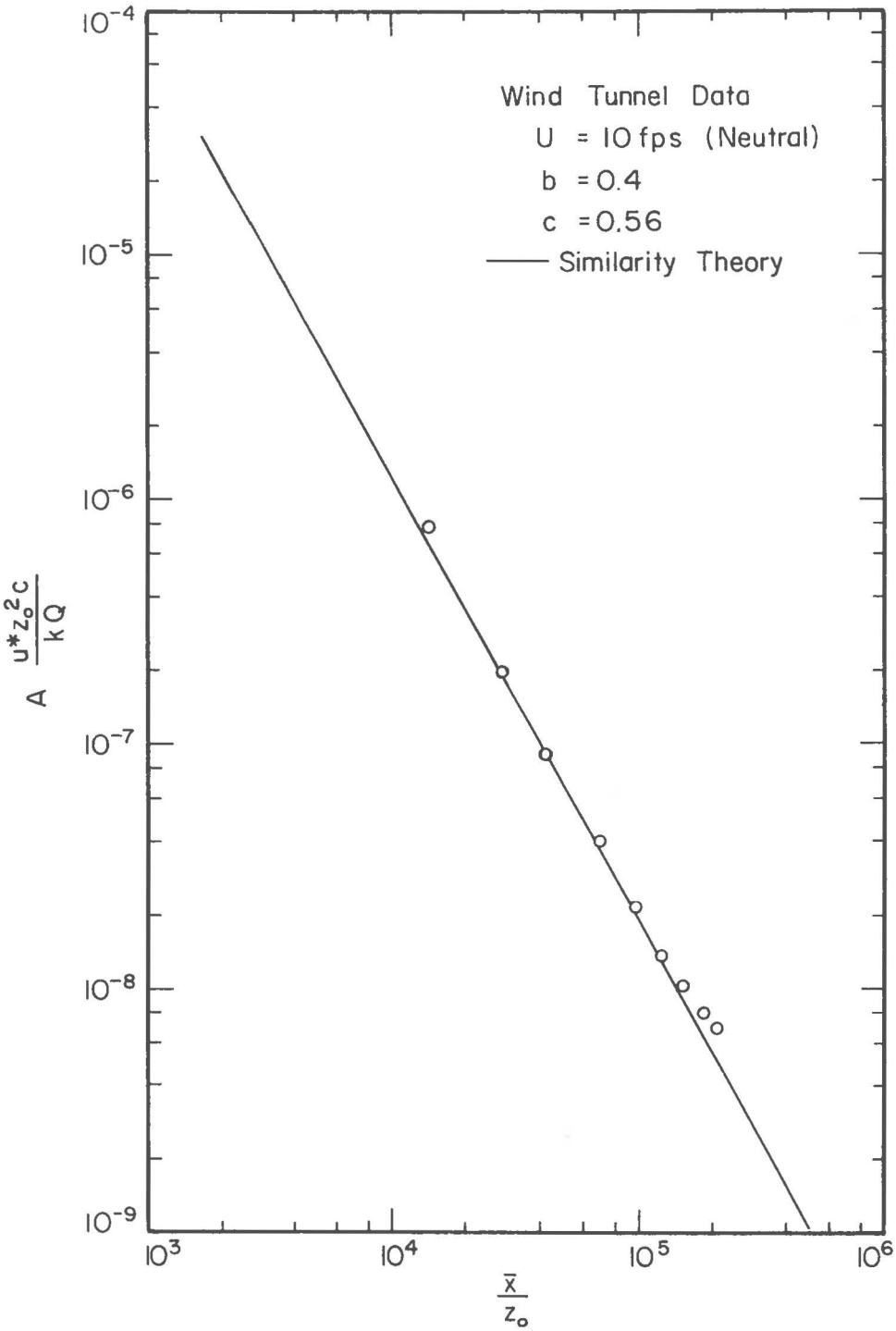

Fig. 46. Comparison of maximum ground concentration for ground source with similarity theory; u_∞ = 10 fps neutral

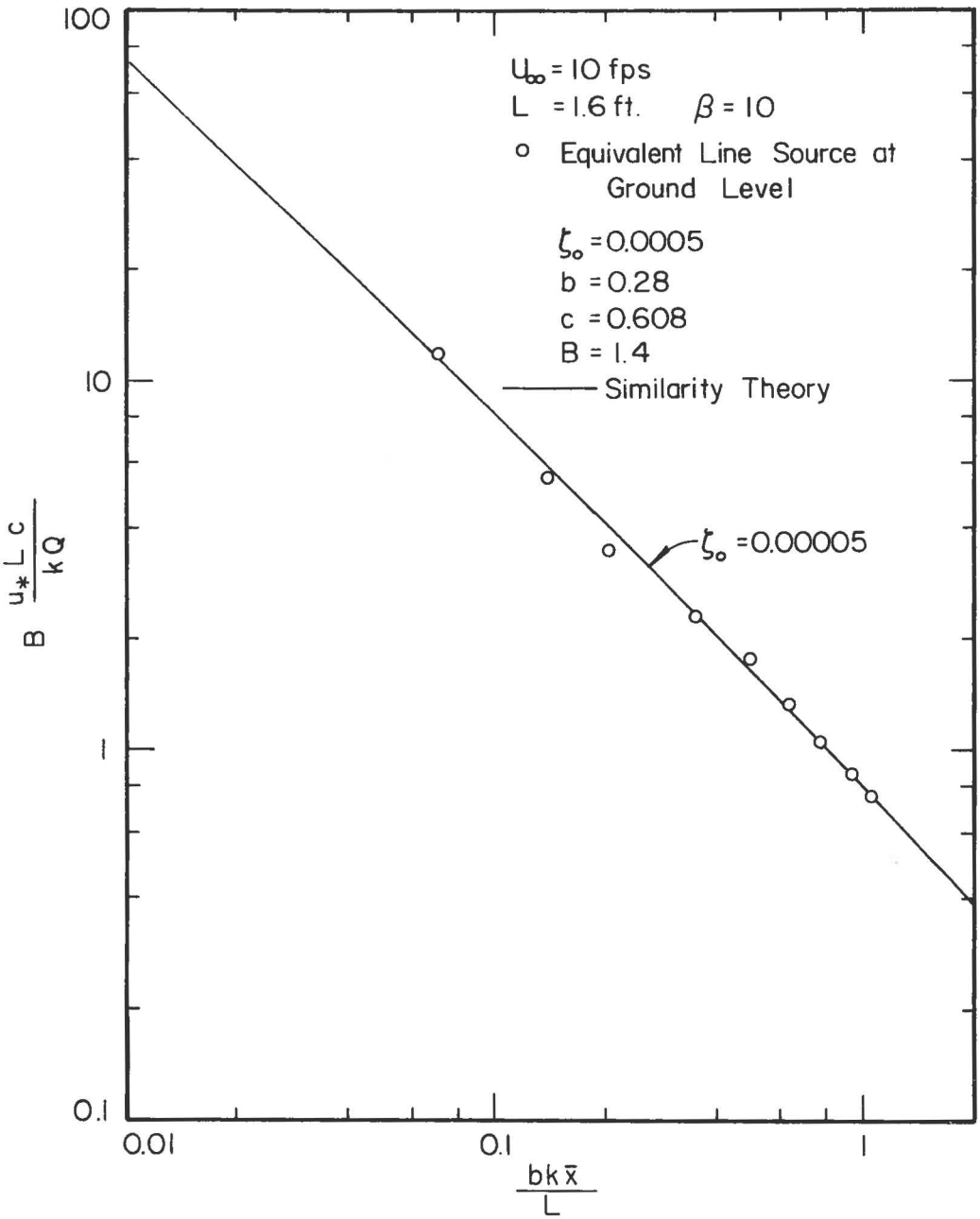

Fig. 47. Comparison of ground level concentration for equivalent line source at ground level; u_∞ = 10 fps stable $\Delta T = 80°F$

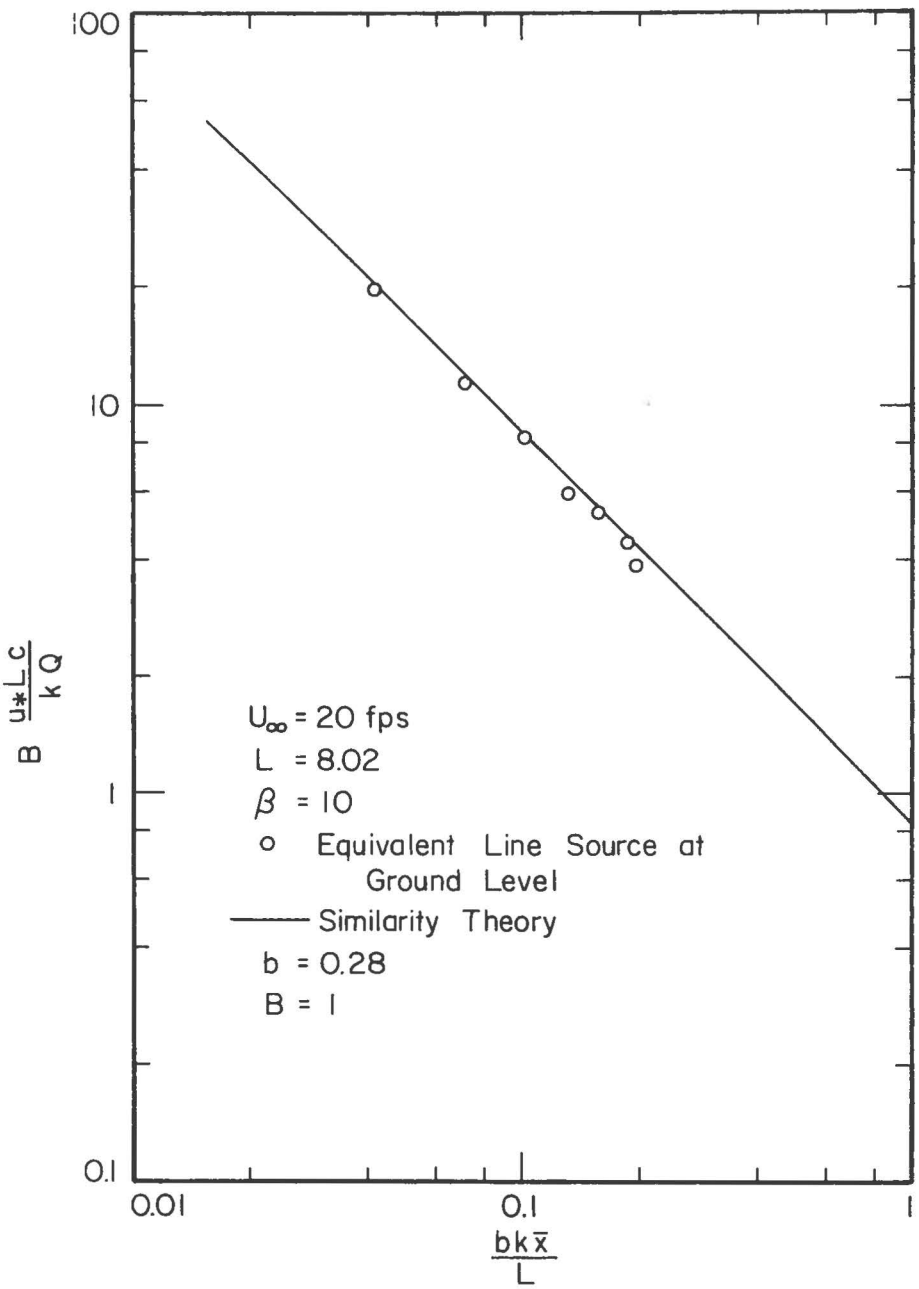

Fig. 48. Comparison of ground level concentration for equivalent line source at ground level; u_∞ = 20 fps stable, ΔT = 80°F

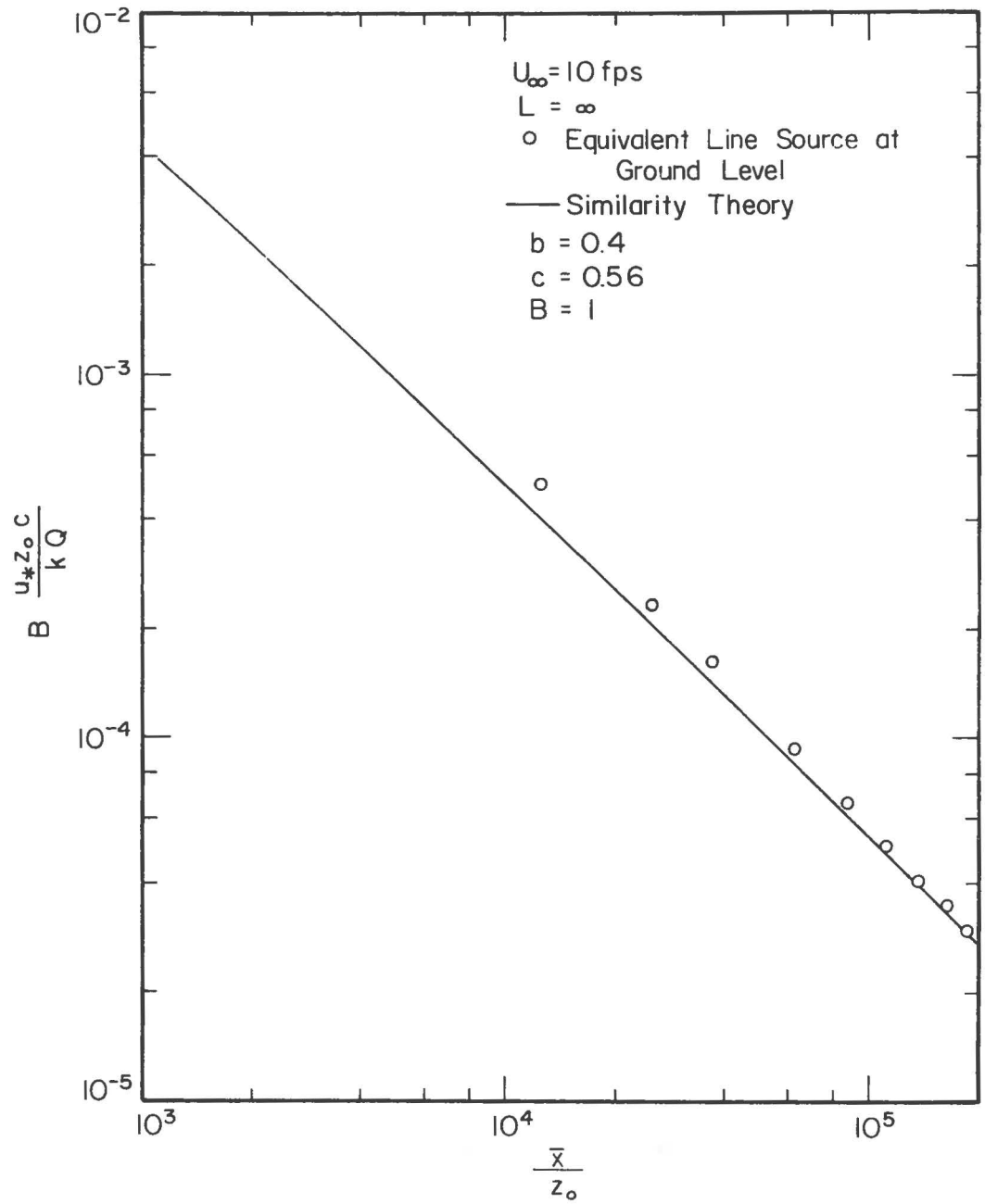

Fig. 49. Comparison of ground level concentration for equivalent line source at ground level; u_∞ = 10 fps neutral

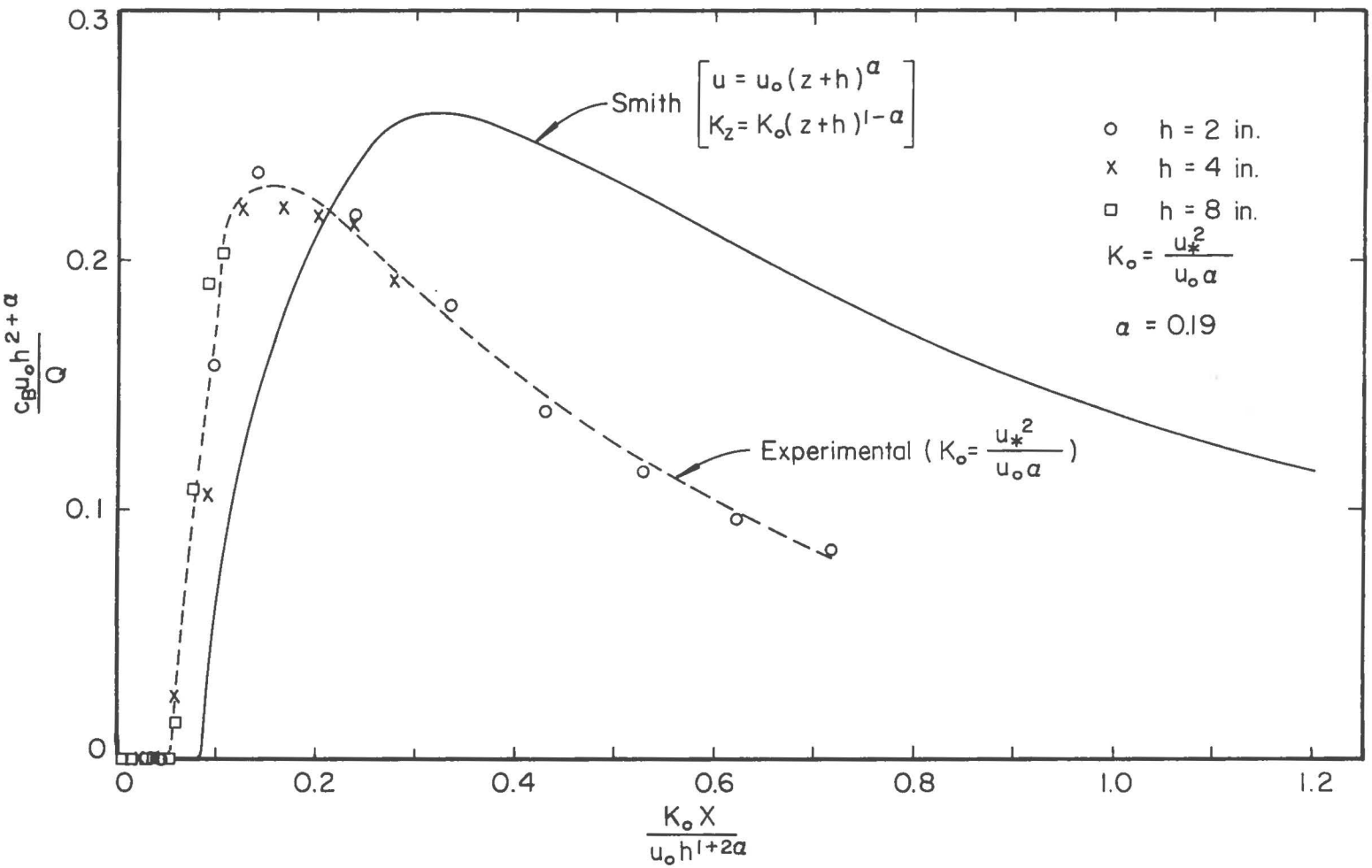

Fig. 50. Comparison of maximum boundary concentration for various elevated sources with Smith's theory

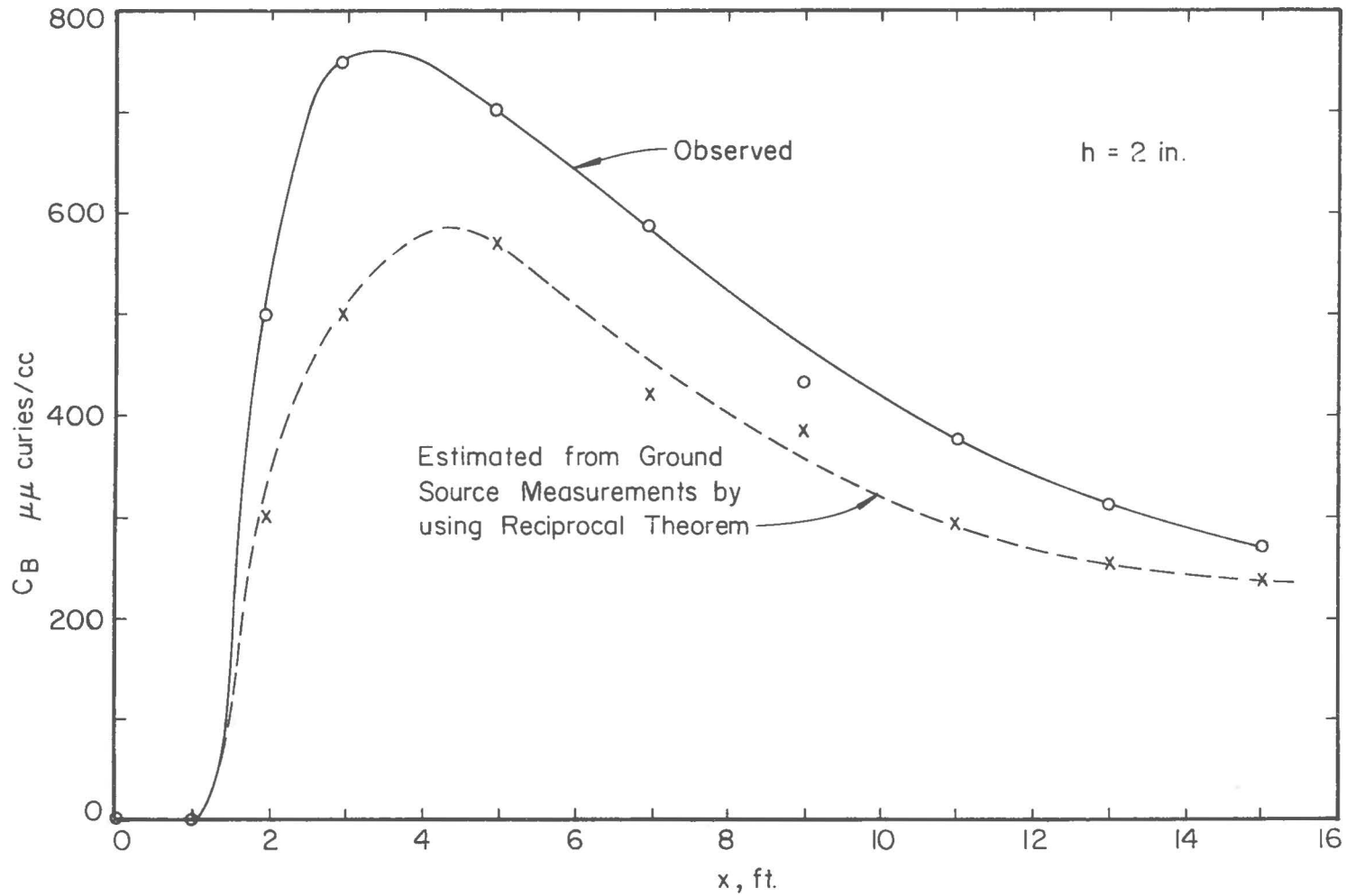

Fig. 51. Comparison of maximum boundary concentrations for an elevated source with those obtained from ground source data by application of Smith's reciprocal theorem; H = 2", u_∞ = 10 fps stable ΔT = 80°F

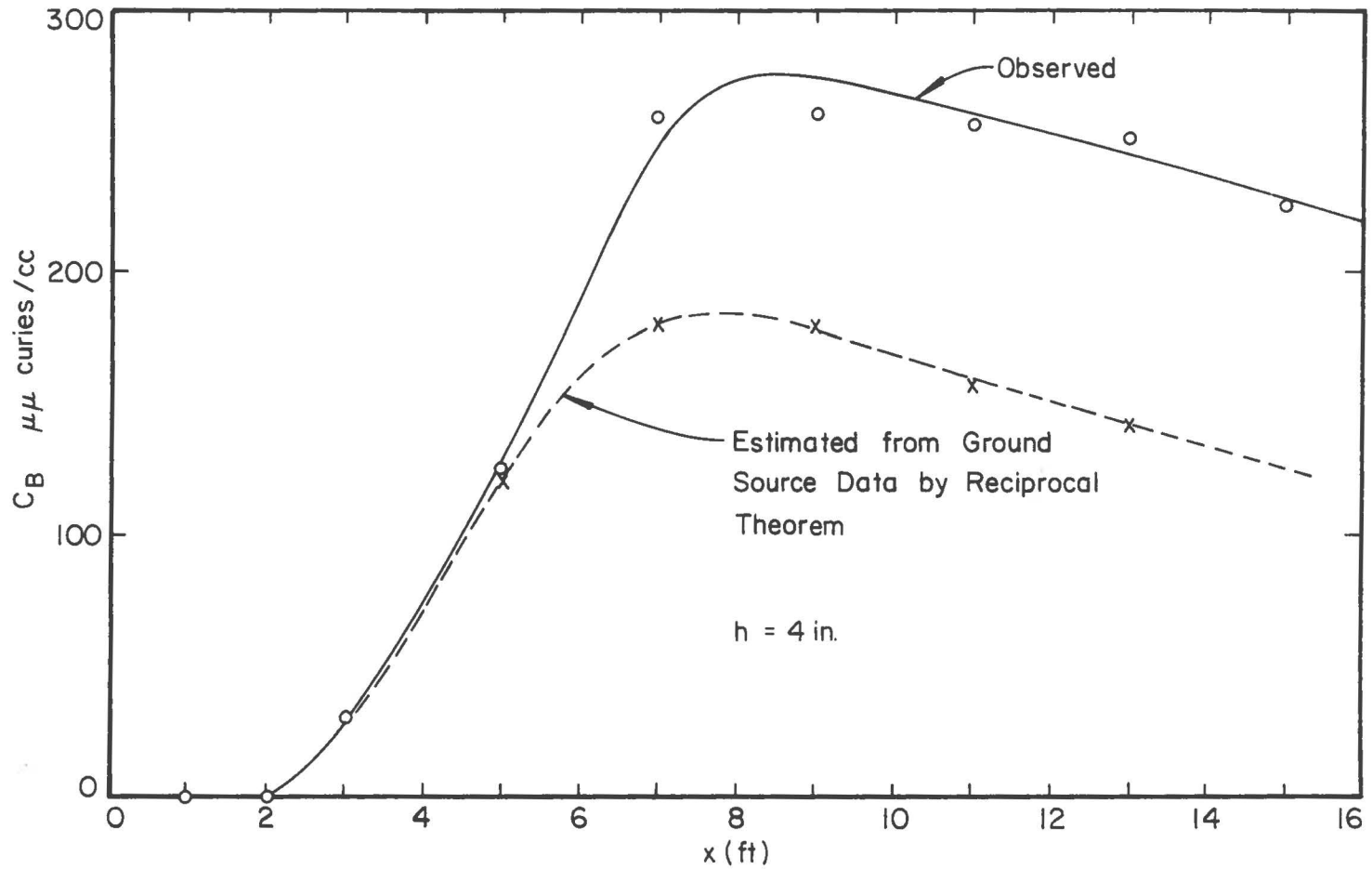

Fig. 52. Comparison of maximum boundary concentrations for an elevated source with those obtained from ground source data by application of Smith's reciprocal theorem; H = 4", u_∞ = 10 fps stable, ΔT = 80°F

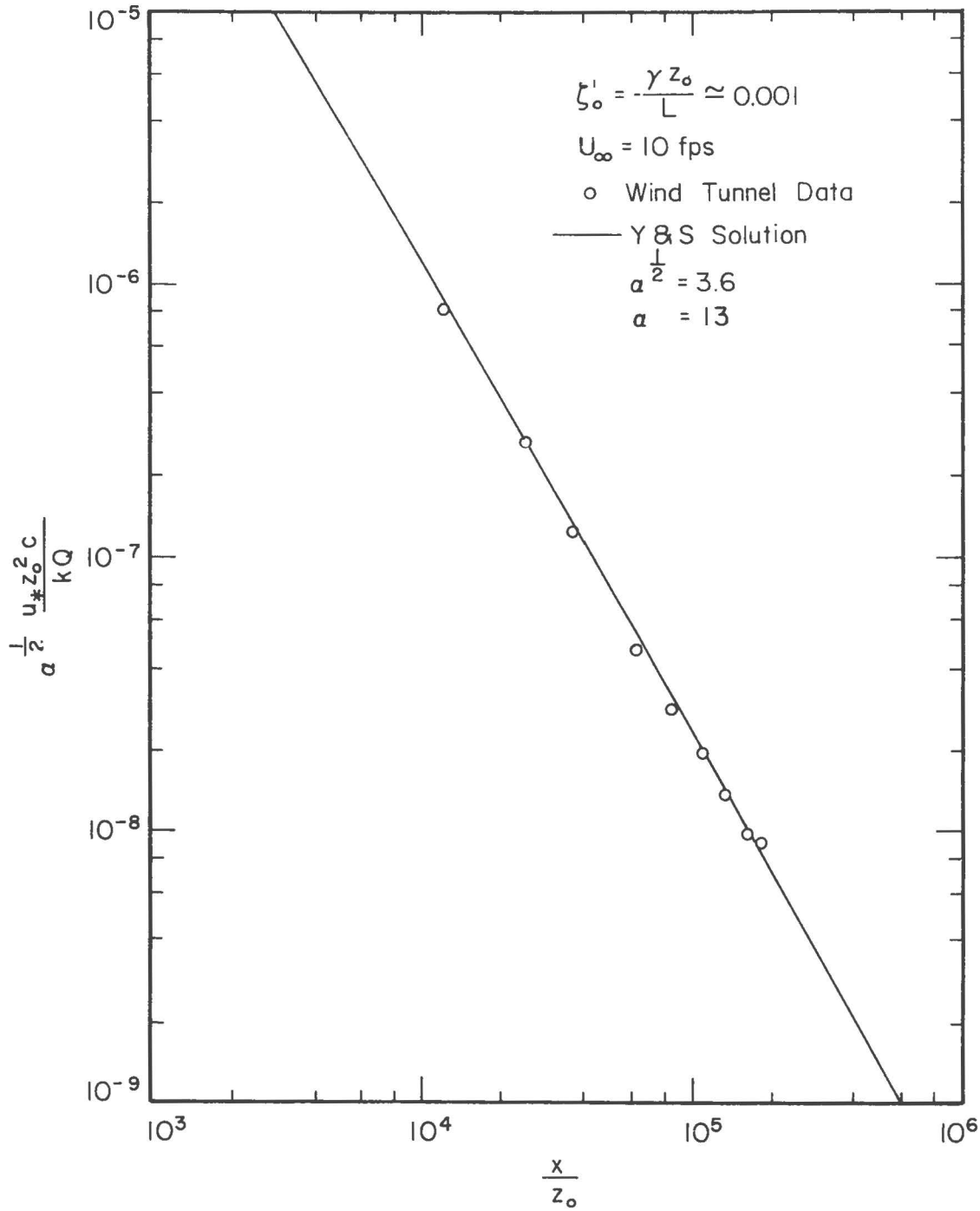

Fig. 53. Determination of α by comparison of the maximum ground concentration data with Y & S solution, $\zeta_o' = -.001$

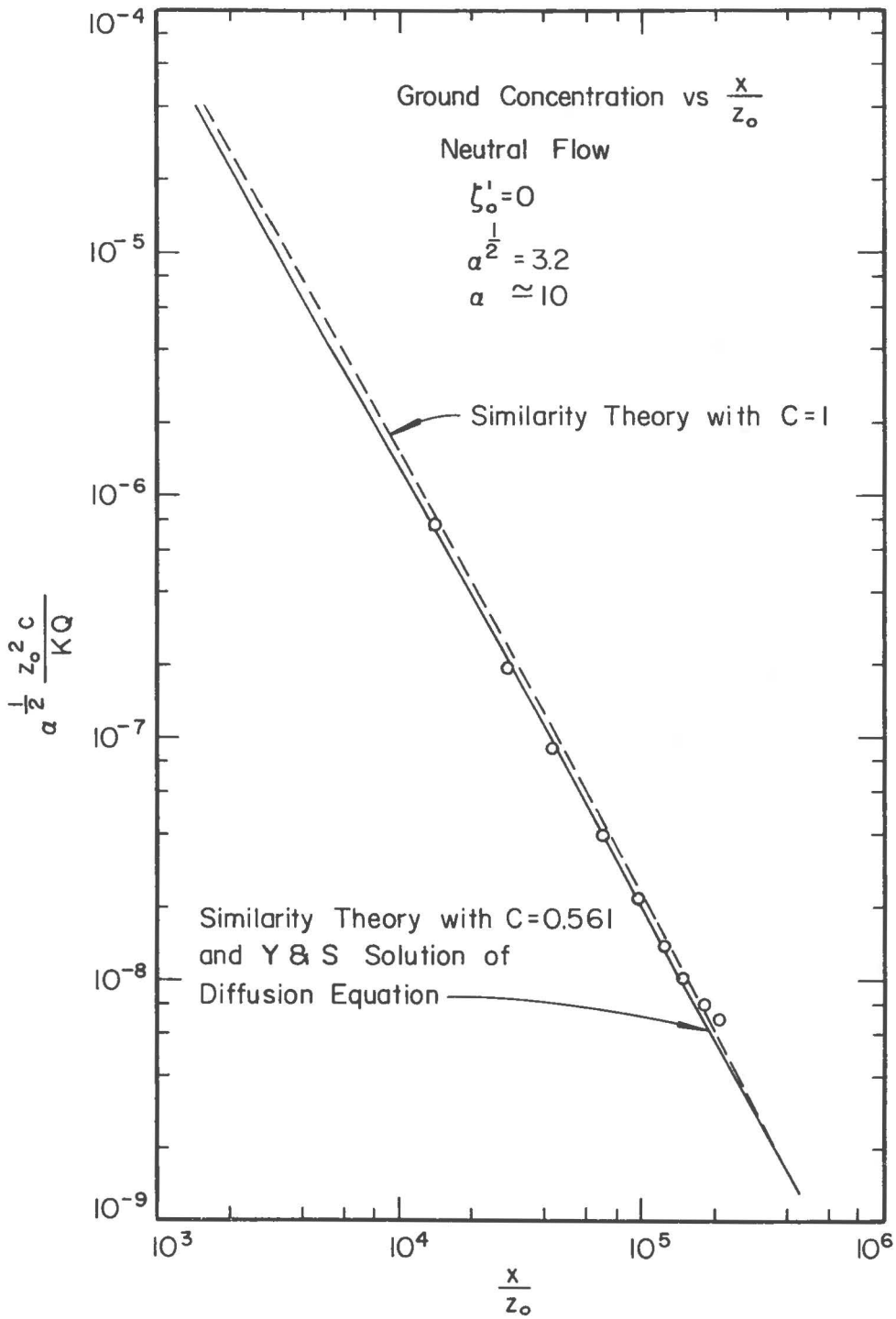

Fig. 54. Determination of α by comparison of the maximum ground concentration data with Y & S solution $\zeta_o' = 0$

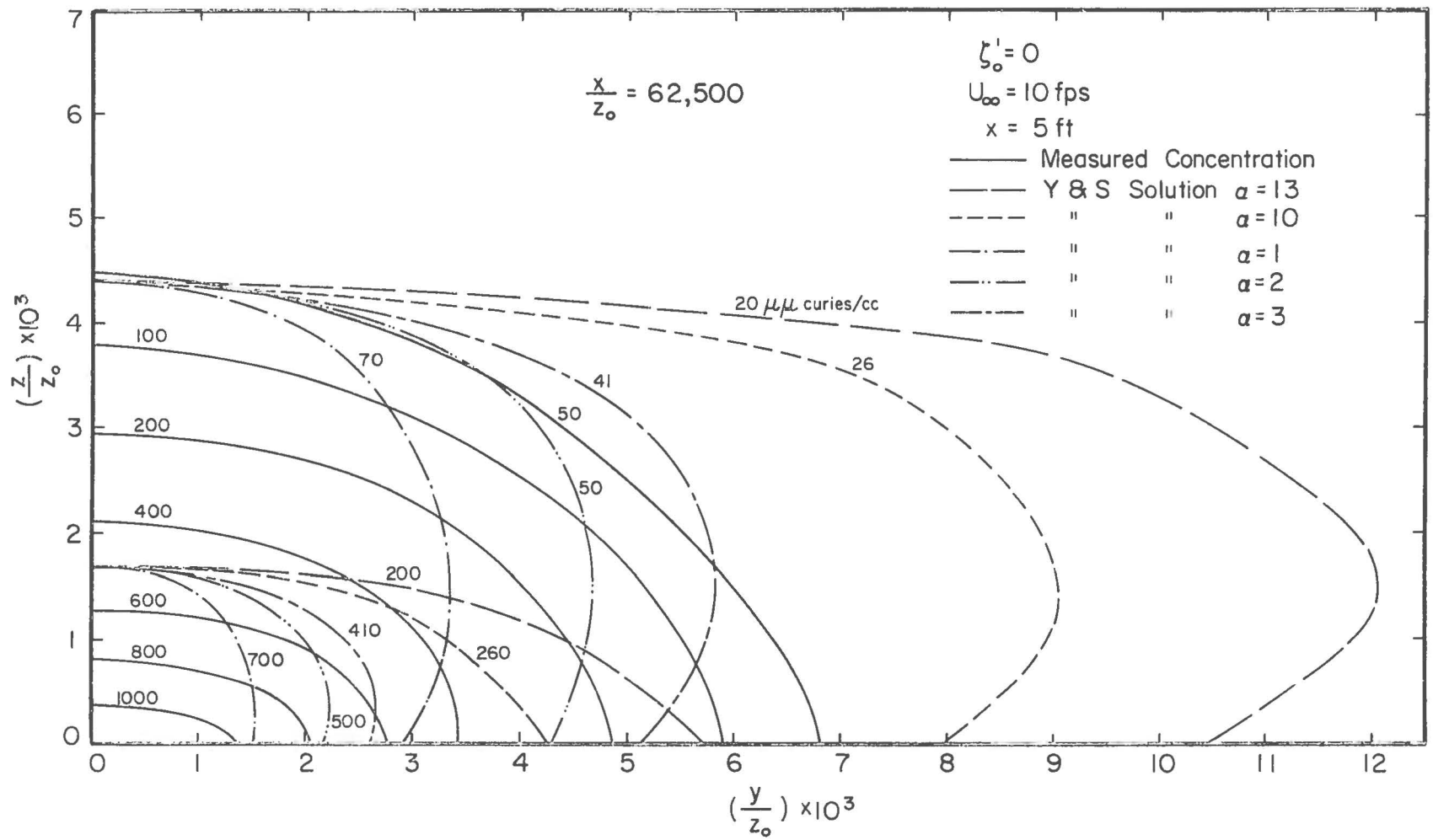

Fig. 55. Comparison of observed isopleths of concentration with Y & S solution for various α values; $\zeta_o' = 0$, $x/z_o = 62{,}500$

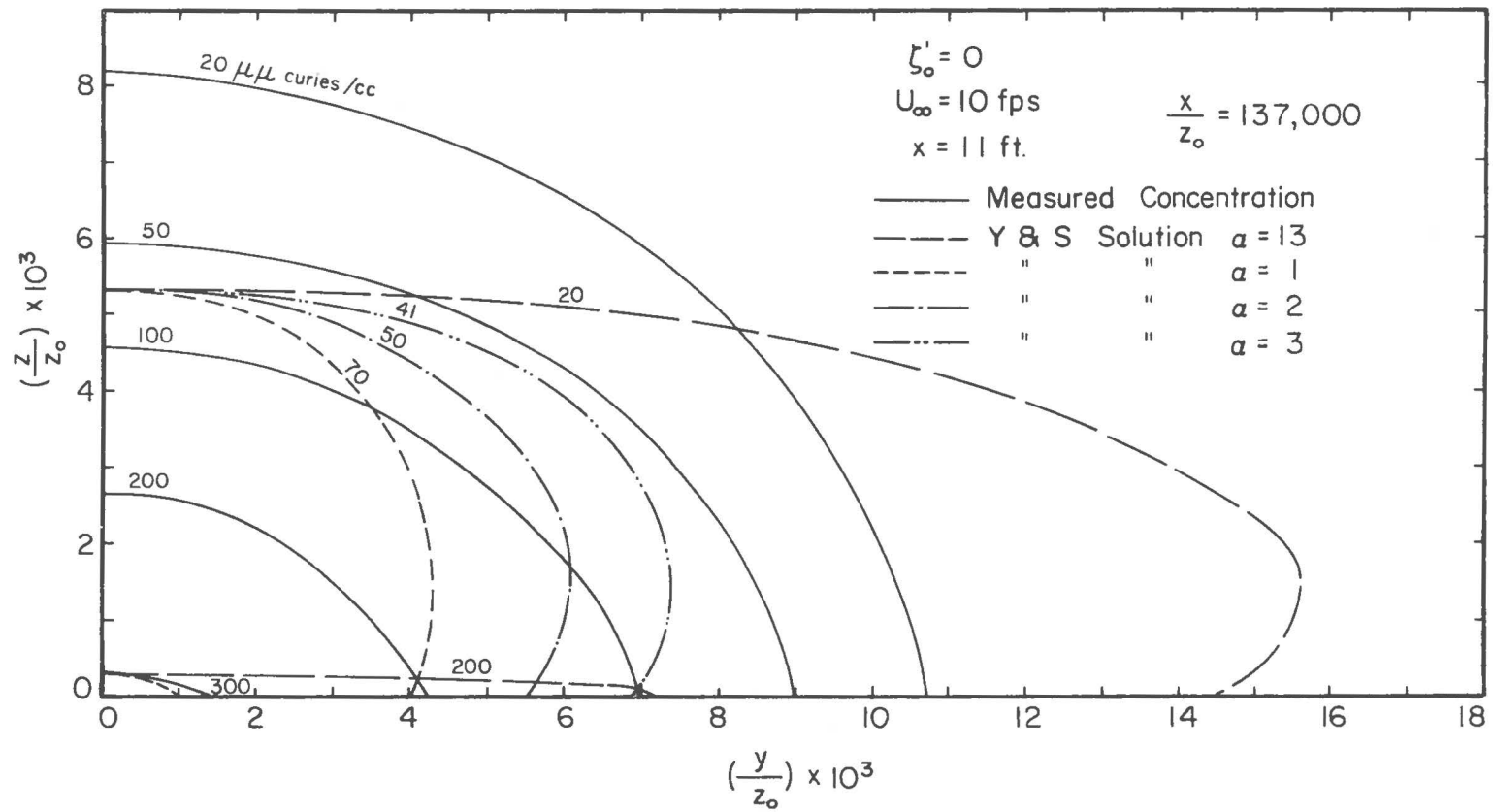

Fig. 56. Comparison of observed isopleths of concentration with Y & S solution for various α values; $\zeta_o' = 0$, $x/z_o = 137{,}000$

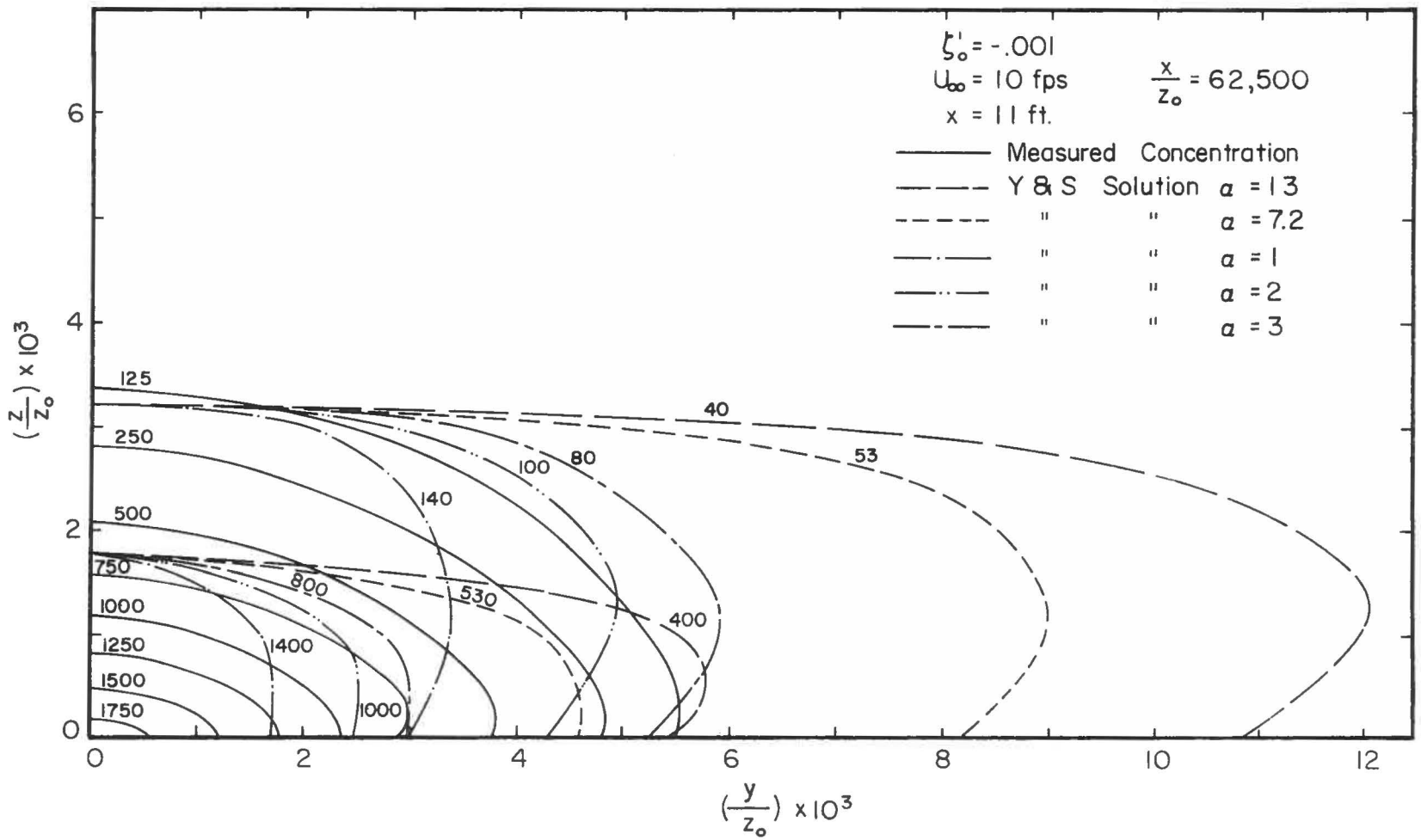

Fig. 57. Comparison of observed isopleths of concentration with Y & S solution for various α values; $\zeta_o' = -.001$, $x/z_o = 62{,}500$

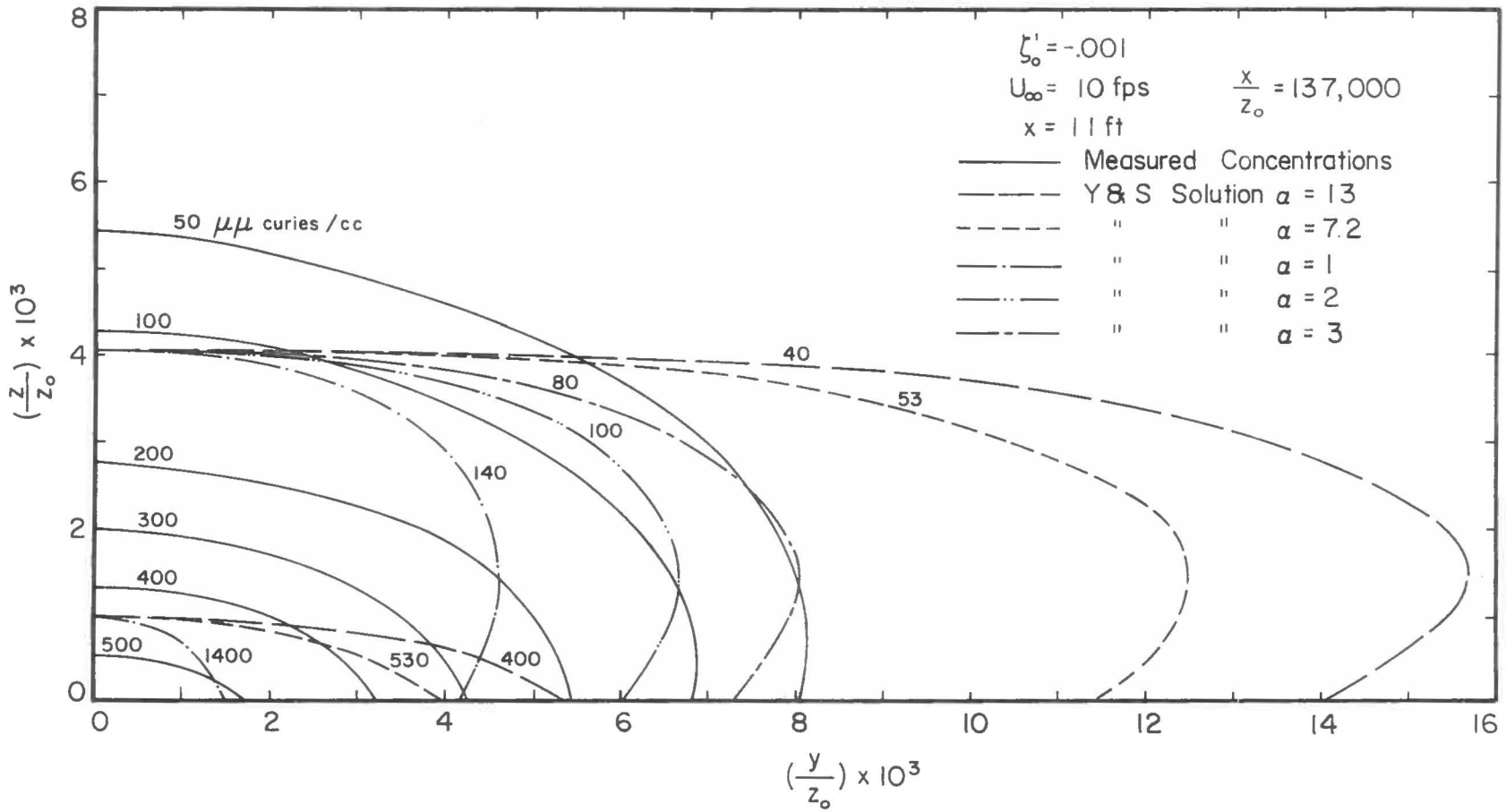

Fig. 58. Comparison of observed isopleths of concentration with Y & S solution for various α values; $\zeta_o' = -.001$, $x/z_o = 137{,}000$

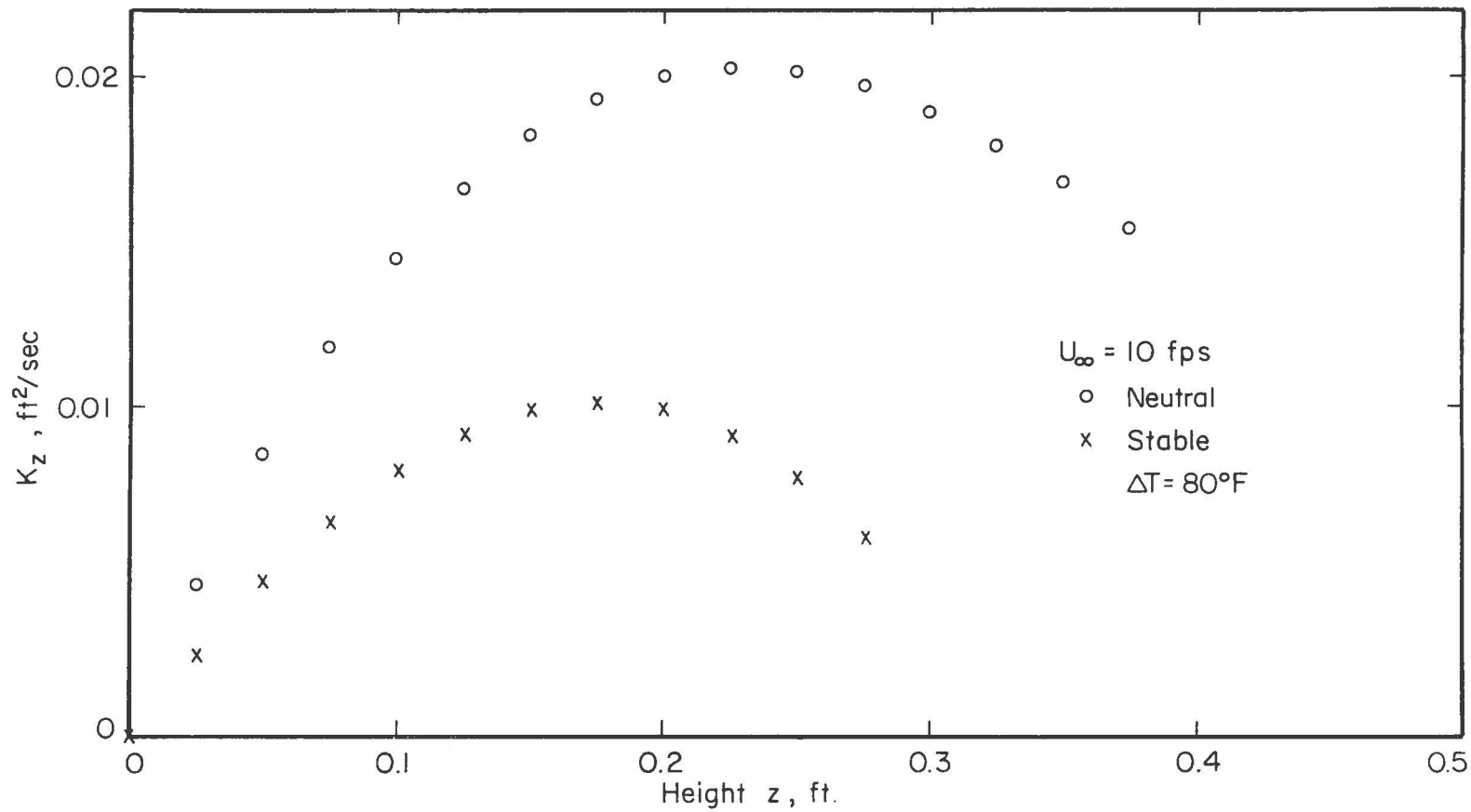

Fig. 59. Mass diffusivity computed from diffusion data in stable and neutral conditions

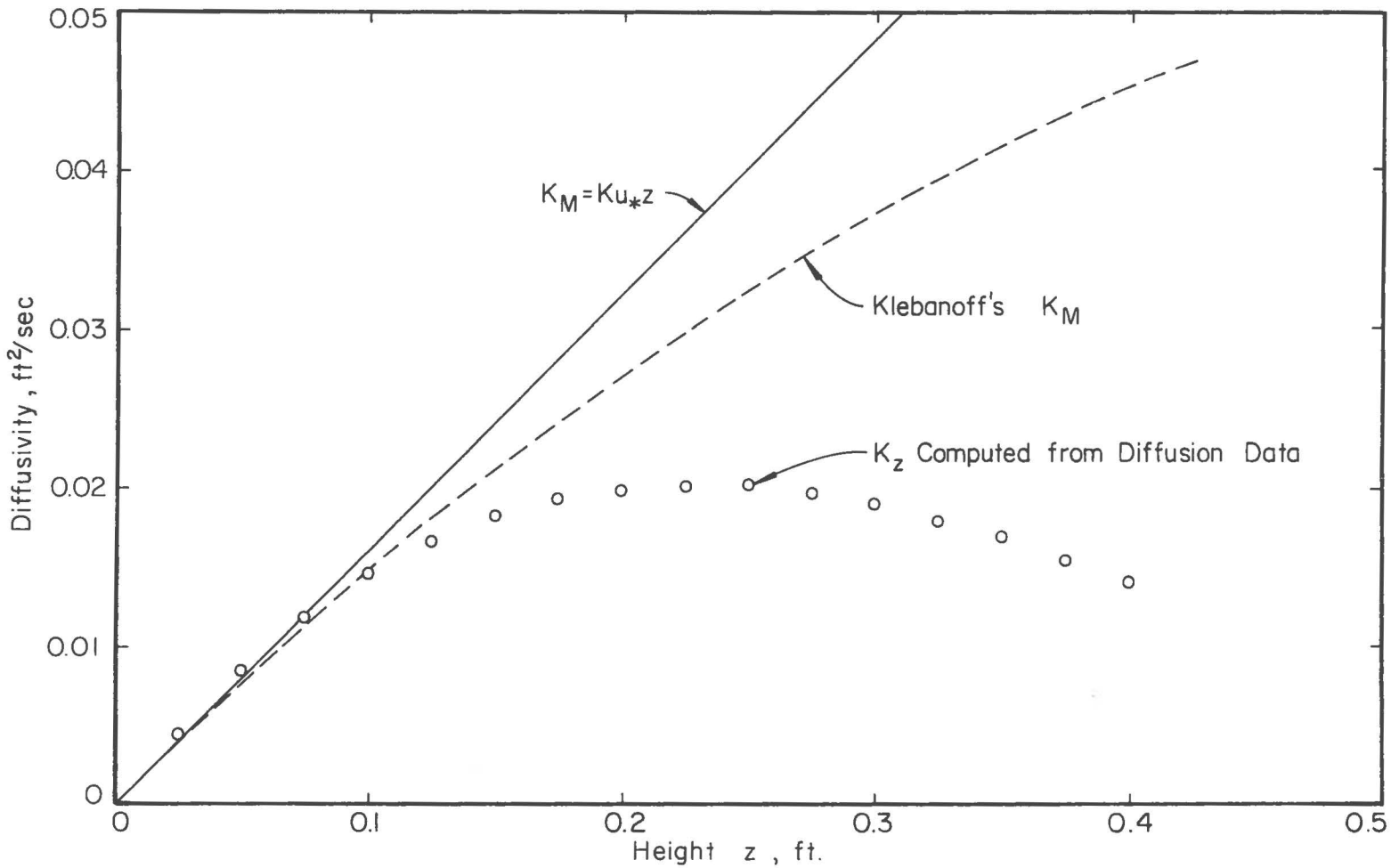

Fig. 60. Comparison of computed mass diffusivity with Klebanoff's measurements in neutral flow

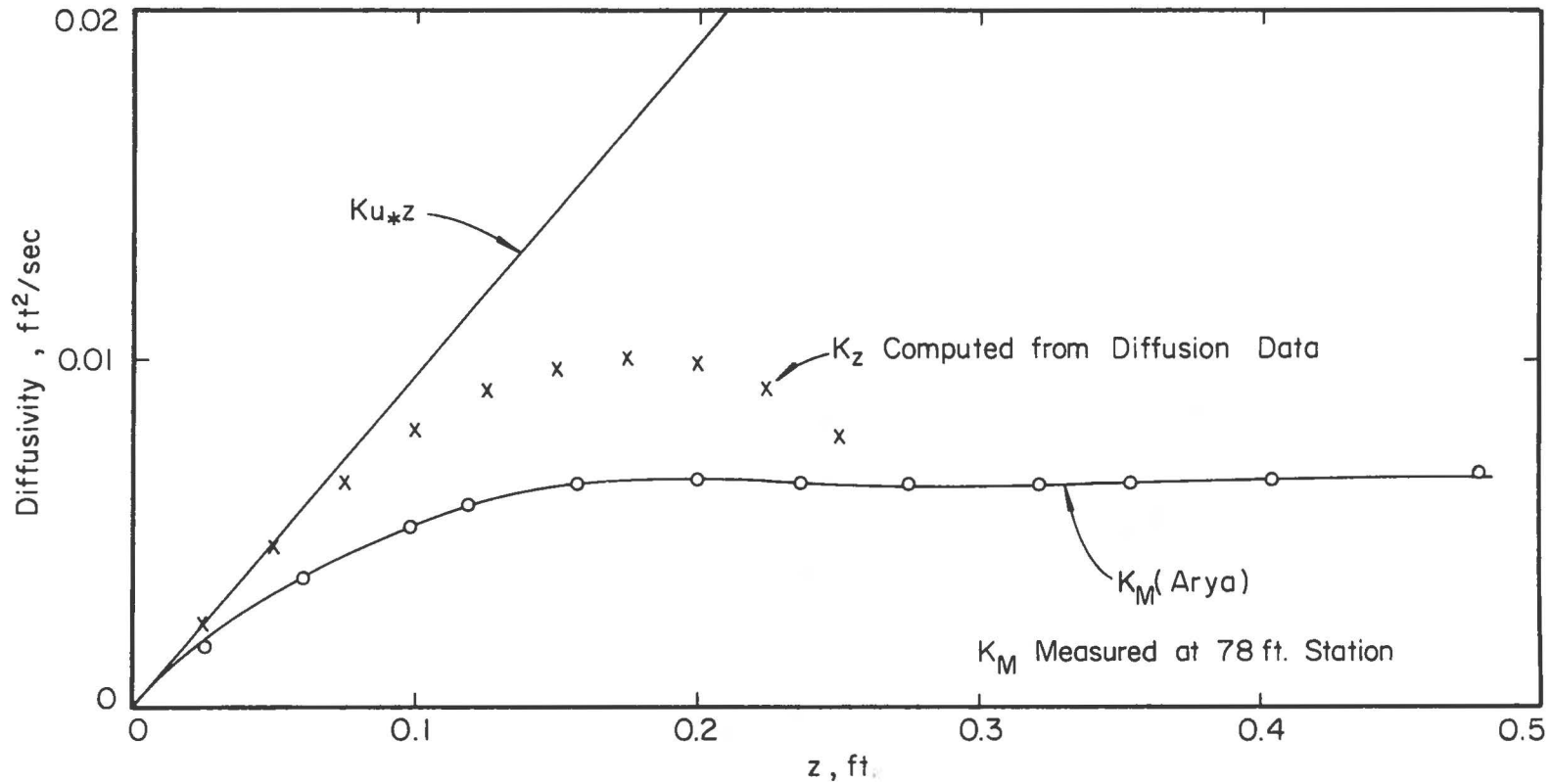

Fig. 61. Comparison of computed mass diffusivity with Arya's measurements in stable flow

Unclassified
Security Classification

DOCUMENT CONTROL DATA - R&D

(Security classification of title, body of abstract and indexing annotation must be entered when the overall report is classified)

1. ORIGINATING ACTIVITY (Corporate author)	2a. REPORT SECURITY CLASSIFICATION
Colorado State University Foothills Campus Fort Collins, Colorado 80521	Unclassified
	2b. GROUP

3. REPORT TITLE

"Turbulent Diffusion in a Stably Stratified Shear Layer"

4. DESCRIPTIVE NOTES (Type of report and inclusive dates)

Technical Report

5. AUTHOR(S) (Last name, first name, initial)

Chaudhry, F. H., and Meroney, R. N.

6. REPORT DATE	7a. TOTAL NO. OF PAGES	7b. NO. OF REFS
September 1969	185	73

8a. CONTRACT OR GRANT NO.	9a. ORIGINATOR'S REPORT NUMBER(S)
DAAB07-68-C-0423	CER69-70FHC-RNM12
b. PROJECT NO.	
c.	9b. OTHER REPORT NO(S) (Any other numbers that may be assigned this report)
d.	

10. AVAILABILITY/LIMITATION NOTICES

Distribution of this report is unlimited

11. SUPPLEMENTARY NOTES	12. SPONSORING MILITARY ACTIVITY
	U. S. Army Electronics Command Fort Monmouth, N. J.

13. ABSTRACT

Diffusion of a passive substance released from a continuous point source in a stably stratified shear layer is investigated both theoretically and experimentally. Using Monin-Obukhov's velocity profile and assuming a vertical eddy diffusivity which is a power function of the stability parameter z/L, the Eulerian turbulent diffusion equation is solved to obtain expressions for vertical and longitudinal velocities of the center of mass of a cloud in the constant stress region. These expressions give physical substance to those suggested by Gifford (1962) and Cermak (1963) as intuitive extensions ob Batchelor's Lagrangian similarity theory. The two constants of this theory viz, b and c are also determined by this analysis. It is shown that it may not be consistent to regard b equal to k, the Von-Karman constant, in the case of diabatic flows.

The experimental investigation was made in the Micrometeorological wind tunnel at the Fluid Dynamics and Diffusion Laboratory of Colorado State University. The wind tunnel has a 6' x 6' x 80' test section. A stably stratified shear layer was produced by heating the air and cooling the wind tunnel floor. Detailed observations of the diffusion field, downwind ground and elevated point sources, have been made using Krypton-85 as a tracer. The

(Continued on attached sheet)

DD FORM 1 JAN 64 1473

Unclassified
Security Classification

14 KEY WORDS	LINK A		LINK B		LINK C	
	ROLE	WT	ROLE	WT	ROLE	WT
Air Pollution Atmospheric Surface Layer Boundary Layers Diffusion Fluid Mechanics Radioactive Tracers Simulation Thermal Stratification Turbulence Wind Tunnel						

INSTRUCTIONS

1. ORIGINATING ACTIVITY: Enter the name and address of the contractor, subcontractor, grantee, Department of Defense activity or other organization *(corporate author)* issuing the report.

2*a*. REPORT SECURITY CLASSIFICATION: Enter the overall security classification of the report. Indicate whether "Restricted Data" is included. Marking is to be in accordance with appropriate security regulations.

2*b*. GROUP: Automatic downgrading is specified in DoD Directive 5200.10 and Armed Forces Industrial Manual. Enter the group number. Also, when applicable, show that optional markings have been used for Group 3 and Group 4 as authorized.

3. REPORT TITLE: Enter the complete report title in all capital letters. Titles in all cases should be unclassified. If a meaningful title cannot be selected without classification, show title classification in all capitals in parenthesis immediately following the title.

4. DESCRIPTIVE NOTES: If appropriate, enter the type of report, e.g., interim, progress, summary, annual, or final. Give the inclusive dates when a specific reporting period is covered.

5. AUTHOR(S): Enter the name(s) of author(s) as shown on or in the report. Enter last name, first name, middle initial. If military, show rank and branch of service. The name of the principal author is an absolute minimum requirement.

6. REPORT DATE: Enter the date of the report as day, month, year; or month, year. If more than one date appears on the report, use date of publication.

7*a*. TOTAL NUMBER OF PAGES: The total page count should follow normal pagination procedures, i.e., enter the number of pages containing information.

7*b*. NUMBER OF REFERENCES: Enter the total number of references cited in the report.

8*a*. CONTRACT OR GRANT NUMBER: If appropriate, enter the applicable number of the contract or grant under which the report was written.

8*b*, 8*c*, & 8*d*. PROJECT NUMBER: Enter the appropriate military department identification, such as project number, subproject number, system numbers, task number, etc.

9*a*. ORIGINATOR'S REPORT NUMBER(S): Enter the official report number by which the document will be identified and controlled by the originating activity. This number must be unique to this report.

9*b*. OTHER REPORT NUMBER(S): If the report has been assigned any other report numbers *(either by the originator or by the sponsor)*, also enter this number(s).

10. AVAILABILITY/LIMITATION NOTICES: Enter any limitations on further dissemination of the report, other than those imposed by security classification, using standard statements such as:

(1) "Qualified requesters may obtain copies of this report from DDC."

(2) "Foreign announcement and dissemination of this report by DDC is not authorized."

(3) "U. S. Government agencies may obtain copies of this report directly from DDC. Other qualified DDC users shall request through _____."

(4) "U. S. military agencies may obtain copies of this report directly from DDC. Other qualified users shall request through _____."

(5) "All distribution of this report is controlled. Qualified DDC users shall request through _____."

If the report has been furnished to the Office of Technical Services, Department of Commerce, for sale to the public, indicate this fact and enter the price, if known.

11. SUPPLEMENTARY NOTES: Use for additional explanatory notes.

12. SPONSORING MILITARY ACTIVITY: Enter the name of the departmental project office or laboratory sponsoring *(paying for)* the research and development. Include address.

13. ABSTRACT: Enter an abstract giving a brief and factual summary of the document indicative of the report, even though it may also appear elsewhere in the body of the technical report. If additional space is required, a continuation sheet shall be attached.

It is highly desirable that the abstract of classified reports be unclassified. Each paragraph of the abstract shall end with an indication of the military security classification of the information in the paragraph, represented as *(TS)*, *(S)*, *(C)*, or *(U)*.

There is no limitation on the length of the abstract. However, the suggested length is from 150 to 225 words.

14. KEY WORDS: Key words are technically meaningful terms or short phrases that characterize a report and may be used as index entries for cataloging the report. Key words must be selected so that no security classification is required. Idenfiers, such as equipment model designation, trade name, military project code name, geographic location, may be used as key words but will be followed by an indication of technical context. The assignment of links, rules, and weights is optional.

Continuation of Abstract:

concentration characteristics obtained from diffusion experiments show excellent agreement with those observed in the atmosphere. The index m, describing the power law variation of ground level concentration with distance, matches with the reliable field estimates. The data compares well with the predictions of similarity theory. It appears that the parameters evaluated in the field by Klug (1968) hold also for the wind tunnel data. The data support the assumption of a Gaussian effect of source height, for elevated releases, on the ground level concentration. An examination of the available solutions to the three dimensional diffusion equation as compared to the data suggests that the detailed diffusion patterns obtained from the wind tunnel experiments may be preferrable over such solutions because they require arbitrary specification of a lateral diffusivity.

MINIMUM BASIC DISTRIBUTION LIST FOR USAMC SCIENTIFIC AND TECHNICAL REPORTS IN METEOROLOGY AND ATMOSPHERIC SCIENCES

Commanding General (1)
U. S. Army Materiel Command
Attn: AMCRD-RV-A
Washington, D. C. 20315

Commanding General (1)
U. S. Army Electronics Command
Attn: AMSEL-EW
Fort Monmouth, New Jersey 07703

Commanding General (1)
U. S. Army Test and Evaluation Command
Attn: NBC Directorate
Aberdeen Proving Ground, Maryland 21005

Commanding Officer (1)
U. S. Army Ballistics Research Laboratories
Attn: AMXBR-IA
Aberdeen Proving Ground, Maryland 21005

Chief, Atmospheric Physics Division (2)
Atmospheric Sciences Laboratory
U. S. Army Electronics Command
Fort Monmouth, New Jersey 07703

U. S. Army Munitions Command (1)
Attn: Irving Solomon
Operations Research Group
Edgewood Arsenal, Maryland 21010

Commanding Officer (1)
U. S. Army Dugway Proving Ground
Attn: Meteorology Division
Dugway, Utah 84022

Commanding Officer (1)
U. S. Army CDC, CBR Agency
Attn: Mr. N. W. Bush
Fort McClellan, Alabama 36205

Commanding General (1)
U. S. Army Test and Evaluation Command
Attn: AMSTE-EL
Aberdeen Proving Ground, Maryland 21005

Assistant Chief of Staff for Force Development (1)
CBR Nuclear Operations Directorate
Department of the Army
Washington, D. C. 20310

Director (1)
Atmospheric Sciences Programs
National Sciences Foundation
Washington, D. C. 20550

Assistant Secretary of Defense (1)
Research and Engineering
Attn: Technical Library
Washington, D. C. 20301

R. A. Taft Sanitary Engineering Center (1)
Public Health Service
4676 Columbia Parkway
Cincinnati, Ohio

Dr. Hans A. Panofsky (1)
Department of Meteorology
The Pennsylvania State University
University Park, Pennsylvania

Commanding General (1)
U. S. Continental Army Command
Attn: Reconnaissance Branch ODCS for Intelligence
Fort Monroe, Virginia 23351

Commander (1)
Air Force Cambridge Research Laboratories
Attn: CRZW
1065 Main Street
Waltham, Massachusetts

President (1)
U. S. Army Artillery Board
Fort Sill, Oklahoma 73504

National Center for Atmospheric Research (1)
Attn: Library
Boulder, Colorado

Dr. J. E. Cermak, Head (15)
Fluid Mechanics Program
Colorado State University
Fort Collins, Colorado 80521

Author (1)

Chief of Research and Development (1)
Department of the Army
Attn: CRD/M
Washington, D. C. 20310

Commanding General (1)
U. S. Army Missile Command
Attn: AMSMI-RRA
Redstone Arsenal, Alabama 35809

Commanding General (1)
U. S. Army Natick Laboratories
Attn: Earth Sciences Division
Natick, Massachusetts 01762

Director, U. S. Army Engineer (1)
Waterways Experiment Station
Attn: WES-FV
Vicksburg, Mississippi 39181

Chief, Atmospheric Sciences Research Division (5)
Atmospheric Sciences Laboratory
U. S. Army Electronics Command
Fort Huachuca, Arizona 85613

Commanding Officer (1)
U. S. Army Frankford Arsenal
Attn: SMUFA-1140
Philadelphia, Pennsylvania 19137

Commandant (1)
U. S. Army Artillery and Missile School
Attn: Target Acquisition Department
Fort Sill, Oklahoma 73504

Commanding General (1)
U. S. Army Test and Evaluation Command
Attn: AMSTE-BAF
Aberdeen Proving Ground, Maryland 21005

Office of Chief Communications - Electronics (1)
Department of the Army
Attn: Electronics Systems Directorate
Washington, D. C. 20315

Chief of Naval Operations (1)
Department of the Navy
Attn: Code 427
Washington, D. C. 20350

Director (1)
Bureau of Research and Development
Federal Aviation Agency
Washington, D. C. 20553

Director of Meteorological Systems (1)
Office of Applications (FM)
National Aeronautics and Space Administration
Washington, D. C. 20546

Director (1)
Atmospheric Physics and Chemistry Laboratory
Environmental Science Services Administration
Boulder, Colorado

Andrew Morse (1)
Army Aeronautical Activity
Ames Research Center
Moffett Field, California 94035

Commanding Officer (2)
U. S. Army Cold Regions Research and Engineering Laboratories
Attn: Environmental Research Branch
Hanover, New Hampshire 03755

Mr. Ned L. Kragness (1)
U. S. Army Aviation Materiel Command
SMOSM-E
12th and Spruce Streets
Saint Louis, Missouri 63166

Commanding Officer, U. S. Army (1)
Artillery Combat Development Agency
Fort Sill, Oklahoma 73504

Commander, USAR Air Weather Service (MATS) (1)
Attn: AWSSS/TIPD
Scott Air Force Base, Illinois

Dr. John Bogusky (1)
7310 Cedardale Drive
Alexandria, Virginia 22308

Commanding General (1)
U. S. Army Combat Development Command
Attn: CDCMR-E
Fort Belvoir, Virginia 22060

Commanding General (1)
U. S. Army Munitions Command
Attn: AMSMU-RE-R
Dover, New Jersey 07801

Commanding Officer (1)
U. S. Army Ballistics Research Laboratories
Attn: AMXBR-B
Aberdeen Proving Ground, Maryland 21005

Director (2)
Atmospheric Sciences Laboratory
U. S. Army Electronics Command
White Sands Missile Range, New Mexico 88002

Chief, Atmospheric Sciences Office (2)
Atmospheric Sciences Laboratory
U. S. Army Electronics Command
White Sands Missile Range, New Mexico 88002

Commanding Officer (1)
U. S. Army Picatinny Arsenal
Attn: SMUPA-TV-3
Dover, New Jersey 07801

Commanding Officer (1)
U. S. Army Communications - Electronics Combat Development Agency
Fort Monmouth, New Jersey 07703

Commanding General (1)
Deseret Test Center
Attn: Design and Analysis Division
Fort Douglas, Utah 84113

Commandant (1)
U. S. Army CBR School Micrometeorological Section
Fort McClellan, Alabama 36205

Assistant Chief of Staff for Intelligence (1)
Department of the Army
Attn: ACSI-DERSI
Washington, D. C. 20310

Commanding Officer (1)
U. S. Naval Weather Research Facility
U. S. Naval Air Station, Building R-48
Norfolk, Virginia 23511

Chief, Fallout Studies Branch (1)
Division of Biology and Medicine
Atomic Energy Commission
Washington, D. C. 20545

Director (1)
U. S. Weather Bureau
Attn: Librarian
Washington, D. C. 20235

Dr. Albert Miller (1)
Department of Meteorology
San Jose State College
San Jose, California 95114

Mrs. Francis L. Wheedon (1)
Army Research Office
3045 Columbia Pike
Arlington, Virginia 22201

Commander (1)
Air Force Cambridge Research Laboratories
Attn: CRXL
L. G. Hanscom Field
Bedford, Massachusetts

Harry Moses, Asso. Meteorologist (1)
Radiological Physics Division
Argonne National Laboratory
9700 S. Cass Avenue
Argonne, Illinois 60440

Defense Documentation Center (20)
Cameron Station
Alexandria, Virginia 22314

Office of U. S. Naval Weather Service (1)
U. S. Naval Air Station
Washington, D. C. 20390

Dr. Gerald Gill (1)
University of Michigan
Ann Arbor, Michigan 48103

Continuation of Abstract:

concentration characteristics obtained from diffusion experiments show excellent agreement with those observed in the atmosphere. The index m, describing the power law variation of ground level concentration with distance, matches with the reliable field estimates. The data compares well with the predictions of similarity theory. It appears that the parameters evaluated in the field by Klug (1968) hold also for the wind tunnel data. The data support the assumption of a Gaussian effect of source height, for elevated releases, on the ground level concentration. An examination of the available solutions to the three dimensional diffusion equation as compared to the data suggests that the detailed diffusion patterns obtained from the wind tunnel experiments may be preferrable over such solutions because they require arbitrary specification of a lateral diffusivity.

MINIMUM BASIC DISTRIBUTION LIST FOR USAMC SCIENTIFIC AND TECHNICAL REPORTS IN METEOROLOGY AND ATMOSPHERIC SCIENCES

Commanding General (1)
U. S. Army Materiel Command
Attn: AMCRD-RV-A
Washington, D. C. 20315

Commanding General (1)
U. S. Army Electronics Command
Attn: AMSEL-EW
Fort Monmouth, New Jersey 07703

Commanding General (1)
U. S. Army Test and Evaluation Command
Attn: NBC Directorate
Aberdeen Proving Ground, Maryland 21005

Commanding Officer (1)
U. S. Army Ballistics Research Laboratories
Attn: AMXBR-IA
Aberdeen Proving Ground, Maryland 21005

Chief, Atmospheric Physics Division (2)
Atmospheric Sciences Laboratory
U. S. Army Electronics Command
Fort Monmouth, New Jersey 07703

U. S. Army Munitions Command (1)
Attn: Irving Solomon
Operations Research Group
Edgewood Arsenal, Maryland 21010

Commanding Officer (1)
U. S. Army Dugway Proving Ground
Attn: Meteorology Division
Dugway, Utah 84022

Commanding Officer (1)
U. S. Army CDC, CBR Agency
Attn: Mr. N. W. Bush
Fort McClellan, Alabama 36205

Commanding General (1)
U. S. Army Test and Evaluation Command
Attn: AMSTE-EL
Aberdeen Proving Ground, Maryland 21005

Assistant Chief of Staff for Force Development (1)
CBR Nuclear Operations Directorate
Department of the Army
Washington, D. C. 20310

Director (1)
Atmospheric Sciences Programs
National Sciences Foundation
Washington, D. C. 20550

Assistant Secretary of Defense (1)
Research and Engineering
Attn: Technical Library
Washington, D. C. 20301

R. A. Taft Sanitary Engineering Center (1)
Public Health Service
4676 Columbia Parkway
Cincinnati, Ohio

Dr. Hans A. Panofsky (1)
Department of Meteorology
The Pennsylvania State University
University Park, Pennsylvania

Commanding General (1)
U. S. Continental Army Command
Attn: Reconnaissance Branch ODCS for Intelligence
Fort Monroe, Virginia 23351

Commander (1)
Air Force Cambridge Research Laboratories
Attn: CRZW
1065 Main Street
Waltham, Massachusetts

President (1)
U. S. Army Artillery Board
Fort Sill, Oklahoma 73504

National Center for Atmospheric Research (1)
Attn: Library
Boulder, Colorado

Dr. J. E. Cermak, Head (15)
Fluid Mechanics Program
Colorado State University
Fort Collins, Colorado 80521

Author (1)

Chief of Research and Development (1)
Department of the Army
Attn: CRD/M
Washington, D. C. 20310

Commanding General (1)
U. S. Army Missile Command
Attn: AMSMI-RRA
Redstone Arsenal, Alabama 35809

Commanding General (1)
U. S. Army Natick Laboratories
Attn: Earth Sciences Division
Natick, Massachusetts 01762

Director, U. S. Army Engineer (1)
Waterways Experiment Station
Attn: WES-FV
Vicksburg, Mississippi 39181

Chief, Atmospheric Sciences Research Division (5)
Atmospheric Sciences Laboratory
U. S. Army Electronics Command
Fort Huachuca, Arizona 85613

Commanding Officer (1)
U. S. Army Frankford Arsenal
Attn: SMUFA-1140
Philadelphia, Pennsylvania 19137

Commandant (1)
U. S. Army Artillery and Missile School
Attn: Target Acquisition Department
Fort Sill, Oklahoma 73504

Commanding General (1)
U. S. Army Test and Evaluation Command
Attn: AMSTE-BAF
Aberdeen Proving Ground, Maryland 21005

Office of Chief Communications - Electronics (1)
Department of the Army
Attn: Electronics Systems Directorate
Washington, D. C. 20315

Chief of Naval Operations (1)
Department of the Navy
Attn: Code 427
Washington, D. C. 20350

Director (1)
Bureau of Research and Development
Federal Aviation Agency
Washington, D. C. 20553

Director of Meteorological Systems (1)
Office of Applications (FM)
National Aeronautics and Space Administration
Washington, D. C. 20546

Director (1)
Atmospheric Physics and Chemistry Laboratory
Environmental Science Services Administration
Boulder, Colorado

Andrew Morse (1)
Army Aeronautical Activity
Ames Research Center
Moffett Field, California 94035

Commanding Officer (2)
U. S. Army Cold Regions Research and Engineering Laboratories
Attn: Environmental Research Branch
Hanover, New Hampshire 03755

Mr. Ned L. Kragness (1)
U. S. Army Aviation Materiel Command
SMOSM-E
12th and Spruce Streets
Saint Louis, Missouri 63166

Commanding Officer, U. S. Army (1)
Artillery Combat Development Agency
Fort Sill, Oklahoma 73504

Commander, USAR Air Weather Service (MATS) (1)
Attn: AWSSS/TIPD
Scott Air Force Base, Illinois

Dr. John Bogusky (1)
7310 Cedardale Drive
Alexandria, Virginia 22308

Commanding General (1)
U. S. Army Combat Development Command
Attn: CDCMR-E
Fort Belvoir, Virginia 22060

Commanding General (1)
U. S. Army Munitions Command
Attn: AMSMU-RE-R
Dover, New Jersey 07801

Commanding Officer (1)
U. S. Army Ballistics Research Laboratories
Attn: AMXBR-B
Aberdeen Proving Ground, Maryland 21005

Director (2)
Atmospheric Sciences Laboratory
U. S. Army Electronics Command
White Sands Missile Range, New Mexico 88002

Chief, Atmospheric Sciences Office (2)
Atmospheric Sciences Laboratory
U. S. Army Electronics Command
White Sands Missile Range, New Mexico 88002

Commanding Officer (1)
U. S. Army Picatinny Arsenal
Attn: SMUPA-TV-3
Dover, New Jersey 07801

Commanding Officer (1)
U. S. Army Communications - Electronics Combat Development Agency
Fort Monmouth, New Jersey 07703

Commanding General (1)
Deseret Test Center
Attn: Design and Analysis Division
Fort Douglas, Utah 84113

Commandant (1)
U. S. Army CBR School Micrometeorological Section
Fort McClellan, Alabama 36205

Assistant Chief of Staff for Intelligence (1)
Department of the Army
Attn: ACSI-DERSI
Washington, D. C. 20310

Commanding Officer (1)
U. S. Naval Weather Research Facility
U. S. Naval Air Station, Building R-48
Norfolk, Virginia 23511

Chief, Fallout Studies Branch (1)
Division of Biology and Medicine
Atomic Energy Commission
Washington, D. C. 20545

Director (1)
U. S. Weather Bureau
Attn: Librarian
Washington, D. C. 20235

Dr. Albert Miller (1)
Department of Meteorology
San Jose State College
San Jose, California 95114

Mrs. Francis L. Wheedon (1)
Army Research Office
3045 Columbia Pike
Arlington, Virginia 22201

Commander (1)
Air Force Cambridge Research Laboratories
Attn: CRXL
L. G. Hanscom Field
Bedford, Massachusetts

Harry Moses, Asso. Meteorologist (1)
Radiological Physics Division
Argonne National Laboratory
9700 S. Cass Avenue
Argonne, Illinois 60440

Defense Documentation Center (20)
Cameron Station
Alexandria, Virginia 22314

Office of U. S. Naval Weather Service (1)
U. S. Naval Air Station
Washington, D. C. 20390

Dr. Gerald Gill (1)
University of Michigan
Ann Arbor, Michigan 48103